

國立臺灣大學生命科學院漁業科學研究所



碩士論文

Institute of Fisheries Science

College of Life Science

National Taiwan University

Master's Thesis

Wnt/ β -catenin 訊息傳遞路徑對文昌魚胚胎發育之影響

The role of Wnt/ β -catenin signaling pathway
in amphioxus embryonic development

葉書碩

Shu-Shuo Yeh

指導教授：楊姍樺 博士

游智凱 博士

呂在明 博士

Advisors: Shan-Hua Yang, Ph.D.,


Jr-Kai Yu, Ph.D.,

Tsai-Ming Lu, Ph.D.

中華民國 113 年 2 月

February, 2024

謝辭



首先我要先謝謝楊老師在大學時的訓練，還記得剛開始實驗室只有幾張桌椅，漸漸的儀器與成員越來越多，也有機會接觸到很多不同的領域，透過練習生物資訊分析，後來才有機會認識中研院的呂老師。謝謝呂老師在生物資訊分析、實驗與論文修改上不厭其煩的指導。謝謝游老師與蘇老師在 meeting 時給予很多研究上的建議，點出我的盲點，也讓我們有充足的資源可以進行實驗。實驗過程有許多需要學長姐的經驗傳承，謝謝坤龍、靖益、函儒、宜芝在實驗上的建議與幫助，還有在哲毅在討論分析時給我很多的方向。也謝謝潔婷姐、孟貞、穎潔、家齊、家桓還有子沛學姐在實驗室生活中大大小小的協助。還有先前做胚胎實驗的政儀，有他的研究我才能接著做後續的分析。無論是在研究上或是生活上幫助過我的朋友們，謝謝你們。謝謝所有人在這段期間的指教與包容。

摘要



訊息傳遞路徑在基因調控中扮演關鍵的角色，進而影響胚胎各胚層的分化與發育。在後生動物中，Wnt/ β -catenin 訊息傳遞路徑決定體軸的調控以及胚層的分化。先前研究指出，若在受精後的文昌魚胚胎中過度啟動 Wnt/ β -catenin 訊息傳遞路徑會使中胚層和內胚層擴張，並使外胚層消失。然而在此過程中整體基因的表現以及變化仍然未知。透過核糖核酸定序，我們分析了文昌魚胚胎發育過程中過度啟動 Wnt/ β -catenin 訊息傳遞路徑對下游基因的影響。我們使用 1-azakenpaullone (GSK-3 β 的小分子抑制劑) 在胚胎一細胞時期到神經胚期 (neurula stage) 過度啟動整顆胚胎的 Wnt/ β -catenin 訊息傳遞路徑。我們發現，中胚層與內胚層的標誌基因 (marker gene) 受到正調控，而外胚層的標誌基因則受到負調控。在基因集富集分析 (Gene Ontology enrichment analysis) 中發現受到過度啟動 Wnt/ β -catenin 訊息傳遞路徑影響的基因與 Wnt、BMP、Nodal、FGF 和 Notch 等訊息傳遞路徑相關；而受到負調控的基因則與外胚層的纖毛和神經元等組織相關，暗示外胚層的組織分化受到了抑制。我們觀察到，在胚胎發育過程中，內胚層和中胚層的標誌基因擴張，而外胚層的標誌基因則消失。然而，在部分胚胎中，中胚層與內胚層的基因並未表現，暗示在過度啟動 Wnt/ β -catenin 訊息傳遞路徑後，中胚層與內胚層的形成可能受到其他訊息傳遞路徑的調控。本研究證實在早期胚胎發育期間過度啟動 Wnt/ β -catenin 訊息傳遞路徑會影響許多調控體軸與胚層的訊息傳遞路徑，並使中胚層與內胚層擴張和外胚層消失。

關鍵詞：Wnt/ β -catenin 訊息傳遞路徑、文昌魚、胚胎發育、胚層調控、發育生物學、原位雜合技術、核糖核酸定序

Abstract



Signaling pathways comprise an essential part of developmental gene regulatory networks. The activities of signaling pathways lead to changes of the gene regulatory states, and consequently determine different cell fates in particular areas within a developing embryo. In a wide range of metazoan animals, the canonical Wnt/ β -catenin pathway has been implicated in playing important functions for defining the initial axes and specifying different germ layers of the embryo. Previous studies showed that Wnt/ β -catenin signaling is active in the nuclei of vegetal hemisphere in early amphioxus embryos. Overactivation of Wnt/ β -catenin signaling greatly expands mesoderm and endoderm at the expense of ectoderm. However, changes of global gene expression profile after overactivation of Wnt/ β -catenin signaling pathway during amphioxus embryogenesis remain unclear. Here we use RNA-seq approach to globally examine developmental genes downstream of Wnt/ β -catenin signaling pathway during amphioxus embryogenesis. We used 1-azakenpaullone, which is a small molecule inhibitor of GSK-3 β , to globally activate Wnt/ β -catenin signaling pathway in amphioxus embryos at one-cell stage to early neurula stage. Our results showed that germ layer marker genes in mesoderm and endoderm were up-regulated, while ectoderm marker genes were down-regulated. Genes involved in Wnt, BMP, Nodal, FGF and Notch signaling pathways were influenced; while genes related to ectoderm derived structures such as cilia and neurons were down-regulated, signifying ectoderm loss. Overactivation of Wnt/ β -catenin signaling led to mesoderm and endoderm expansion, accompanied by the loss of ectoderm. However, in some inhibitor-treated embryos, mesoderm and endoderm genes were not expressed, suggesting that the formation of these germ layers might be regulated by other signaling pathways following the overactivation of the Wnt/ β -catenin pathway.

Overactivation of Wnt/ β -catenin signaling pathway during early embryo development influenced genes in Wnt, BMP, Nodal, FGF and Notch signaling pathways, and led to mesoderm and endoderm expansion at the expense of ectoderm.

Keywords: Wnt/ β -catenin signaling pathway; Amphioxus; Embryogenesis; Germ layer determination; Developmental biology; Whole-mount *in situ* hybridization; RNA Sequencing

Table of Contents



謝辭	II
摘要	III
Abstract.....	IV
Table of Contents.....	VI
List of Figures.....	VIII
List of Tables	XI
Introduction	1
Cephalochordates are early branching groups of chordates	1
Signaling pathways regulate embryo development and influence germ layers determination	2
Diverse roles of Wnt/ β -Catenin signaling in embryonic development across metazoan.....	3
Amphioxus as the basal chordate to answer evolution of developmental mechanism	6
Materials and methods.....	9
Animals, embryos, and drug treatments	9
RNA extraction and next generation sequencing (NGS).....	9
Sequence trimming	10
Sequence alignment and expression quantification.....	10
Sample variation examination and differentially expressed gene selection	11
Over Representation Analysis	11
Gene Set Enrichment Analysis (GSEA).....	11

Whole-mount <i>in situ</i> hybridization.....	13
Annotation reference construction and gene name assignment.....	15
Results	19
Transcriptome alignment and expression quantification.....	19
Azakenpaullone treatment influenced mRNA expression in the amphioxus embryo	19
Differential gene expression analysis	20
Gene set enrichment analysis	22
Examine gene expression patterns of germ layer marker genes by whole-mount <i>in situ</i> hybridization	23
Discussion.....	28
Global activation of Wnt/ β -catenin signaling expands mesoderm and endoderm at the expense of ectoderm	28
Genes involved in BMP, Nodal, Notch, Wnt and FGF signaling pathway were differentially expressed.....	31
References	89



List of Figures



Figure 1. Development stages of amphioxus.....	35
Figure 2. Diagram of gradients of four major signaling pathways (Nodal/Vg1, BMPs, Wnt/ β -catenin, and FGFs) in early amphioxus embryos.....	36
Figure 3. Overview of Wnt/ β -catenin signaling pathway (Ota et al., 2016).	37
Figure 4. Process of RNA-seq analysis.	38
Figure 5. Pipeline of constructing GO annotation reference.....	39
Figure 6. Distinct impacts of Azkp treatments on the samples	40
Figure 7. DEGs after Azkp treatment.....	41
Figure 8. Transcription factors in DEGs.	42
Figure 9. Heatmap of selected genes in DEGs.....	43
Figure 10. BMP signaling pathway map.....	44
Figure 11. Nodal signaling pathway map.....	45
Figure 12. Notch signaling pathway map.....	46
Figure 13. Wnt/ β -catenin signaling pathway map.....	47
Figure 14. Fibroblast growth factor signaling pathway map (MAPK signaling).....	48
Figure 15. Top 20 significant GO terms in biological process in up-regulated DEGs...	49
Figure 16. Top 20 significant GO terms in biological process in down-regulated DEGs.	50
Figure 17. Selected GO terms in biological process related to germ layer development in up-regulated DEGs.....	51
Figure 18. Selected GO terms in biological process related to germ layer development in down-regulated DEGs.	52

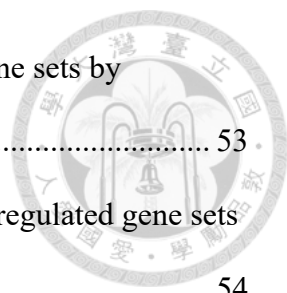


Figure 19. Top 20 GO terms in biological process in up-regulated gene sets by normalized enrichment score (NES)..... 53

Figure 20. Top 20 GO terms in biological process enriched in down-regulated gene sets by normalized enrichment score (NES)..... 54

Figure 21. GO terms related to germ layer development in biological process in up-regulated genes by normalized enrichment score (NES)..... 55

Figure 22. GO terms related to germ layer development in biological process in down-regulated gene sets by normalized enrichment score (NES). 56

Figure 23. *Dll* expression at G3 stage in DMSO and Azkp treated embryos..... 57

Figure 24. *Hex* expression at the blastula, G3, G5 and N2 stages in DMSO and Azkp-treated embryos..... 58

Figure 25. *SoxF* expression at the blastula, G3, G5 and N2 stage in DMSO and Azkp-treated embryos..... 60

Figure 26. *Hey1* expression at the blastula, G3, G5 and N2 stage in DMSO and Azkp-treated embryos..... 61

Figure 27. *FoxAa* expression at the blastula, G3, G5 and N2 stage in DMSO and Azkp-treated embryos..... 62

Figure 28. *Gooseoid* expression at the blastula, G3, G5 and N2 stage in DMSO and Azkp-treated embryos..... 64

Figure 29. *Brachyury1* expression at the blastula, G3, G5 and N2 stage in DMSO and Azkp-treated embryos..... 66

Figure 30. *AP2* expression at the blastula, G3, G5 and N2 stage in DMSO and Azkp-treated embryos..... 67

Figure 31. *FoxJ1* expression at the blastula, G3, G5 and N2 stage in DMSO and Azkp-treated embryos..... 69

Figure 32. <i>Dll</i> expression at the blastula, G3, G5 and N2 stage in DMSO and Azkp-treated embryos.....	70
Figure 33. <i>SoxB1a</i> expression at the blastula, G3, G5 and N2 stage in DMSO and Azkp-treated embryos.....	72
Figure 34. <i>Neurogenin</i> expression at the blastula, G3, G5 and N2 stage in DMSO and Azkp-treated embryos.....	73

List of Tables



Table 1. Number of terms found in annotation result using different database as reference.	74
Table 2. Published genes in <i>Branchiostoma sp.</i>	75
Table 3. RNA sequence counts in each analysis step.....	85
Table 4. Down-regulated gene set in KEGG pathway by GSEA.....	86
Table 5. Up-regulated gene set in KEGG pathway by GSEA.....	87
Table 6. Gene set members involved in Notch signaling pathway in GSEA analysis. ...	88

Introduction

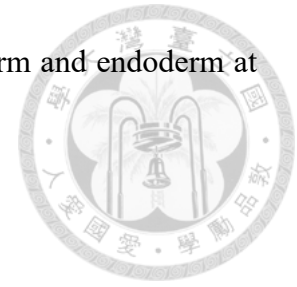


Cephalochordates are early branching groups of chordates

Chordates are categorized into three subphyla: Vertebrata, Tunicata, and Cephalochordata. Cephalochordata, commonly referred to as lancelets or amphioxus, are identified as the sister group to both Vertebrata and Tunicata. Cephalochordates are the most basal extant chordate that did not go through whole genome duplication (Holland et al., 1994; Putnam et al., 2008), and share same features such as notochord and the dorsal hollow nerve cord the with other chordates (Gee, 1996). As the most basal extant lineage in Chordata, amphioxus represents a significant model to understand the basal status of chordates during embryo development.

Amphioxus embryo development include five stages: cleavage, gastrula, neurula, tailbud and larva. Each of these stages is characterized by unique morphological and developmental characteristics (Figure 1). The process begins with cleavage, the fertilized egg undergoes cell division that increase cell number without enlarging the size of embryo (Hall, 1998; Holland & Onai, 2012). At 8-cell stage, the 3rd cleavage separates the embryo into animal half, which primarily contributes to ectoderm formation, and a vegetal half, which gives rise to both mesoderm and endoderm. If separated at 8-cell stage, the animal halves typically develop into ciliated ectodermal vesicles, whereas the vegetal halves predominantly form mesendoderm derivatives. (Holland & Holland, 2007). Gastrulation starts with invagination of the cells at the vegetal side. The invaginating cells correspond to the presumptive mesendoderm, while the non-invaginating cells of the outer layer will form the future ectoderm (Holland & Onai, 2012). During neurulation, the embryo starts to form somites and notochord. Followed by the tailbud stage, the embryo elongates due to maturation and elongation of the somites. The larval mouth

opens on the left side of the developing animal by fusion of ectoderm and endoderm at larva stage (Carvalho et al., 2021).

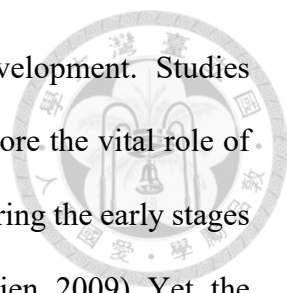


Signaling pathways regulate embryo development and influence germ layers determination

Embryo development is regulated by transcription factors and signaling pathways, both of which are crucial for regulating gene expression and mediating cellular interactions (Hall, 1998). These mechanisms collectively govern the specification, determination, and development of germ layers. Notably, various signaling pathways play a significant role in the regulation of embryo development and germ layer specification during the cleavage and gastrula stages in amphioxus (Figure 2).

The formation of three germ layers—ectoderm, mesoderm, and endoderm—is a fundamental aspect of embryo development in deuterostomes, providing the basis for all organs and tissues (Hall, 1998). The ectoderm develops into the nervous system and epidermis. The mesoderm forms muscle, connective tissue, vascular system, and skeletal structures. The endoderm differentiates into digestive structures including the gut and glandular cells. (Hall, 1998). Gastrulation is a critical phase where the mesoderm undergoes invagination, leading to the distinct separation and spatial arrangement of the mesoderm and endoderm. This process is characterized by the coordinated and dynamic rearrangement of mesendoderm cells, essential for the establishment of specific cell lineages and fates. Such coordination underscores the complexity and precision required in early embryonic development for the proper formation of germ layers.

The interplay, either cooperative or antagonistic, among signaling pathways is pivotal in regulating germ layer specification. A deeper understanding of these signaling



mechanisms can shed light on the intricacies of embryonic development. Studies encompassing a range of deuterostome and protostome taxa underscore the vital role of Wnt/ β -catenin signaling in establishing the anterior-posterior axis during the early stages of embryogenesis in bilaterians (Martindale, 2005; Petersen & Reddien, 2009). Yet, the precise influence of Wnt/ β -catenin signaling on germ layer formation in early embryonic development remains an area requiring further exploration.

Diverse roles of Wnt/ β -Catenin signaling in embryonic development across metazoan

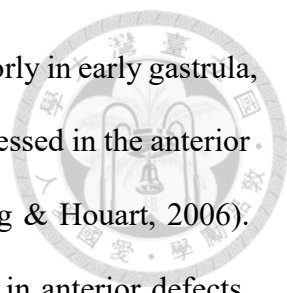
In metazoans, the Wnt signaling pathway plays a pivotal role in embryonic development, influencing a range of processes including the specification of vegetal cell fates, determination of embryonic polarity, patterning of the anteroposterior axis and posterior growth (Petersen & Reddien, 2009). Three main types have been described: Wnt/ β -catenin (canonical Wnt) signaling pathway (Figure 3), planar cell polarity (PCP) and calcium pathway (Strutt, 2003; Veeman et al., 2003).

The Wnt/ β -catenin signaling pathway consists of Wnt ligands, frizzled (FZD) receptors, co-receptors low-density lipoprotein receptor-related proteins (LRP), signaling intermediates *Dishevelleds* (DVL), β -catenin destruction complex, transcriptional coactivator β -catenin and transcription factors T cell factor and lymphoid enhancer factor (TCF/LEF) (Logan & Nusse, 2004; Moon et al., 2004). Phosphorylated β -catenin is recognized and ubiquitinated by ubiquitin ligase E3 and is subsequently degraded by the proteasome. Upon Wnt ligand binding to its receptors, the capacity of the destruction complex to phosphorylate cytosolic β -catenin is inhibited. Unphosphorylated β -catenin accumulates in the cytosol, translocates into the nucleus, and activates Wnt target gene expression, via its integration with the TCF/LEF family of transcription factors, which is

important for cellular proliferation, differentiation, and survival (Königshoff & Eickelberg, 2010; Ota et al., 2016). Nuclear accumulation of β -catenin signifies the activation of the Wnt/ β -catenin signaling pathway, playing a key role in embryo development.

Wnt ligands are expressed posteriorly during embryonic development in most bilaterians, and they promote posteriorly polarized features (Petersen & Reddien, 2009). Wnt signaling patterns the AP axis in deuterostome embryos. Activation of Wnt/ β -catenin signaling at the posterior end of the embryo specifies posterior cell fates and induces a posterior signaling center. In addition, the inhibition of Wnt/ β -catenin signaling at the anterior side is necessary for the differentiation of anterior structures (Petersen & Reddien, 2009; Range, 2014).

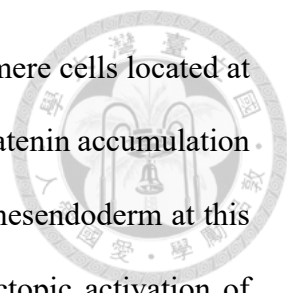
In vertebrates, the maternal Wnt/ β -catenin pathway is primarily used for setting up the dorsoventral axis and is only a minor player in germ layer specification (Marikawa, 2006). In *Xenopus*, although the inhibition of Wnt/ β -catenin signaling at blastula stage abrogates the body axis, the embryo still gastrulates and forms three germ layers. When β -catenin is depleted in frog embryos at blastula stage, the dorsal mesodermal markers are down-regulated, but ventral and general mesodermal markers are robustly expressed (Heasman et al., 1994). Also, the overactivation of Wnt/ β -catenin signaling at two cell stage does not induce mesoderm or endoderm in the ectoderm (Carnac et al., 1996; Sokol, 1993). Overactivation of Wnt signaling from fertilized egg to late gastrula stage directs embryos toward a posterior identity during gastrulation, whereas inhibiting Wnt signaling promotes an anterior identity (Kiecker & Niehrs, 2001). In *Xenopus*, Wnt/ β -catenin pathway plays a pivotal role in determining cell fate along the anteroposterior axis during early development.



In zebrafish, Wnt ligands *Wnt3a* and *Wnt8* are expressed posteriorly in early gastrula, tailbud and somite stages, while Wnt inhibitors sFRP family are expressed in the anterior neurectoderm from the tailbud stage (Shimizu et al., 2005; Tendeng & Houart, 2006). Overactivation of Wnt signaling by mutant of *Tcf3* function results in anterior defects, including absence of eyes, forebrain and midbrain (Kim et al., 2000). Inhibition of Wnt ligand genes cause posterior defects including head enlargement, failure to form posterior mesoderm (Erter et al., 2001; Rhinn et al., 2005).

In the mammalian model, specifically in mice, embryos with β -catenin-null and *Wnt3* mutations fail to undergo gastrulation (Huelsen et al., 2000). *Wnt3* and β -catenin knockout mice fail to form primitive streak (Haegel et al., 1995; Liu et al., 1999), whereas knockout of the Wnt inhibitor *Dkk1* results in an anterior truncation (Mukhopadhyay et al., 2001). Additionally, in transgenic mice expressing β -catenin resistant to GSK3 β -mediated degradation, overactivation of Wnt/ β -catenin signaling in mouse embryonic ectoderm through the expression of the constitutively active β -catenin leads to premature epithelial-mesenchymal transformation. This modification illustrates the capability of Wnt/ β -catenin signaling to initiate mesoderm formation from ectodermal cells (Kemler et al., 2004; Marikawa, 2006).

In the tunicate *Ciona intestinalis*, during the initial specification of the germ layers (occurring between the 8- and 16-cell stages), all cells except for the ectoderm require Wnt/ β -catenin signaling (Hudson et al., 2013). Subsequently, at the 32-cell stage, a crucial shift occurs wherein mesendodermal cells exhibit divergent responses to Wnt/ β -catenin signaling. This divergence is integral to the determination of endoderm and mesoderm fates, with Wnt/ β -catenin signaling being activated in endoderm cells and deactivated in mesoderm cells (Hudson et al., 2013).



In sea urchin, β -catenin nuclearization occurs in the four micromere cells located at the vegetal pole as early as the 16-cell stage; by the 60-cell stage, β -catenin accumulation in the nucleus extends to all vegetal cells, which are designated as mesendoderm at this developmental phase (Logan et al., 1999; Weitzel et al., 2004). Ectopic activation of Wnt/ β -catenin signaling leads to embryo becoming vegetalized and posteriorized (Logan et al., 1999; Wikramanayake et al., 1998). Mesendoderm-specific genes are up-regulated and anterior neuroectodermal genes are down-regulated by Wnt/ β -catenin signaling overactivation (Sun et al., 2021). Wnt/ β -catenin signaling plays an important role in mesendoderm specification and regulates posterior cell fate in the sea urchin.

In hemichordate *Saccoglossus kowalevskii*, initial mesendoderm specification is promoted and ectoderm specification is suppressed by Wnt/ β -catenin signaling during A/V axial patterning (Darras et al., 2011).

Amphioxus as the basal chordate to answer evolution of developmental mechanism

In amphioxus, nuclear β -catenin is found asymmetrically distributed in amphioxus at the vegetal hemisphere since the 32-cell stage, and the expression remains vegetally expressed until gastrulation (Kozmikova & Kozmik, 2020). At the late gastrula stage, nuclear β -catenin is expressed dorsally, and is concentrated posteriorly (Kozmikova & Kozmik, 2020). Ectopic activation of Wnt/ β -catenin signaling at the 16-cell stage has been demonstrated to inhibit gastrulation, and concurrently reduces the expression of ectodermal genes, such as *Foxq2* and *Distalless* (Onai, 2019). This suggests that Wnt/ β -catenin signaling exerts a negative regulatory effect on the specification of ectoderm during gastrulation. Another study has showed that ectopic activation of Wnt/ β -catenin signaling after fertilization provokes the expression of dorsal genes *Chordin* and *Gooseoid* (Kozmikova & Kozmik, 2020). However, there are few discussions about the

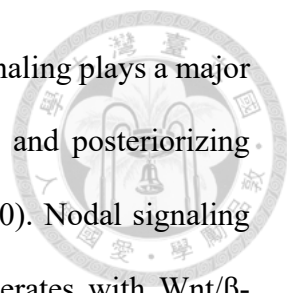
influence on germ layers. Whether Wnt/ β -catenin signaling pathway regulates amphioxus germ layer determination is not well understood.

To exam the influence of Wnt/ β -catenin signaling pathway, previous studies in our laboratory have shown that during the cleavage stage, global activation of Wnt/ β -catenin signaling leads to mesoderm and endoderm expansion and the loss of ectoderm. Hence, a global view of genes downstream of the Wnt/ β -catenin signaling pathway in early embryo development is necessary for understanding the functions of the signaling pathway in the amphioxus system. Furthermore, a more detailed examination on germ layers to answer whether Wnt/ β -catenin signaling pathway regulates amphioxus germ layer determination is necessary.

Based on previous studies, we hypothesized that overactivation of Wnt/ β -catenin signaling would result in the expansion of the mesendoderm at the expense of ectoderm loss. Therefore, we used an RNA-seq approach to globally examine downstream genes of the Wnt/ β -catenin signaling pathway during amphioxus development. 1-azakenpaullone (Azkp), a small molecule inhibitor of the β -catenin destruction complex GSK-3 β (Kunick et al., 2004), was used to globally activate Wnt/ β -catenin signaling level in amphioxus embryos. The differential expression analysis was applied to compare gene expression profiles between control and Azkp-treated embryos.

Gene set enrichment analysis (GSEA) was employed to evaluate the impact of global activation of the Wnt/ β -catenin signaling pathway on gene sets. To gain further insights into the functional implications of these differentially expressed genes, Gene Ontology (GO) term enrichment analysis was conducted to identify the biological processes significantly associated with the differentially expressed genes.

We investigated signaling molecules involved in the establishment of the embryonic axis and germ layers, focusing on genes within the BMP, Nodal, Wnt/ β -catenin, FGF and



Notch signaling pathways. Antagonism between Nodal and BMP signaling plays a major role in axial patterning, as BMP signaling mediates a ventralizing and posteriorizing influence, opposing Nodal signaling in amphioxus (Onai et al., 2010). Nodal signaling pathway, a key inducer in the organizer of amphioxus, also cooperates with Wnt/ β -catenin signaling pathway to promote dorsal cell fate and dorsoanterior/ventroposterior axis in amphioxus gastrula (Onai, 2019). Inhibition of Notch signaling reduced mesendoderm marker genes in amphioxus late gastrula stage, indicating Notch signaling controls mesendoderm specification during gastrulation in amphioxus (Onai, 2019). Furthermore, suppression of Notch signaling resulted in the reduction of Wnt/ β -catenin signaling genes *Wnt8* in the mesoderm, implying a synergistic interaction between Notch and Wnt/ β -catenin signaling pathways in mesoderm development (Onai, 2019). FGF signaling is necessary during amphioxus gastrulation, and it also forms the most anterior somites through the MAPK pathway (Bertrand et al., 2011)

To exam whether germ layer is influenced by overactivation of Wnt/ β -catenin signaling pathway, we used *in situ* hybridization to examine the expression patterns of transcription factors that are differentially expressed and recognized as germ layer markers. Examination on these marker genes at blastula to neurula stage embryos showed the impacts of global activation of the Wnt/ β -catenin signaling pathway to germ layer determination during amphioxus development.

Materials and methods



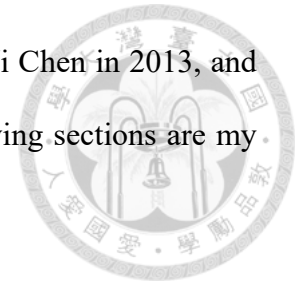
Animals, embryos, and drug treatments

Amphioxus (*B. floridae*) adults were collected in Tampa Bay, Florida, USA, during the summer breeding season. The gametes were obtained by electric stimulation and spontaneous spawning. Fertilization and subsequent culturing of the embryos were carried out as previously described (Yu & Holland, 2009). Small molecule inhibitor 1-azakenpaullone (Azkp, Merck), the ATP-competitive kinase which can specifically block the activity of GSK-3 β , was dissolved in DMSO (Sigma-Aldrich) to prepare a 10 mM stock solution. The experimental embryos were treated with inhibitors at low concentration 2 μ M or high concentration 10 μ M at 1-cell stage, and the control embryos were treated with an equal amount of DMSO in filtered seawater. DMSO have been used for drug solvent and control treatment for decades since there is no harm to embryos under 0.1%. Both the experimental and control embryos are harvested at the same time when the control embryos reached to N2 stage (~ 9hpf) for total RNA extraction.

RNA extraction and next generation sequencing (NGS)

RNA was extracted from amphioxus embryos originating from two different batches, dated 2013/8/7 and 2013/9/6. For embryos at the N2 stage, RNA extraction was carried out using the RNeasy Plus Micro Kit (QIAGEN). Subsequently, this RNA was subjected to multiplexed sequencing on a HiSeq 2500 sequencer (Illumina), utilizing a paired-end 2x101 base pair format. The sequencing yielded an average read depth of 61,778,816 paired reads per sample.

The experiments mentioned above was conducted by Cheng-Yi Chen in 2013, and RNA extraction was conducted by Che-Yi Lin in 2017. The following sections are my own research findings.



Sequence trimming

RNA-seq analysis process is shown in Figure 4. The qualities of reads were assessed by fastp (Chen et al., 2018). Adapters were trimmed by Trimmomatic v0.39 (Bolger et al., 2014), first 13 bases were cut due to uncoordinated GC content. If leading or trailing bases quality were below 20, the bases were removed and the next base would be investigated. Reads were scanned with a 4-base wide sliding window, cutting when the average quality per base dropped below 15. Reads length below 36 were dropped.

Sequence alignment and expression quantification

RNA reads were mapped to *B. floridae* genome from NCBI with RefSeq assembly accession: GCF_000003815.2, using STAR 2.7.10a (Dobin & Gingeras, 2015). Output format was set as BAM file, chromosomes/contigs/scaffolds information were not sorted. Alignment would be output only if the normalized read length is higher than or equal to 0.45.

Raw reads were count by *featureCounts* v2.0.2 (Liao et al., 2014) in paired end mode. Read pairs would be counted instead of reads. Fragments for pair-end read would be counted instead of reads. Only fragments that successfully aligned in both ends would be considered for summarization. Chimeric fragments would not be counted, and multi mapping reads and multi-overlapping reads were excluded.

Sample variation examination and differentially expressed gene selection

The R package DESeq2 version 1.40.2 (Love et al., 2014) was applied to conduct a count-based quality check and depict relationships between samples. Principles of Correlation Analysis (PCA) was used to exam if Azkp treatment would cause sample variation. Hierarchical clustering, employing Euclidean distances and Ward's minimum variance method, was used to define clusters in heatmap. Data in heatmap was normalized to facilitate comparison across different genes and samples.

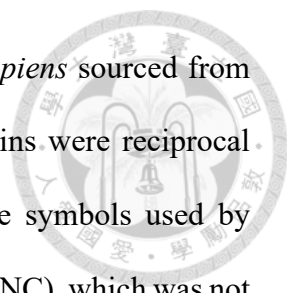
The gene expression matrix was analyzed using DESeq2. Genes were considered differentially expressed when the adjusted p-value (p-adj) was lower than 0.05, fold change greater than 2.

Over Representation Analysis

Differentially expressed genes (DEGs) underwent gene ontology (GO) enrichment analysis using OmicsBox (Götz et al., 2008), with prior annotation references established. Fisher exact test was used to identify enriched GO terms, with an adjusted p-value threshold set at 0.05. Terms with genes fewer than 15 or more than 500 were excluded. The composition of enriched terms was examined using the R package wordcloud v2.6. Hierarchical classification result of GO terms was generated by OmicsBox. Visualization was performed using R package ggplot2.

Gene Set Enrichment Analysis (GSEA)

GSEA by broad institute was used to exam enriched biological pathways (Subramanian et al., 2005). However, the MsigDB database employed by GSEA did not include gene IDs for *B. floridae*. Therefore, to facilitate the analysis, it was necessary to identify orthologous genes between amphioxus and humans. This was achieved through



bidirectional blast, using protein sequences of amphioxus and *H. sapiens* sourced from the UniProt database (Accession: GCF_000001405.40). 8443 proteins were reciprocal best hit, 8240 genes possessed expression profiles. However, gene symbols used by MsigDB were named by HUGO Gene Nomenclature Committee (HGNC), which was not aligned with UniProt. To address this discrepancy, a transformation was executed using SynGO (Koopmans et al., 2019). Sequence expression was examined before analysis operation. Total read counts lower than 16 were filtered. For sequences expressed exclusively in treatment or control, 0 were set as 0.01 to avoid fold change ratio calculation error. To ensure the normalization of read counts across all samples, library sizes were adjusted by TMM normalization. Manual inspections were conducted to identify any genes that may have been erroneously excluded. Ultimately, 7127 sequences were retained for the GSEA analysis.

The parameters used in the GSEA analysis were configured as follows: The database selections included C2 (Canonical pathways) and C5 (ontology gene sets). The number of permutations was set to 1000 iterations. The Azkp treatment and DMSO control groups were designated as distinct phenotype labels. The “collapse” mode was chosen to eliminate genes that existed in input data but not in the database. Additionally, the permutation type was specified as “Gene_set” for samples fewer than 7. Gene sets larger than 500 or smaller than 5 genes were excluded. The chip platform utilized was “Human_Gene_Symbol_with_Remapping_MsigDB.v2023.1.Hs.chip.”

KEGG pathways and GO terms were considered significant by following parameters: FDR (False Discovery Rate) < 0.25, ES (Enrichment Score) > 0.5, and a peak gene set score exceeding 3500. The results were visualized using the R package ggplot2.

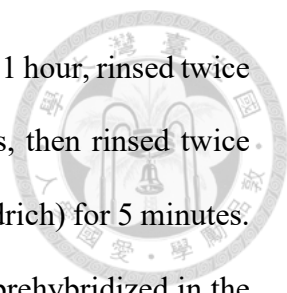
Whole-mount *in situ* hybridization

Embryos treated with 10 μ M Azkp from fertilize egg until N2 stage were used (2013/6/28). A control group was treated with 0.1% DMSO. Embryos collected at blastula, G3, G5 and N2 stage were used for whole-mount *in situ* hybridization. Additionally, another batch (2013/8/23) treated with 10 μ M Azkp from 2/4 cell stage until N2 stage was used.

To synthesize riboprobes, we used a primer matching the vector sequence next to the 3' end of the cDNA insert with a T7 promoter sequence (Promega) added to its 5' end as a reverse primer (pDONR222-T7-Reverse, 5'-TAATACGTCTCACTATAGGGAGGGGATATCAGCTGGATG-3') and a primer matching the vector sequence adjacent to the 5' end of the cDNA insert with SP6 promoter (Promega) sequence added as a forward primer (pDONR222-SP6-Forward, 5'-ATTTAGGTGACACTATAGAAGACGGCCAGTCTTAAGCTC-3') using PCR condition below: 2 min 96 °C; 25 cycles of 20 sec 96 °C, 30 sec 53 °C, 3 min 72 °C; 3 min 72 °C.

PCR products were purified by QIAquick® PCR Purification kit (QIAGEN) for DIG-labeled riboprobe synthesis. T7 or SP6 RNA polymerase were used to synthesized antisense and sense riboprobes. The concentration and quality of DIG-labeled RNA probes were examined using Nanodrop Spectrophotometer and gel electrophoresis.

All solutions for *in situ* hybridization experiments were prepared using Diethyl Pyrocarbonate-treated water (DEPC-H₂O, Sigma-Aldrich) as solvent. Fixed embryos were stored in 70% EtOH. Embryos were rehydrated with PBS (Gibco) containing 0.1% Tween 20 (Sigma-Aldrich), washed three times with PBST for 5 minutes, soaked in 5 μ g/ml Proteinase K (Invitrogen) for 3 minutes, then add 10 μ l 10% glycine (Avantor) to stop proteinase K, quickly change solution to 2 mg/ml glycine in PBST for 5 minutes.



The embryos then fixed in 4% paraformaldehyde (Sigma-Aldrich) for 1 hour, rinsed twice with the 0.1M triethanolamine (Sigma-Aldrich) for 1 and 5 minutes, then rinsed twice with PBST adding 2.5 μ l/ml and 5 μ l/ml acetic anhydride (Sigma-Aldrich) for 5 minutes. Wash twice with the PBST for 1 and 5 minutes. The embryos were prehybridized in the pre-hybridization buffer and hybridization buffer (50% deionized formamide (Merck), 100 μ g/mL Heparin (Sigma-Aldrich), 5X SSC (Invitrogen), 0.1% Tween 20, 5mM EDTA (Ambion), 1X Denhardt's solution (Invitrogen), DEPC-treated water (Sigma-Aldrich). Hybridization buffer was made with 1mg/ml yeast total RNA (Ambion)) for at least 1 hour at 60°C. Hybridization was performed in the hybridization buffer containing probe (>100 ng/ml) overnight at 60°C.

After hybridization, embryos were washed with wash solution I (50% formamide, 5X SSC, 1% SDS) for 5 minutes twice and 15 minutes twice at 60°C, then washed with wash solution II (50% formamide, 2X SSC, 1% SDS (Invitrogen)) for 5 minutes at 60°C, 10 and 15 minutes at room temperature without shaking, then washed with wash solution III (2X SSC, 0.1% Tween 20) for five minutes without shaking, 20 minutes with 2ul RNase A (10mg/ml, Roche) and 1ul RNase T1 (10000 U/ml, Roche) in 1 ml wash solution III at 37°C, then wash with wash solution III for 20 minutes twice, then wash in wash solution IV (0.2X SSC, 0.1% Tween 20) for 20 minutes, then wash in wash solution V (2mg/ml BSA (Sigma-Aldrich), 0.1% Tween 20) for five minutes. After these washes, the embryos were incubated in the blocking solution (sheep serum (Jackson ImmunoResearch) in wash solution V, 1:10) for at least 1 hour at room temperature, then incubate with the blocking solution containing antibody conjugated with alkaline phosphatase (1:3000; Roche) overnight at 4°C. After immunoreaction, embryos were washed with PBST for 20 minutes 4 times, then rinse with AP buffer without MgCl₂ (Sigma-Aldric) (100mM Tris pH 9.5 (J.T. Baker), 100mM NaCl, 0.1% Tween 20) for 10

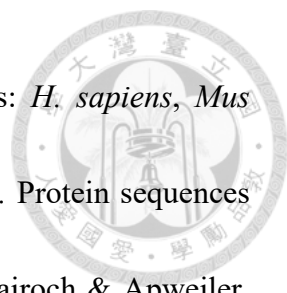
minutes, then rinse with AP buffer for 10 minutes three times. Color development was performed using alkaline phosphatase-conjugated anti-DIG antibodies with NBT (nitro blue tetrazolium, Roche) and BCIP (5-bromo-4-chloro-3-indolyl-phosphate, Roche) as substrates.

After staining, embryos were washed with PBST for 10 minutes, fixed with 4% paraformaldehyde in PBS for 1 hour, washed with PBST for at least 1 hour to reduce background, then store in 80% glycerol in PBST with 0.1% sodium azide (Sigma-Aldrich). Images were taken using a Zeiss Axio Imager A2 microscope with a Zeiss AxioCam MRc CCD camera.

Annotation reference construction and gene name assignment

The protein sequences, genome sequences (Fast Adaptive Shrinkage Threshold Algorithm, FASTA) and annotation features (General Feature Format, GFF) of *B. floridae* were obtained from the National Center for Biotechnology Information (NCBI) with RefSeq assembly accession: GCF_000003815.2. Each protein ID corresponded to multiple gene IDs, indicating the presence of numerous isoforms within each protein. To remove isoform gene, protein IDs were assigned to their corresponding gene ID with the longest sequence.

To construct annotation reference, the protein sequences of *B. floridae* were blasted to the NCBI non-redundant (nr) database, focusing on a subset of Metazoan species by blastp v2.11.0 (McGinnis & Madden, 2004). To compare blast result from different



subsets, blastp were also performed against five model organisms: *H. sapiens*, *Mus musculus*, *Danio rerio*, *Gallus gallus* and *Drosophila melanogaster*. Protein sequences of these model organisms were sourced from nr and Swiss-Prot (Bairoch & Apweiler, 1996). To increase annotations, the sequence from all five species were integrated to create a comprehensive reference.

Pipeline of constructing GO annotation reference is shown in figure 5. The mapping of GO terms and annotation was followed by Blast2GO suite (Götz et al., 2008). The blast results were generated using either a local server or OmicsBox's integrated blast function. For local blast, the output format was configured as XML to ensure compatibility with OmicsBox. Within OmicsBox, GO mapping and GO annotation were executed to obtain annotation information. GO terms from EggNOG and InterProScan were amalgamated into OmicsBox, enhancing the annotation reference. A comprehensive reference was established by merging GO terms after the input of all data.

In comparison to model organisms, the gene annotation of *B. floridae* was relatively limited. OmicsBox was used to combine numerous annotation references to reveal more comprehensive information. Proteins of *B. floridae* blasted to three databases were compared: (1) focus on a subset of metazoan species in the NCBI non-redundant (nr) database, (2) five model organisms including *H. sapiens*, *M. musculus*, *G. gallus*, *D. rerio*, and *D. melanogaster* in nr database, (3) five model organisms in Swiss-Prot databases. Genes of model organisms were well-annotated, making them valuable resources for constructing an annotation reference.

Amount of GO terms with keywords related to germ layers and development found in each reference were recorded (Table 1). Notably, the reference constructed from the nr

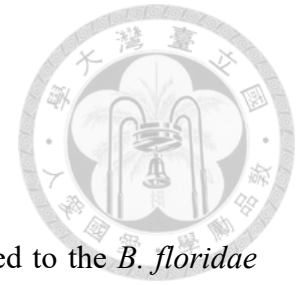
database's five model organisms contained the most terms. The reference built by the nr database focusing on metazoan had half the number of GO terms as the one built from five model organisms. The reference provided by the Swiss Prot database, had the fewest terms. Therefore, the reference produced from the five model organisms by nr database was selected as annotation reference.

For the genes in *B. floridae*, a transformation between gene IDs and corresponding gene symbols was necessary for further interpretation. In genome sequence of *B. floridae*, for example, the gene ID of *brachyury1* is “LOC118423429”. The nomenclature does not intuitively correspond to its commonly known gene name, thereby making direct association challenging. In my study, 179 published genes in *B. floridae* (Table 2) were listed and assigned to the genes with highest similarity. Rest of the genes were assigned to published data from *B. lanceolatum* and *H. sapiens*. Gene names from *B. lanceolatum* were assigned by name of human in HUGO Gene Nomenclature Committee (Seal et al., 2023). Union of gene names is necessary for comparison between *Branchiostoma*. The remaining genes were blasted to three references including *B. lanceolatum* (Marlétaz et al., 2018), *H. sapiens* from UniProt database and entire UniProt database. Gene nomenclature was assigned based on the priority order of *B. lanceolatum*, human and UniProt database matches.

For transcription factors (TFs) in *B. floridae*, TFs were extracted from annotation reference and genome sequences of *B. floridae*, union of two results were defined as TFs. Genes annotated by four GO terms were extracted and listed as TFs (Ayers et al., 2023). Including DNA-binding transcription factor activity (GO:0003700), sequence-specific DNA binding (GO:0043565), transcription factor binding (GO:0008134) and transcription regulator complex (GO:0005667). Hidden Markov Model (HMM) was employed to categorize TF families in genome sequences. HMM files for 59 out of 72 TF

families were download from the Pfam database (v35.0), the remaining files were obtained from AnimalTFDB 3.0 (Hu et al., 2018). Hmsearch (Johnson et al., 2010) was hired to search TFs, E-value thresholds were configured as follow: 1E-02 for bHLH family, 1E-03 for HMG, Homeobox, zf-BED and zf-C2H2, 1E-20 for zf-CCCH and 1E-04 for all the other families. 2079 TFs were found in annotation reference, 2174 TFs were found by Hmsearch. The union of two results contains 2665 TFs.

Results



Transcriptome alignment and expression quantification

To access the expression of each gene, sequences were mapped to the *B. floridae* reference genome. All reads achieved a quality score higher than 38 which indicates good quality, as scores above 30 are generally considered satisfactory. The proportion of reads successfully mapped to the genome varied from 78% to 86%. The percentage of sequences mapped to multiple loci also differed among the samples, ranging from 8% to 16% (Table 3). The primary reasons for sequences remaining unmapped were insufficient length and ambiguity. After mapping the reads to the genome, subsequent procedure was to quantify the number of reads aligned to each gene. A total of 29721 genes were assigned. The assignment rate for alignments ranged between 83% to 85%, with unassigned alignments predominantly resulting from multiple mapping. The quality and mapping rate were sufficient for subsequent analysis.

Azakenpaullone treatment influenced mRNA expression in the amphioxus embryo

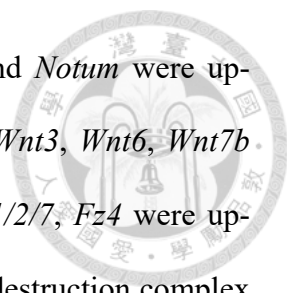
To assess variations between treatments, sample correlation heatmap and principal component analysis (PCA) were utilized. Variations in Azkp efficacy across different concentration treatments were observed (Figure 6A). Notably, the samples were clearly separated by different treatments, suggesting that Azkp treatment significantly affects gene expression in amphioxus embryos. However, in the case of the 2 μ M Azkp treatment, one batch displayed a closer resemblance to the DMSO treatment group (Figure 6B). Consequently, subsequent analyses focused exclusively on comparing the 10 μ M Azkp treatment with the DMSO treatment.

Differential gene expression analysis

Between 10 μ M Azkp-treated and control samples, a total of 5181 genes exhibited differential expression, comprising 1686 up-regulated and 3495 down-regulated genes (Figure 7). Among the up-regulated DEGs, *Kremen*-like showed the most prominent increase, and *Mucin2*-like also exhibited a drastical increase. In the down-regulated genes, *Tlx* showed the most prominent decrease and *Keratin1* exhibit the most significant p-value (Figure 7).

Among the identified differentially expressed TFs, 247 were up-regulated and 278 were down-regulated. Selected transcription factors representing known germ layer markers were highlighted among differentially expressed genes (Figure 8). Among up-regulated genes, endoderm marker genes *FoxAa*, *FoxAb*, *Hex*, *Otx* and *SoxF* were up-regulated. Mesoderm marker genes *SoxF*, *MESP*, *Hey1*, *Goosecoid*, *Brachyury1* and *Brachyury2* were up-regulated. Neuroectoderm marker genes *SoxB1a*, *SoxB1b*, *Ash*, *Neurogenin*, *EmxA*, *FoxQ2c*, *Tlx* and *Elav* were down-regulated. Non-neural ectoderm marker genes *AP2*, *FoxJ1*, *Keratin1* and *Dll* were down-regulated. (Figure 9A).

We examined genes involved in signaling pathways crucial for embryo development (Figure 9B). Additionally, the relationships of DEGs and their expression patterns in each signaling pathway are depicted. These figures were modified from the Kyoto Encyclopedia of Genes and Genomes (KEGG) database. In the BMP signaling pathway (Figure 10), the BMP antagonist *Gremlin* was down-regulated, while another antagonist *Chordin* was up-regulated. Signaling ligands *BMP2/4*, *BMP5/8*, along with the mediator *Smad1/5/8* were up-regulated. In the Nodal signaling pathway (Figure 11), *Nodal* was up-regulated, while the inhibitor *INHBB* and downstream target gene *Pitx* were down-regulated. In the Notch signaling pathway (Figure 12), *Delta*, *Fringe*, and downstream target gene *Hey1* were up-regulated. Wnt/ β -catenin signaling pathway exhibited a



complex pattern (Figure 13): inhibitors *Cerberus*, *Dkk1*, *sFRP2* and *Notum* were up-regulated, whereas *Dkk3* was down-regulated. Wnt ligands *Wnt1*, *Wnt3*, *Wnt6*, *Wnt7b* were down-regulated, while *Wnt8* was up-regulated. Receptors *Fz1/2/7*, *Fz4* were up-regulated, while *Fz5/8* was down-regulated. One component of the destruction complex *APC* was up-regulated. β -catenin and downstream transcription factor *Tcf* were up-regulated. In the FGF signaling pathway (Figure 14), ligands including *FGF9/16/20*, *FGFA*, *EGF*, *HGF* and *VEGFC* were down-regulated. Among receptor genes, *FGFR3*, *FLT1* and *MET* were up-regulated, while three other receptor genes *ERBB4*, *NTRK2* and *RET* were down-regulated. Additionally, downstream transcription factor *Elk1* was down-regulated.

Over representation analysis

To delve into the potential functions of DEGs, up-regulated and down-regulated DEGs were separated and performed GO enrichment analysis, respectively. Among the up-regulated DEGs, 811 terms were found to be enriched. In contrast, 182 terms were found to be enriched in the down-regulated DEGs. Ranked by adjusted p-value, top 20 enriched terms in the up-regulated DEGs were associated with DNA/RNA metabolism activities and cellular processes (Figure 15). In contrast, terms in the down-regulated DEGs were associated with cilia movement and assembly (Figure 16).

To examine the influence of Azkp treatment to germ layer determination, enriched terms related to germ layers and signaling pathway were examined. Terms related to all three germ layers were enriched in up-regulated DEGs. Additionally, terms related to Nodal and Notch signaling pathways were enriched (Figure 17). On the other hand, “epidermis development” was the only germ layer related term characterized by down-

regulated DEGs. Remaining terms were mainly associated with neuron development and cilium organization, both of them are derived from ectoderm (Figure 18).



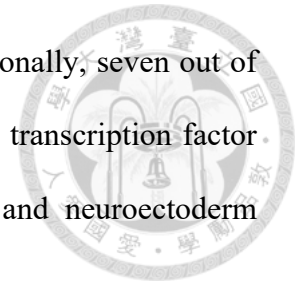
Gene set enrichment analysis

Gene set enrichment analysis was employed to investigate the enrichment of gene sets. Regarding the KEGG pathway, arachidonic acid metabolism was the only down-regulated gene set (Table 4), while seven gene sets were up-regulated (Table 5). Notably, Notch signaling pathway was the only up-regulated gene set related to embryo development.

In gene ontology, the top 20 enriched terms were shown by normalized enrichment score and gene set size (Figure 19). Up-regulated terms were related to RNA metabolism, including “Lateral mesoderm development” and “Determination of left right asymmetry in lateral mesoderm”. On the other hand, three terms in down-regulated gene sets were related to neuron differentiation, including “Noradrenergic neuron differentiation”, “GABAergic neuron differentiation” and “Rostro caudal neural tube patterning” (Figure 20).

To delve deeper into terms associated with germ layer development, a manual examination was conducted. Among the up-regulated gene sets, six terms exhibited enrichment, including “Lateral mesoderm development”, “Nodal signaling pathway”, “Determination of left-right asymmetry in lateral mesoderm”, “Gastrulation with mouth forming second”, “Epithelial cell differentiation involved in prostate gland development”, and “Primitive streak formation” (Figure 21). Conversely, in down-regulated gene sets, terms related to cilium and neuron were enriched. Two terms associated with muscle were enriched, including “Muscle adaptation” and “Muscle cell development” (Figure 22). Seven out of nine terms related to cilium were associated with a transcription factor gene

FoxJ1, which is expressed in ectoderm during development. Additionally, seven out of nine terms related to neuron were associated with proneural bHLH transcription factor *Ash*. Terms involving non-neural ectoderm marker gene *FoxJ1* and neuroectoderm marker gene *Ash* were marked in the plot.

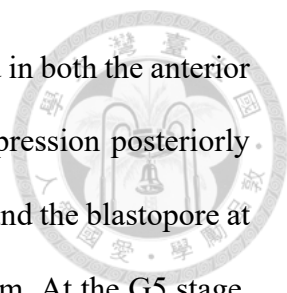


Examine gene expression patterns of germ layer marker genes by whole-mount *in situ* hybridization

To assess the impact of perturbation of Wnt/ β -catenin signaling on germ layer development, also confirm the results of differential expression analysis, we examined 11 differentially expressed transcription factors that are also recognized as markers for germ layer characterization. The expression patterns of germ layer marker genes are as follows: Endoderm markers *Hex*, *FoxAa* and *SoxF* were up-regulated, as were mesoderm markers *Hey1*, *Goosecoid* and *Brachyury1*. Conversely, neuroectoderm markers *Neurogenin* and *SoxB1a*, along with non-neural ectoderm markers *AP2*, *FoxJ1*, and *Dll*, were down-regulated.

In embryos treated with Azkp, 33 out of 78 embryos (42%) did not properly go through gastrulation during G3 stage, and 42 out of 66 (64%) in G5 stage. Furthermore, blastopore was not properly formed among embryos in N2 stage, which indicated that gastrulation was not done properly. Take *Dll* at G3 stage as example, whether embryos went through gastrulation did not influence the gene expression (Figure 23). Despite the aberrant gastrulation, the body axis of the embryo remained identifiable, characterized by larger cells on the posterior side and smaller cells on the animal side.

In the expression of germ layer marker genes, *Hex* exhibited no expression at the blastula stage. During the G3 stage, slight expression was found at the center of vegetal plate, consistent with findings from a previous study (Yu et al., 2007). At the G5 stage,



Hex expression expanded to the anterior endoderm, and was observed in both the anterior and posterior endoderm at the N2 stage, with more pronounced expression posteriorly (Figure 24A). *Azcp* treatment led to the expansion of expression around the blastopore at the G3 stage, suggesting an enlargement of the presumptive endoderm. At the G5 stage, gene expression was up-regulated and expanded in the posterior half of the embryos, while no expression was observed in the rest of the embryos (Figure 24B). At the N2 stage, expression in both anterior and posterior mesoderm was up-regulated and expanded, indicative of endodermal expansion due to *Azcp* treatment (Figure 24A).

SoxF displayed maternal and uniform expression pattern as previously documented (Cattell et al., 2012), which became restricted to the mesendoderm anteriorly and ventrally during late gastrulation. It had the strongest expression in the forming midgut and extend to hindgut at N2 stage (Figure 25A). *Azcp* treatment led to an expansion and up-regulation at the G5 stage, also occurring posteriorly at N2 stage. Notably, in some embryos, *SoxF* expression was absent at the blastula, G3, and N2 stages, suggesting a variable influence of *Azcp* on *SoxF* expression patterns (Figure 25B-D).

Hey1 was expressed as single stripes in the presumptive somite during gastrulation, turned into four stripes in the N2 stage as previously reported (Beaster-Jones et al., 2008). Following *Azcp* treatment, *Hey1* expression was absent at the G3 and G5 stages, but at the N2 stage, the stripes were extended across the entire embryo (Figure 26).

FoxAa was first expressed in anterior ventral endoderm and also in dorsal mesendoderm, corresponding to the presumptive notochord territory and cells of archenteron floor at the G5 stage. Expression in the axial mesoderm and endoderm persisted at the N2 stage as previously documented (Aldea et al., 2015). Following *Azcp* treatment, there was a noticeable expansion of *FoxAa* expression both anteriorly and ventrally at the G5 stage, and this expansion extended anteriorly and posteriorly at the N2

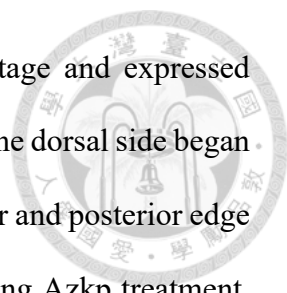
stage (Figure 27A). Notably, four out of six embryos exhibited an absence of *FoxAa* expression at the G5 stage (Figure 27B).

Gooseoid was expressed at the dorsal lip of the blastopore, and extending throughout the axial mesoderm during gastrulation. Its expression later became concentrated in the presumptive notochord region, consistently observed at the N2 stage as previously reported (Neidert et al., 2000). Under Azkp treatment, gene expression was expanded at the G3 and G5 stages, with a posterior expansion at the N2 stage. Remarkably, one out of six embryos exhibited an absence of *Gooseoid* expression during the G5 stage (Figure 28).

Brachyury1 was expressed around the blastopore at the onset of gastrulation, with stronger expression in the dorsal posterior mesoderm while weaker in anterior axial mesoderm at the N2 stage as previously reported (Yuan et al., 2020). Gene expression of embryos treated with Azkp were all expanded (Figure 29A-D).

AP2 marked the epidermal ectoderm at the G3 and G5 stages. The edges of epidermal ectoderm derived from neuroectoderm and migrated to the midline during neurulation as previously reported (Meulemans & Bronner-Fraser, 2002). No *AP2* expression were found by Azkp treatment from G3 to N2 stages (Figure 30A). Notably, there were half embryos with *AP2* expression at G5 stage, and two out of three embryos with slight *AP2* signal at the N2 stage (Figure 30B, C).

FoxJ1 demonstrated a dynamic expression pattern, first observed in the ectoderm, except in the regions surrounding the blastopore at the G3 and G5 stages. At the N2 stage, *FoxJ1* signal was detected in the neural tube and ectoderm as previously reported (Aldea et al., 2015). Notably, following Azkp treatment, *FoxJ1* expression was absent at all examined stages (Figure 31).



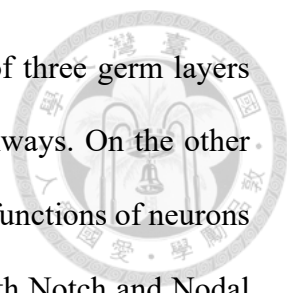
Dll was first detected in animal hemisphere at the blastula stage and expressed throughout the ectoderm at the G3 stage. However, its expression on the dorsal side began to diminish at the G5 stage. During N2 stage, *Dll* expressed at anterior and posterior edge of ectoderm as previous documented (Holland et al., 1996). Following Azkp treatment, *Dll* expression was absent at all stages (Figure 32A), with the exception of a few embryos at the blastula and G3 stages (Figure 32B).

SoxB1a, previously referred to as *AmphiSox1/2/3* (Holland et al., 2000), was detected in the dorsal epiblast, maintaining strong expression throughout gastrulation. During the N2 stage, *SoxB1a* expression became limited to the neural plate (Figure 33A). Except for four out of six embryos at the G5 stage (Figure 33B), there were no expression at any stages after Azkp treatment.

Neurogenin expressed in the presumptive neural plate at the G3 and G5 stages. At the N2 stage, *Neurogenin* expression was down-regulated in the future floor plate and became stripes as previously reported (Holland et al., 2000). There were no *Neurogenin* expression at any stages after Azkp treatment (Figure 34).

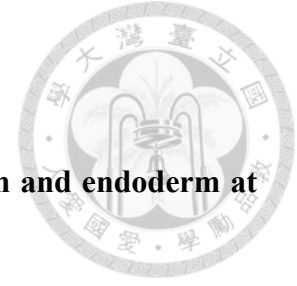
In conclusion, compared to DMSO treated embryos, mesoderm and endoderm marker genes were expanded at the N2 stage in Azkp treated embryos. Conversely, neural and non-neural ectoderm marker genes were diminished in Azkp treated embryos. Suggesting expansion and up-regulation of endoderm and mesoderm, loss in ectoderm due to Azkp treatment. The variable expression patterns observed for mesoderm and endoderm marker genes will be further explored in the discussion section.

In our research, we found that perturbation of Wnt/ β -catenin signaling by Azkp treatment significantly influenced the gene expression in amphioxus embryo. The expression profile showed that mesoderm and endoderm marker genes were up-regulated, while ectoderm marker genes were down-regulated. GO enrichment analysis revealed



that up-regulated genes were involved in regulating the formation of three germ layers and were also associated with BMP, FGF and Notch signaling pathways. On the other hand, down-regulated genes were associated with the formation and functions of neurons and cilia, derived from ectoderm. In GSEA, gene sets associated with Notch and Nodal signaling were up-regulated, while those related to ectodermal tissues, including cilia and neurons, were down-regulated. The expression of germ layer marker genes in embryos showed that global activation of Wnt/ β -catenin signaling during early embryo development results in the expansion of endoderm and mesoderm, with a concurrent reduction of ectoderm.

Discussion

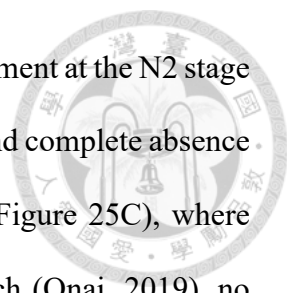


Global activation of Wnt/ β -catenin signaling expands mesoderm and endoderm at the expense of ectoderm

In our study, RNA-seq was utilized to globally examine developmental genes downstream of the Wnt/ β -catenin signaling pathway during amphioxus embryo development. Additionally, the aim was to assess whether germ layer specification is influenced by global activation of Wnt/ β -catenin signaling, as evidenced through *in situ* hybridization.

Transcriptome analysis revealed that overactivation of Wnt/ β -catenin signaling differentially affected marker genes across germ layers. Mesoderm and endoderm marker genes were up-regulated, while ectoderm marker genes were down-regulated. Notably, mesoderm marker genes showed variable levels of up-regulation (Figure 9A). With the exception of *SoxF*, all mesoderm marker genes in one *Azfp*-treated sample exhibited a twofold increase, while in another sample, a fivefold increase was observed. This suggests a degree of variability in the regulatory influence of the Wnt/ β -catenin signaling pathway on mesoderm development. The variability might be due to long term activation of Wnt/ β -catenin signaling pathway.

In situ hybridization results further demonstrate the inconsistent expression patterns of mesoderm and endoderm marker genes among embryos. *Brachyury1* was used in both batches as a positive control, and two batches showed the same results. The inconsistent expression is more possibly due to overactivation of Wnt/ β -catenin signaling, long-term activation of Wnt/ β -catenin signaling might lead to numerous effects on signaling pathways, potentially resulting in different expression patterns of mesoderm and endoderm marker genes.



SoxF exhibited two distinct expression patterns under Azkp treatment at the N2 stage (Figure 25A), with expanded posterior expression in three embryos and complete absence in another. This inconsistency was also observed at the G3 stage (Figure 25C), where *SoxF* was not expressed in half of the embryos. In previous research (Onai, 2019), no expression of *SoxF* was found at the late gastrula stage by BIO (6BIO (2'Z,3'E)-6-bromoindirubin-3'-oxime, a specific inhibitor of GSK3) treatment for 30 minutes at 16-cell stage. Similarly, no expression was found at early neurula stage by injection of *Wnt1* mRNA in unfertilized eggs. These results suggest that the global activation of the Wnt/ β -catenin signaling pathway in unfertilized eggs and at the 16-cell stage both lead to the down-regulation of *SoxF*. The author regarded *SoxF* as inner mesendoderm marker gene, and suggested that Wnt/ β -catenin signaling pathway inhibit the specification of inner mesendoderm. However, *SoxF* showed inconsistent expression in our result compared to previous research. Our findings suggest that the drug selection and treatment duration of Wnt/ β -catenin signaling activation might influence the developmental regulation of mesendoderm genes like *SoxF*.

The absence of *Hey1* expression under Azkp treatment at the G5 stage, followed by its expansion in somites at the N2 stage (Figure 26), suggests that overactivation of the Wnt/ β -catenin signaling pathway initially inhibits *Hey1* expression. Subsequently, influences from other signaling pathways contribute to the expansion of *Hey1* expression at the N2 stage. This pattern indicates the complex interplay between Wnt/ β -catenin signaling and other pathways in regulating gene expression. *Hey1* is a downstream gene of Notch signaling pathway (Zhou et al., 2012), with components such as *Delta* and *Fringe* being up-regulated in our study (Figure 12). This up-regulation within the Notch signaling pathway could be responsible for the increased expression of *Hey1* in the N2 stage. This suggests that prolonged activation of Wnt/ β -catenin signaling may indirectly

affect multiple signaling pathways, leading to varied impacts on signaling pathways and their downstream genes.

The expression of ectoderm marker genes was consistently down-regulated in amphioxus embryos following Azkp treatment, leading to the loss of ectoderm. The result of ectoderm loss in my research is identical to global activation of Wnt/ β -catenin signaling by *Wnt1* mRNA injection in unfertilized eggs (Onai, 2019). The inhibition of ectoderm determination by the Wnt/ β -catenin signaling pathway in amphioxus is consistent with its roles observed in other deuterostome animals such as hemichordate (Darras et al., 2011), echinoderm (Logan et al., 1999) and vertebrates (Martin & Kimelman, 2012). Which showed a conserved function within the deuterostome.

Chordin functions as a BMP signaling antagonist and plays a role in dorsal-ventral patterning in vertebrates (Chang et al., 2001), and it is expressed in both ectoderm and mesoderm at the onset of gastrulation and in the dorsal mesoderm during the neurula stage (Yu et al., 2007). In my analysis, *Chordin* expression was up-regulated, showing a doubling in one Azkp-treated sample and a fivefold increase in the other, indicating variability in the regulatory pattern. However, previous studies showed inconsistencies in *Chordin* expression under Wnt/ β -catenin signaling overactivation. *Chordin* expression is absent at mid gastrula stage by BIO treatment at 16-cell stage, and no significant change at the early neurula stage after *Wnt1* mRNA injection at the one-cell stage (Onai, 2019). Conversely, *Chordin* expansion was observed at the mid gastrula stage under overactivation of Wnt/ β -catenin signaling pathway by GSK3 inhibitor CHIR99021 at the 1-cell stage; the expansion of *Chordin* was also observed at the mid neurula stage by CHIR99021 treatment at the early gastrula stage (Kozmikova & Kozmik, 2020). This indicates a complex regulatory interaction between *Chordin* and the Wnt/ β -catenin signaling pathway. Further investigation into genes expressed in both the mesoderm and

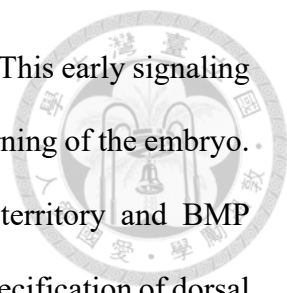
ectoderm during embryonic development elucidates the regulatory mechanisms of Wnt/ β -catenin signaling pathway.

My research demonstrates that global activation of the Wnt/ β -catenin signaling pathway influences germ layer determination in amphioxus, promoting the expansion of mesoderm and endoderm at the expense of ectoderm. This finding underscores the pivotal role of Wnt/ β -catenin signaling pathway in developmental processes. However, the expression patterns of endoderm and mesoderm marker genes, including *SoxF* and *Hey1*, displayed variability. This inconsistency suggests a complex regulatory mechanism of Wnt/ β -catenin signaling pathway, which also indicates influences from other signaling pathways. To elucidate the specific role of the Wnt/ β -catenin signaling pathway in germ layer determination, further investigation involving both short-term overactivation and inhibition of this pathway is necessary. The studies are essential for a comprehensive understanding of the regulatory mechanisms of Wnt/ β -catenin signaling pathway in embryonic development.

Genes involved in BMP, Nodal, Notch, Wnt and FGF signaling pathway were differentially expressed

GSEA showed that genes in Nodal and Notch signaling pathway were influenced by Azkp treatment. Over representation analysis showed that differentially expressed genes were involved in FGF, Nodal and BMP signaling pathways. Over representation analysis focus on differentially expressed genes while GSEA examined all genes in the gene sets, both analyses are necessary for complete examination of downstream genes influenced by Azkp treatment.

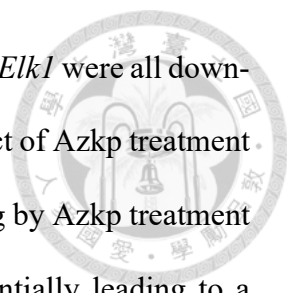
Maternal Wnt/ β -catenin and Nodal signaling plays a pivotal role in inducing a variety of transcription factors and secreted proteins during the cleavage and blastula



stages of embryonic development in amphioxus (Zinski et al., 2018). This early signaling is essential for the initial specification of cell fates and the axial patterning of the embryo. Furthermore, the establishment of Nodal signaling in the dorsal territory and BMP signaling in the ventral territory of embryo is critical for the precise specification of dorsal and ventral cell fates, as well as for axial patterning (Kozmikova et al., 2013). In my research, following Azkp treatment, there was an up-regulation of BMP ligands *BMP2/4* and *BMP5/8*, along with mediators *Smad1/5/8*, and down-regulation of the BMP pathway inhibitor *Gremlin* (Figure 9). This suggests a positive regulatory effect of Azkp treatment on BMP signaling. Additionally, within the Nodal signaling pathway, *Nodal* was found to be up-regulated, while its inhibitor *INHBB* was down-regulated (Figure 10). These findings collectively indicate that overactivation of the Wnt/ β -catenin signaling pathway leads to positive regulation of both BMP and Nodal signaling pathways, further influencing the specification of cell fates and embryonic patterning in amphioxus.

The Wnt/ β -catenin and Notch signaling pathways play crucial roles in controlling mesoderm specification from the early mesendoderm in amphioxus, and Notch signaling was suggested to regulate Wnt/ β -catenin signaling during gastrulation (Onai, 2019). Under Azkp treatment at the N2 stage, *Delta* and *Fringe* were up-regulated, as well as the downstream gene *Hey1*. This suggests a positive regulatory effect of Azkp treatment on Notch signaling at N2 stage. However, gene expression of *Hey1* was not found in G3 and G5 stage under Azkp treatment, indicating a prolong up-regulation of *Hey1*. Further effect of Wnt/ β -catenin signaling overactivation to Notch signaling pathway and *Hey1* during gastrulation was needed to complete the relationship between two signaling pathway.

FGF signaling is necessary during amphioxus gastrulation, and it also forms the most anterior somites through the MAPK pathway (Bertrand et al., 2011). In my research, three FGF receptors *FGFR3*, *FLT1* and *MET* were up-regulated following Azkp treatment.

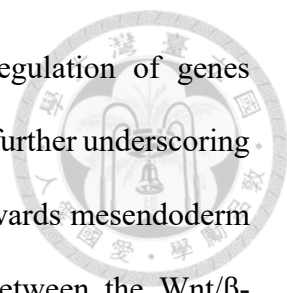


However, five ligands, three receptor genes and the downstream gene *Elk1* were all down-regulated (Figure 9). This pattern indicates a negative regulatory effect of Azkp treatment on FGF signaling. The observed negative regulation of FGF signaling by Azkp treatment could impact the gastrulation process in amphioxus embryos, potentially leading to a failure in proper invagination.

For gene expression in Wnt/ β -catenin signaling, Wnt ligands *Wnt1*, *Wnt3*, *Wnt6*, and *Wnt7b* were down-regulated, whereas *Wnt8* was the only ligand observed to be up-regulated. Additionally, most Wnt inhibitors, including *Cerberus*, *Notum*, *sFRP2*, and *Dkk1* were up-regulated, with *Dkk3* being the sole inhibitor to be down-regulated. In terms of receptors, *Fz1/2/7* and *Fz4* were up-regulated, whereas *Fz5/8* showed a down-regulation. Furthermore, downstream components of the pathway, such as *Dvl*, *APC*, β -*catenin*, and *Tcf* were uniformly up-regulated (Figure 12). The down-regulation of Wnt ligands and up-regulation of inhibitors indicating there is a negative feedback loop of Wnt signaling.

In conclusion, the global activation of the Wnt/ β -catenin signaling pathway impacts germ layer determination in amphioxus embryos, characterized by the down-regulation of ectoderm marker genes and the up-regulation of endoderm and mesoderm marker genes. This shift leads to the loss of ectodermal tissue and the expansion of mesodermal and endodermal tissues. However, the observation of inconsistent gene expression among endoderm and mesoderm marker genes indicates the complexity role of Wnt/ β -catenin signaling role in germ layer specification, further investigation of short-term overactivation effects is necessary to elucidate the underlying regulatory mechanisms.

The overactivation of the Wnt/ β -catenin signaling pathway also affects the expression of genes across multiple signaling pathways, including BMP, Notch, Nodal, Wnt, and FGF signaling pathway, highlighting its extensive influence on embryonic



development. Moreover, this overactivation leads to the down-regulation of genes associated with ectoderm-derived tissues, such as cilium and neuron, further underscoring the pivotal role of signaling in directing embryonic development towards mesendoderm specification in *B. floridae*. Investigating the mutual inhibition between the Wnt/ β -catenin signaling pathway and other signaling pathways could give us more information on germ layer determination during amphioxus embryo development

The findings from this study reveal the critical regulatory function of Wnt/ β -catenin signaling pathway in germ layer determination, driving the embryo towards mesendoderm. This comprehensive impact underscores the need for additional research to fully understand the mechanisms and effects of the Wnt/ β -catenin signaling pathway on embryonic development.

Figures

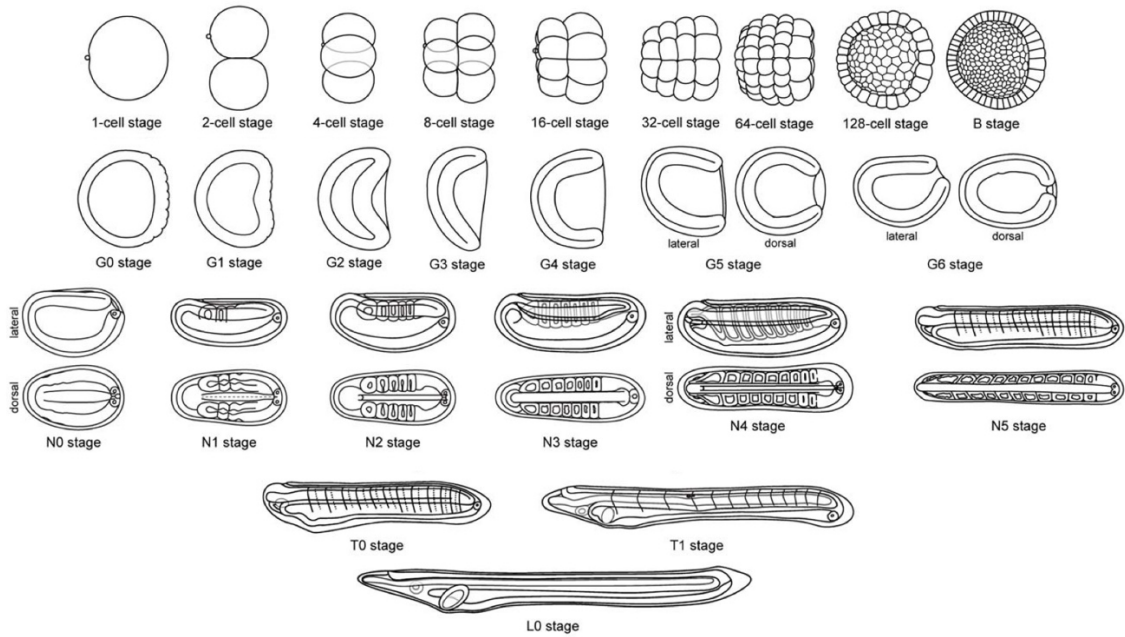


Figure 1. Development stages of amphioxus.

Schematic overview of *Branchiostoma lanceolatum* development, illustrating stages from the 1-cell phase to the L0 stage. The embryos are shown in lateral views, with animal pole and anterior pole to the left, and dorsal side oriented upwards. Adapted from Carvalho's drawings (Carvalho et al., 2021).

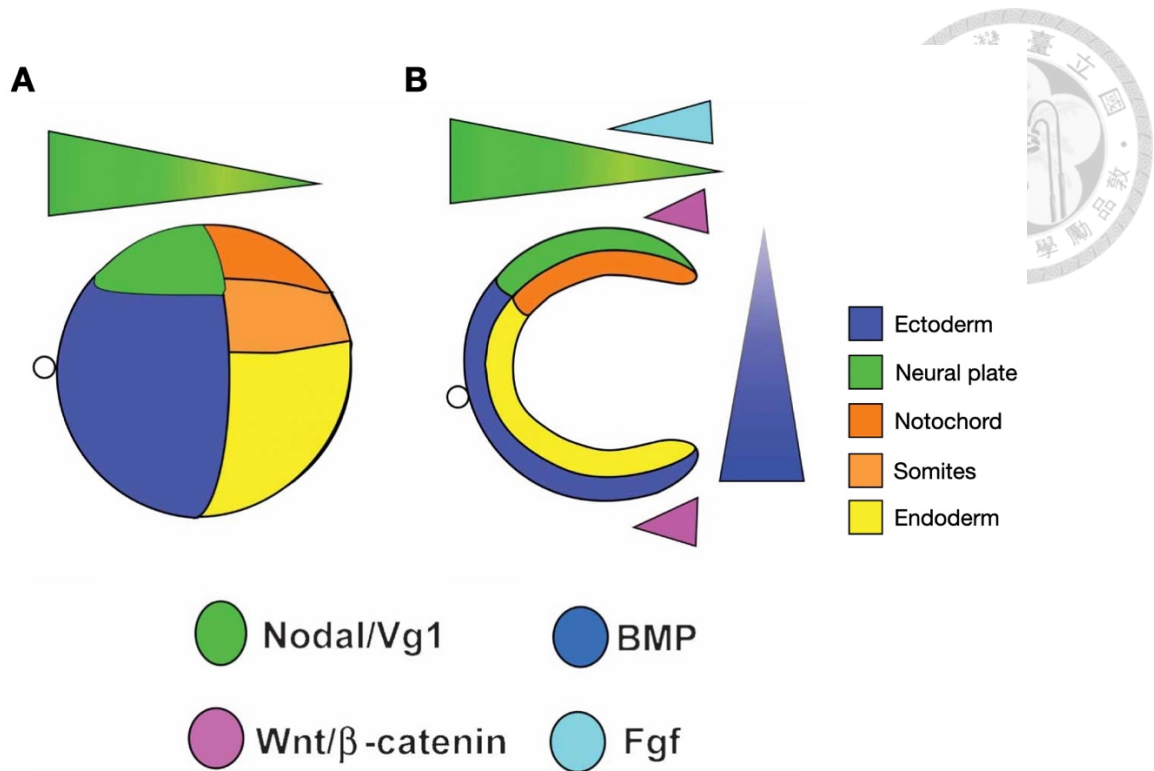


Figure 2. Diagram of gradients of four major signaling pathways (Nodal/Vg1, BMPs, Wnt/ β -catenin, and FGFs) in early amphioxus embryos.

(A) Nodal signaling is high in the animal hemisphere in eggs just after fertilization. BMPs, FGFs, and Wnt/ β -catenin signaling through β -catenin are not expressed in fertilized eggs or cleavage stages. (B) By the mid-gastrula, Nodal/Vg1 signaling is high dorsally and anteriorly, while BMP signaling is highest dorsally and posteriorly, while Wnt/ β -catenin signaling is highest posteriorly. Adapted from Holland's drawings (Holland & Onai, 2012).

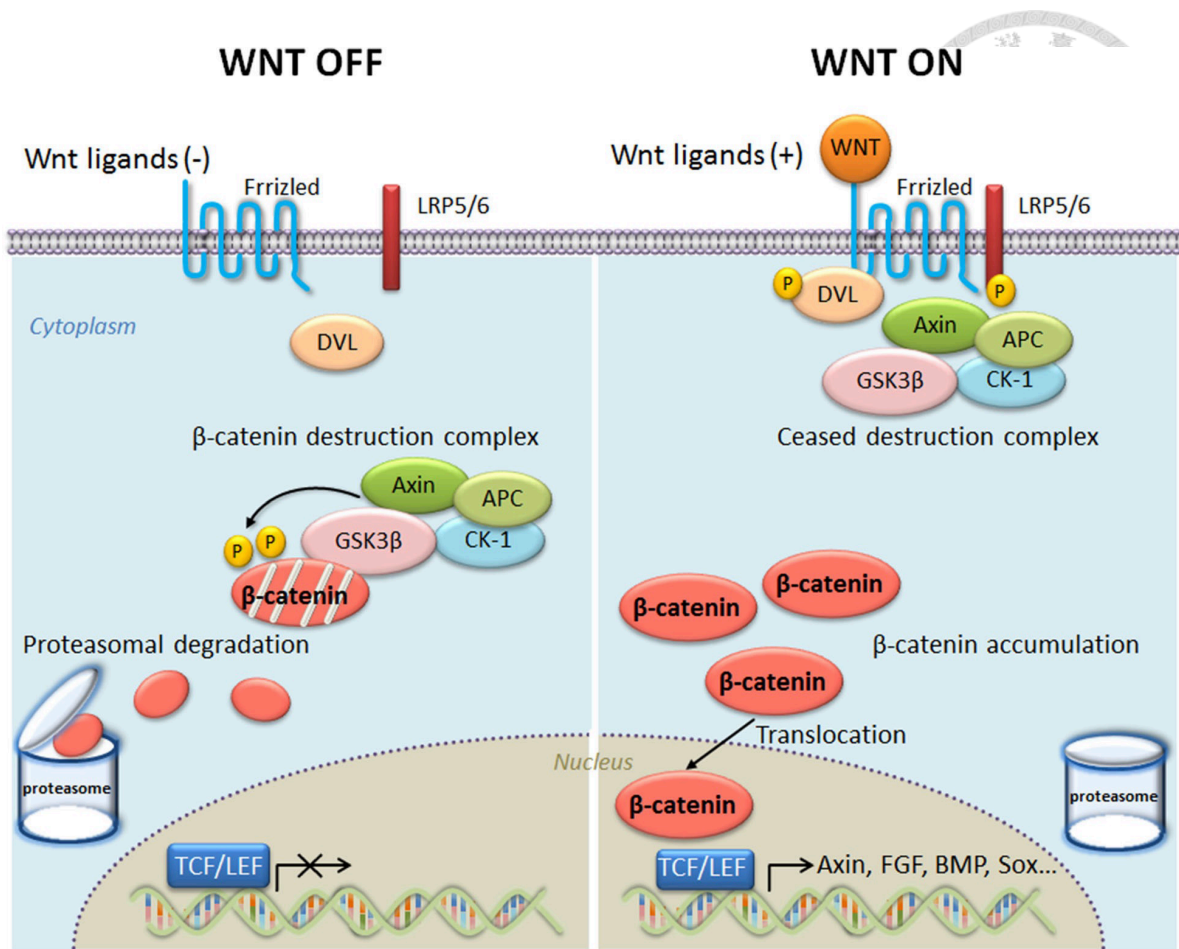


Figure 3. Overview of Wnt/ β -catenin signaling pathway (Ota et al., 2016).

Overview of the WNT/ β -catenin Signaling Mechanism. In the quiescent state, characterized as 'WNT OFF', the destruction complex targets cytosolic β -catenin for phosphorylation. This post-translational modification renders β -catenin recognizable for subsequent degradation via proteasomes. In contrast, under 'WNT ON' conditions with Wnt ligands, signaling leads to the inhibition of the destruction complex's ability to phosphorylate β -catenin in the cytosol. Consequently, unphosphorylated β -catenin accumulates, translocates into the nucleus, and subsequently activates transcription of Wnt-responsive genes, including those regulated by the TCF/LEF1 family of transcription factors.

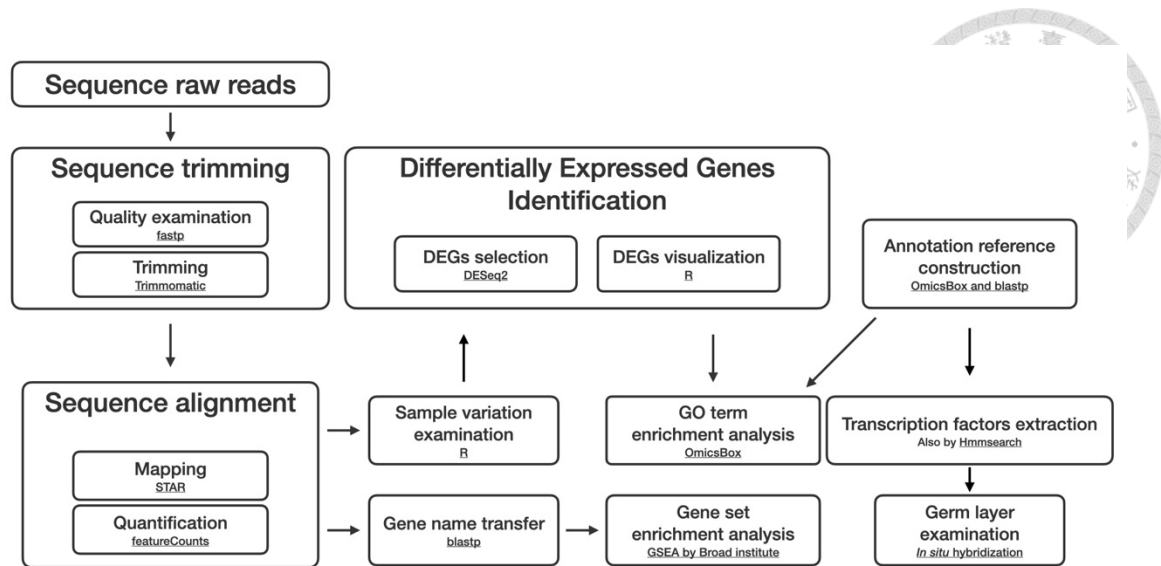


Figure 4. Process of RNA-seq analysis.

The tools utilized at each step are underlined for clarity. Initially, sequence quality was assessed using fastp, and primer trimming was executed with Trimmomatic. Subsequent alignment to the *B. floridae* genome was performed using STAR, and quantification of alignment result was carried out by featureCounts. Gene names were then mapped to *H. sapiens* using bidirectional blast via blastp, which facilitated gene set enrichment analysis. Prior to identifying differentially expressed genes, an initial examination of differences between samples was conducted. These differentially expressed genes were then selected for GO term enrichment analysis, employing the annotation reference constructed by OmicsBox and the blast results. Transcription factors in *B. floridae* were identified based on the annotation reference and Hmmssearch. Finally, transcription factors in each germ layer were selected to examine the impact of Azkp treatment on amphioxus.

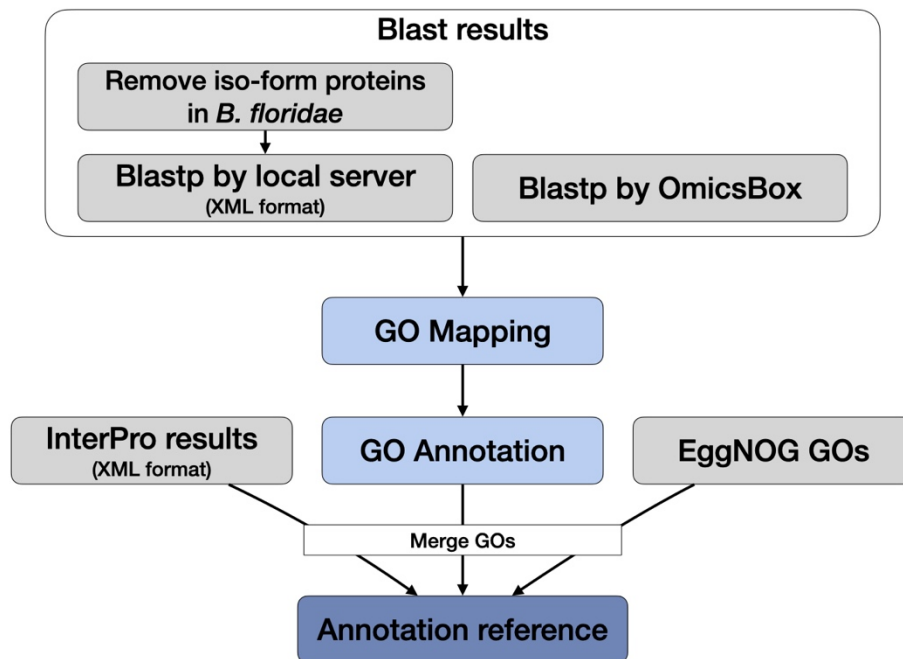


Figure 5. Pipeline of constructing GO annotation reference.

The blast results were generated using either a local server or OmicsBox's integrated blast function. GO mapping and GO annotation were executed in OmicsBox to obtain annotation information. GO terms from EggNOG and InterProScan were amalgamated into OmicsBox, enhancing the annotation reference. A comprehensive reference was established by merging GO terms.

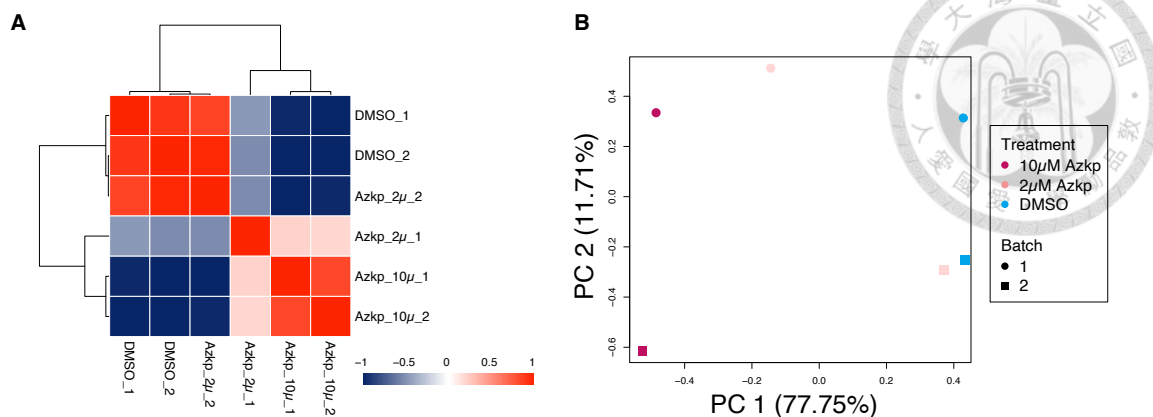


Figure 6. Distinct impacts of Azkp treatments on the samples

(A) Sample correlation heatmap. One sample from the 2 μ l Azkp treatment group exhibits a similarity to the control samples. The heatmap illustrates the similarities between samples, with higher numerical values indicating greater similarity and lower values denoting fewer similarity. Sample names are displayed along the bottom and right axes. Euclidean distances and Ward's minimum variance method were used to define clusters in heatmap. (B) Consistent with the findings from the sample correlation heatmap, one sample in the 2 μ l Azkp treatment demonstrates similarity to the control samples. The shapes represent different batches, while the colors denote various treatments.

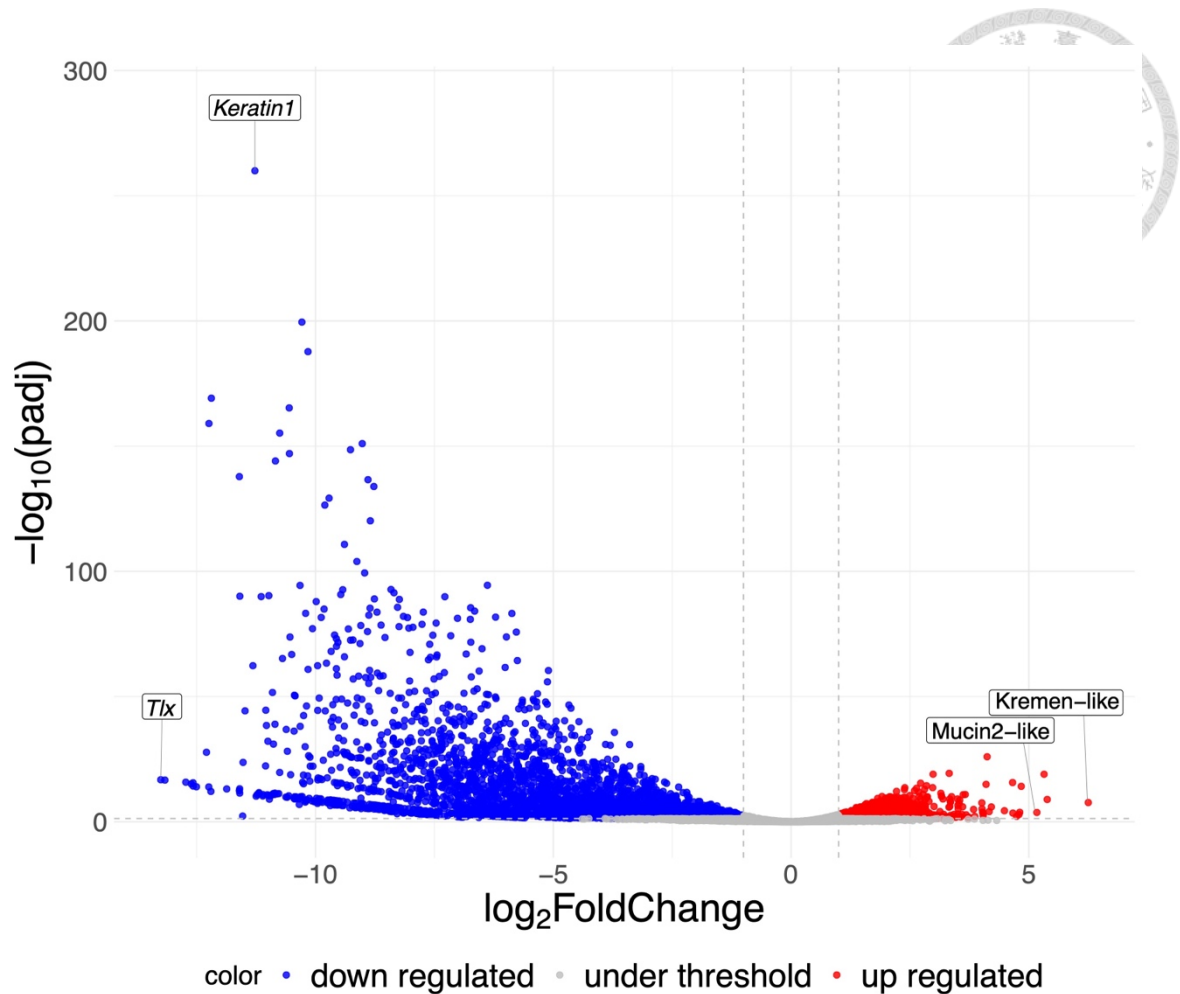


Figure 7. DEGs after Azkp treatment.

Each point represents a gene. DEG threshold: adjusted p-value < 0.05 and fold change >2. X-axis shows the \log_2 fold change, Y-axis shows the $-\log_{10}$ adjusted p-value. Vertical gray dotted lines represent the absolute value of 1 and the horizontal gray dotted line represents an adjusted p-value of 0.05. Fold change and adjusted p-value were calculated by comparing the 10 μ M Azkp treatment to the DMSO treatment. Red dots represent genes that were significantly up-regulated after 10 μ M Azkp treatment. Blue dots represent genes that were significantly down-regulated after 10 μ M Azkp treatment. Grey dots represent genes below the threshold.

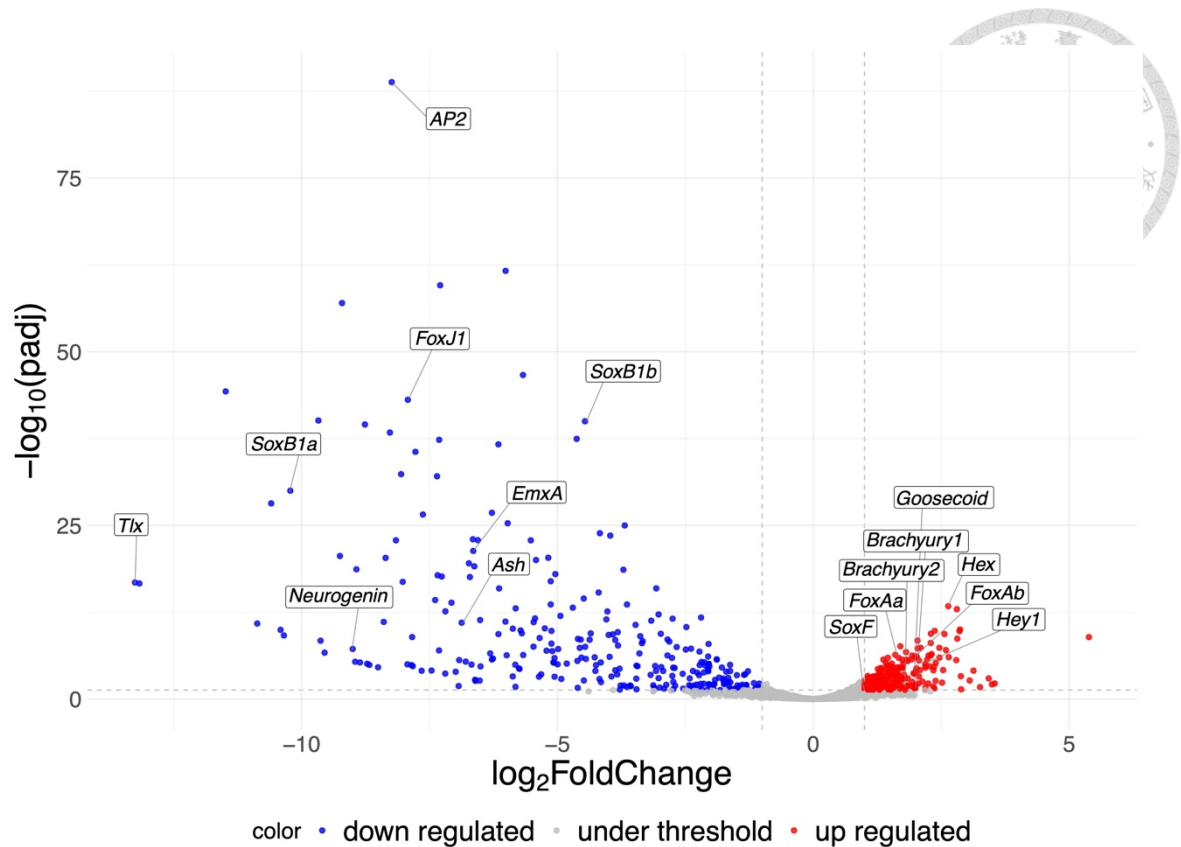


Figure 8. Transcription factors in DEGs.

Each point represents a gene. X-axis shows the log₂ fold change, Y-axis shows -log₁₀ adjusted p-value. Vertical gray dotted lines represent absolute value of 1 and horizontal gray dotted line represents adjusted p-value of 0.05. Fold change and adjusted p-value were calculated by comparing the 10μM Azkp treatment to the DMSO treatment. Red dots represent genes that have been significantly up-regulated after 10μM Azkp treatment. Blue dots represent genes that have been significantly down-regulated after 10μM Azkp treatment. Selected transcription factor genes representing known germ layer markers were highlighted among DEGs. Grey dots represent genes under threshold.

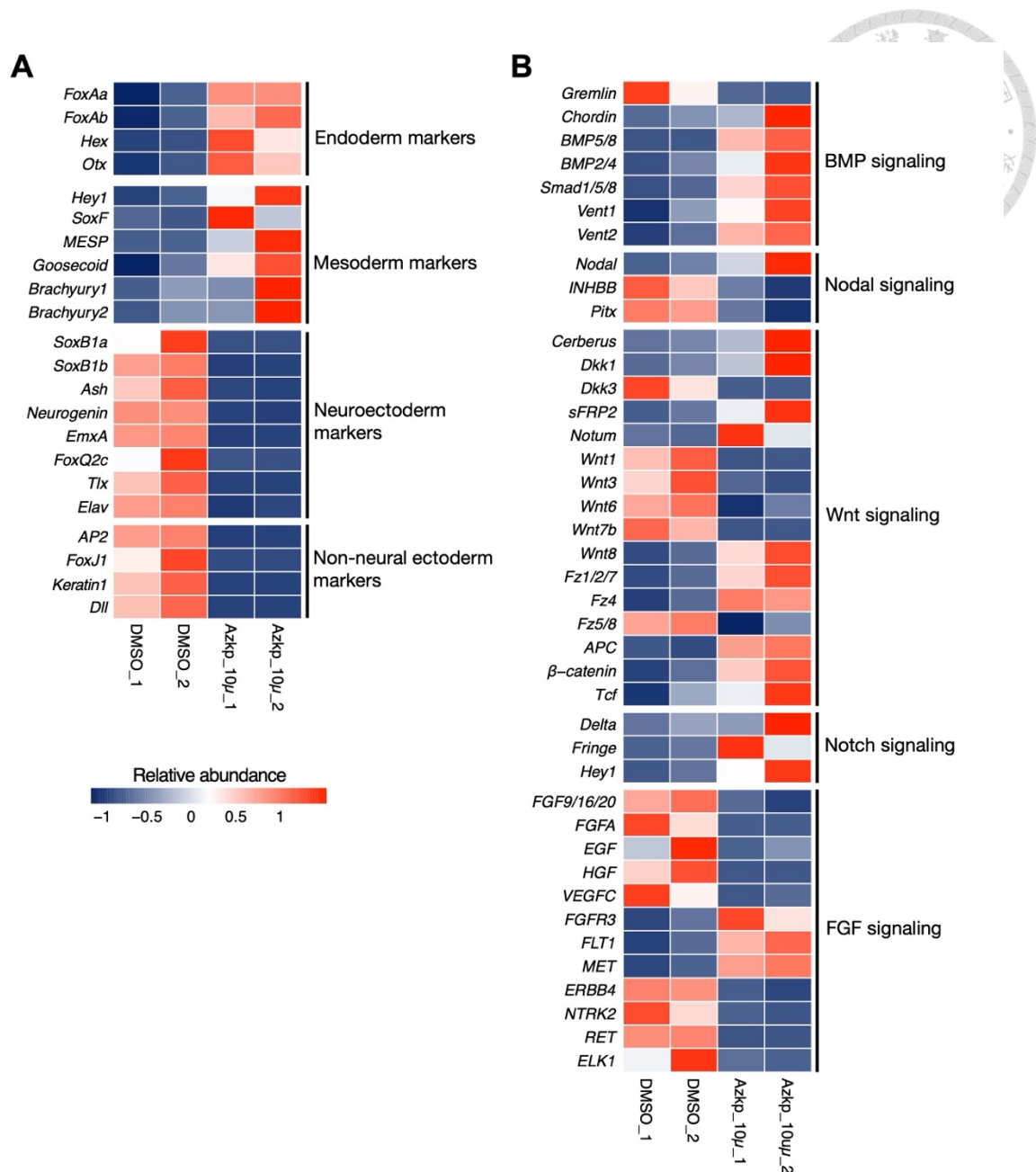


Figure 9. Heatmap of selected genes in DEGs.

(A) Germ layer marker genes have been selected and are labeled with their corresponding germ layers (B) Selected genes are aligned with their respective pathways on the right side. The horizontal axis represents gene names, while the vertical axis represents sample names. Gene expression values for each sample have been normalized to a mean of 0 and a standard deviation of 1. Up-regulated gene expression is depicted in red, whereas down-regulated expression is denoted by blue.

BMP signaling pathway map

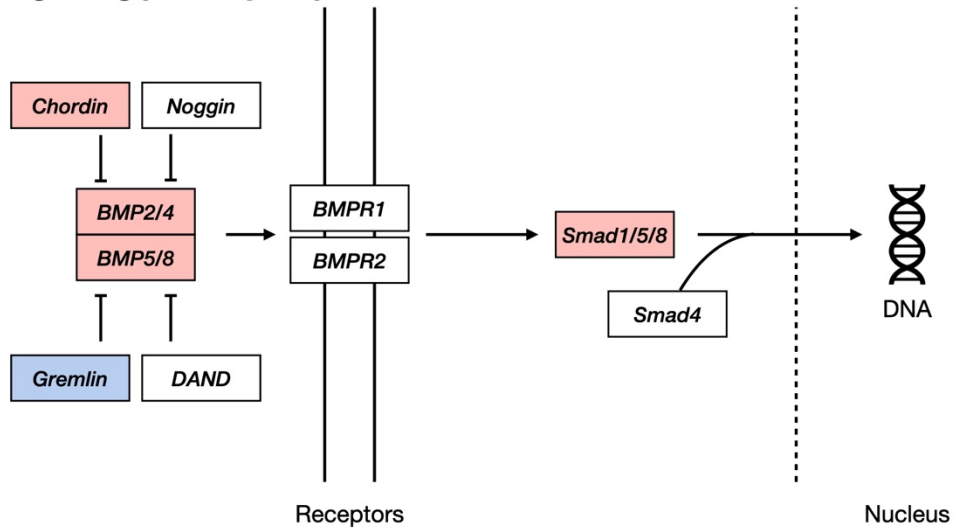


Figure 10. BMP signaling pathway map.

Each block represents a gene. The figure was sourced and modified from the KEGG database. DEGs are marked, up-regulated genes are depicted in red, while down-regulated genes are denoted in blue.

Nodal signaling pathway map

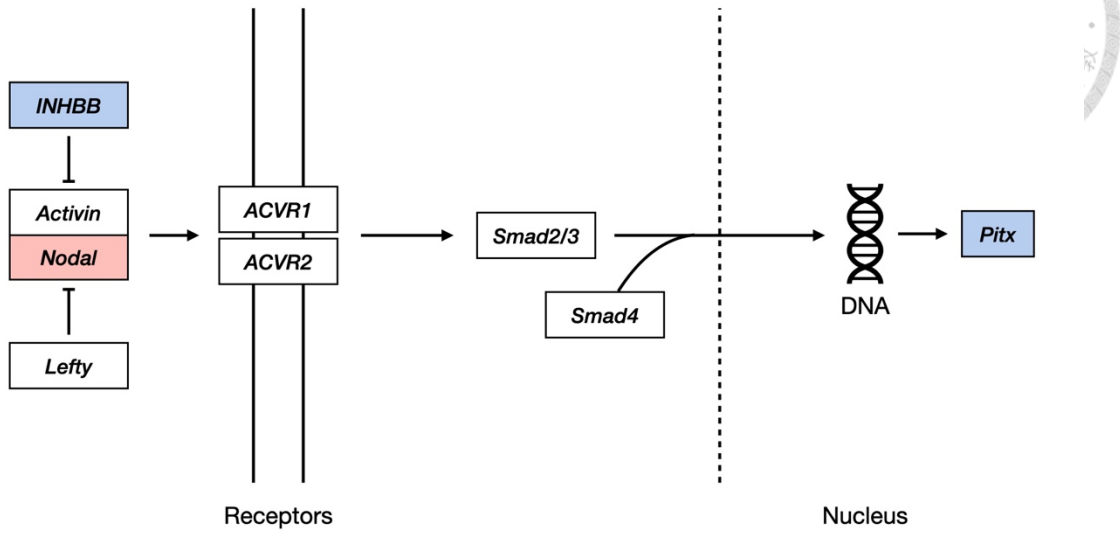


Figure 11. Nodal signaling pathway map.

Each block represents a gene. The figure was sourced and modified from the KEGG database. DEGs are marked, up-regulated genes are depicted in red, while down-regulated genes are denoted in blue.

Notch signaling pathway map

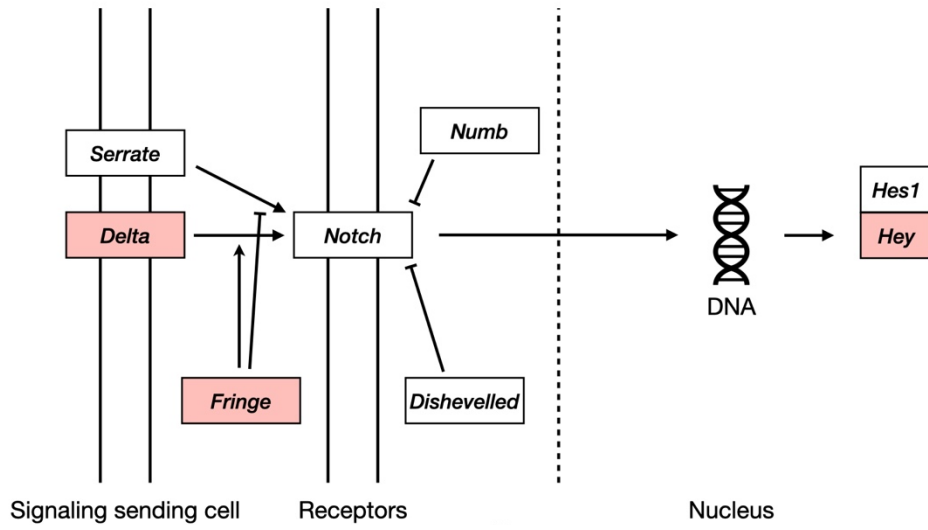


Figure 12. Notch signaling pathway map.

Each block represents a gene. The figure was sourced and modified from the KEGG database. DEGs are marked, up-regulated genes are depicted in red, while down-regulated genes are denoted in blue.

Wnt/ β -catenin signaling pathway map

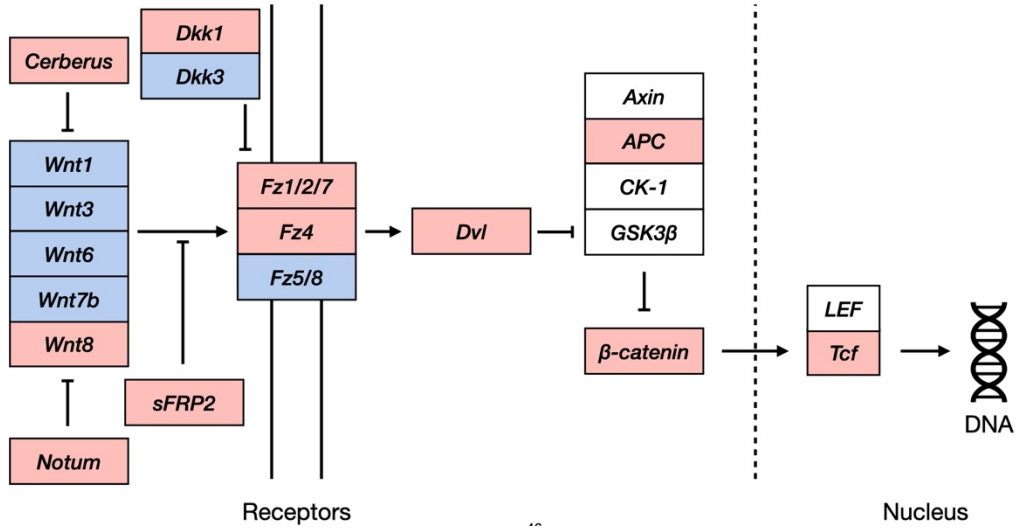


Figure 13. Wnt/ β -catenin signaling pathway map.

Each block represents a gene. The figure was sourced and modified from the KEGG database. DEGs are marked, up-regulated genes are depicted in red, while down-regulated genes are denoted in blue.

Fibroblast growth factor signaling pathway (MAPK)

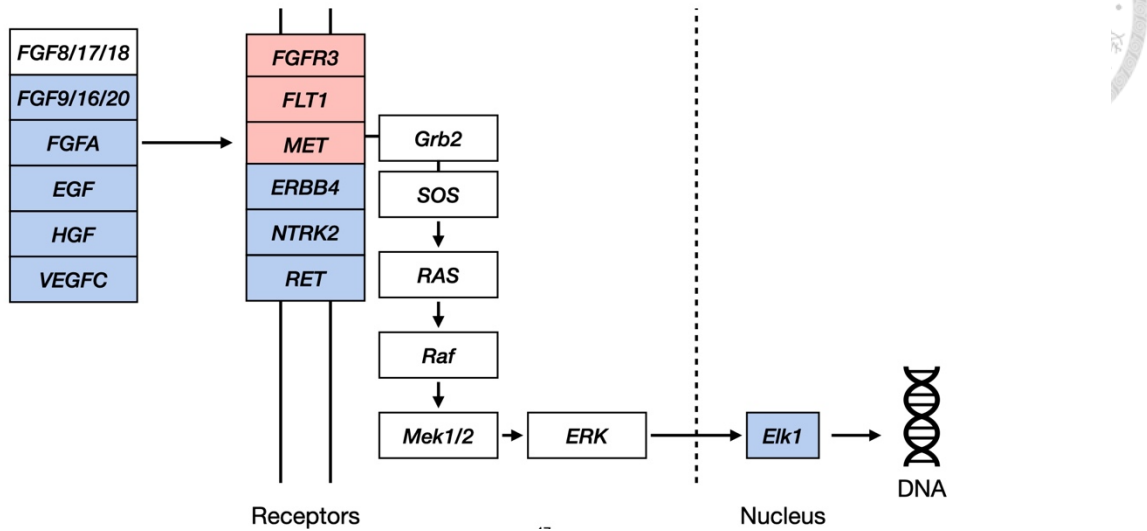


Figure 14. Fibroblast growth factor signaling pathway map (MAPK signaling).

Each block represents a gene. The figure was sourced and modified from the KEGG database. DEGs are marked, up-regulated genes are depicted in red, while down-regulated genes are denoted in blue.

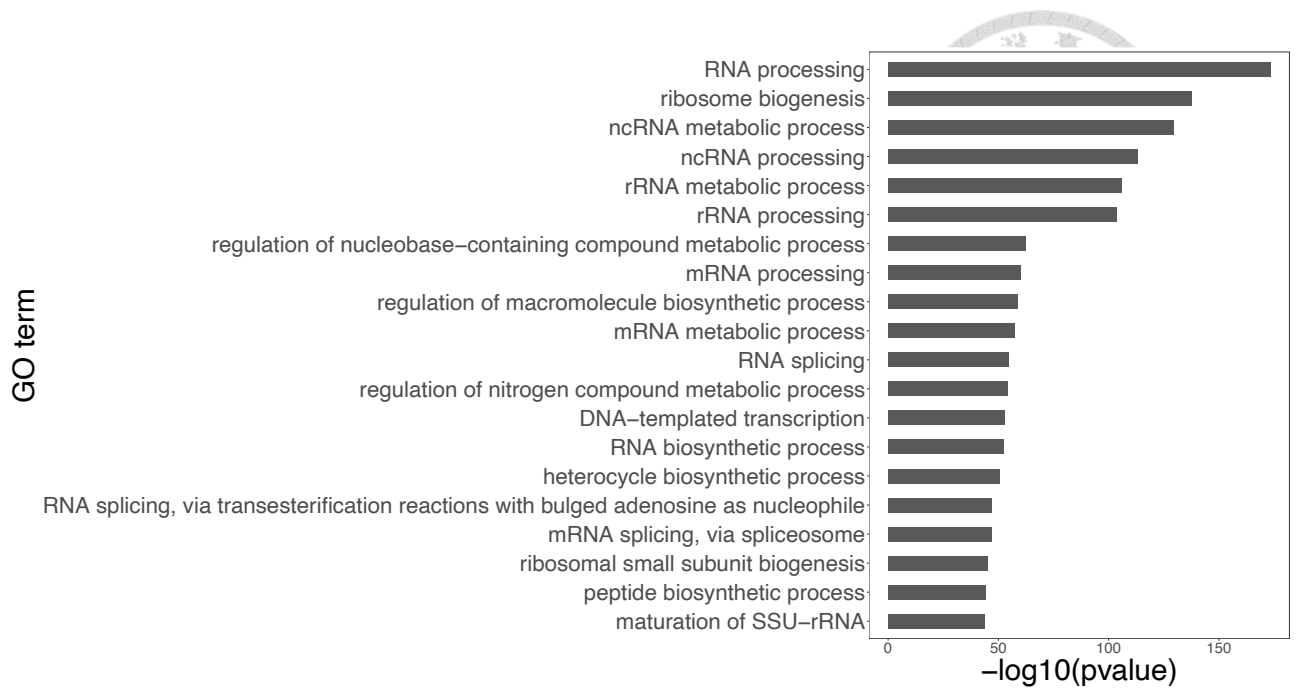


Figure 15. Top 20 significant GO terms in biological process in up-regulated DEGs. X-axis shows the $-\log_{10} p$ -values for the corresponding GO terms, Y-axis shows the name of the GO terms.

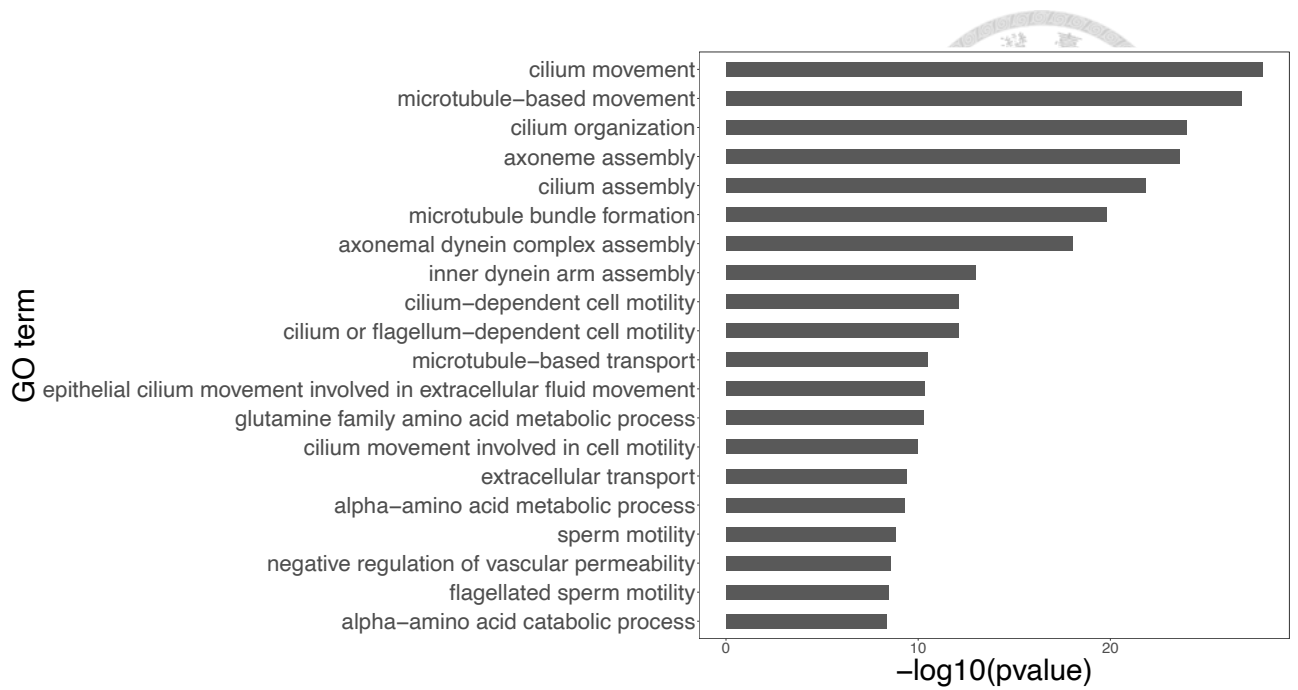


Figure 16. Top 20 significant GO terms in biological process in down-regulated DEGs.

X-axis shows the $-\log_{10} p$ -values for the corresponding GO terms, Y-axis shows the name of the GO terms.

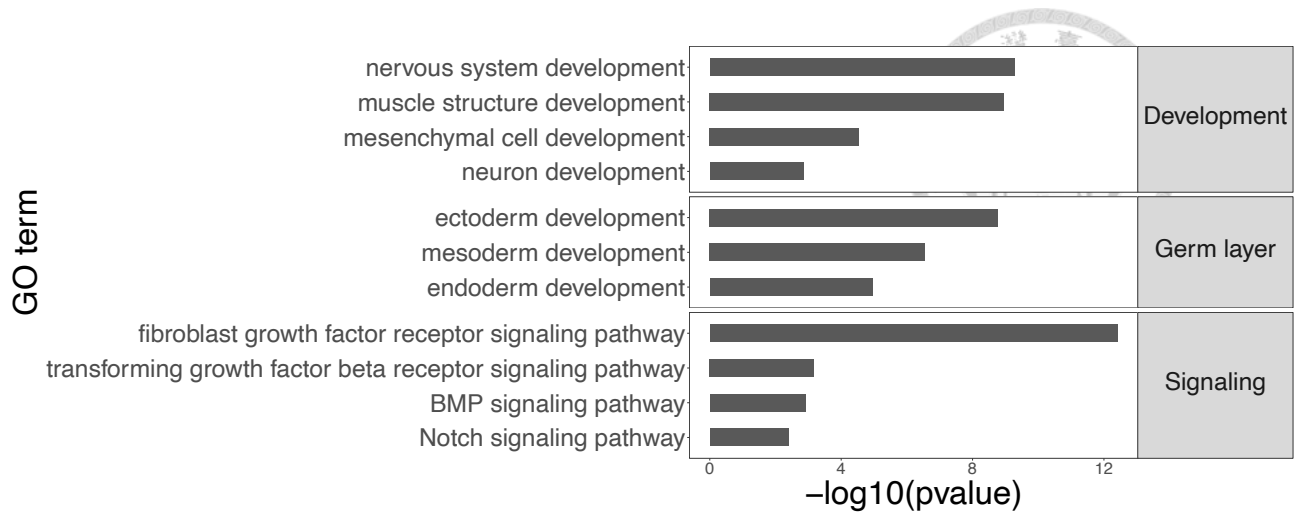


Figure 17. Selected GO terms in biological process related to germ layer development in up-regulated DEGs.

X-axis shows the $-\log_{10} p$ -values for the corresponding GO terms, Y-axis shows the name of the GO terms. Tags on the right represent key words used to select the terms.

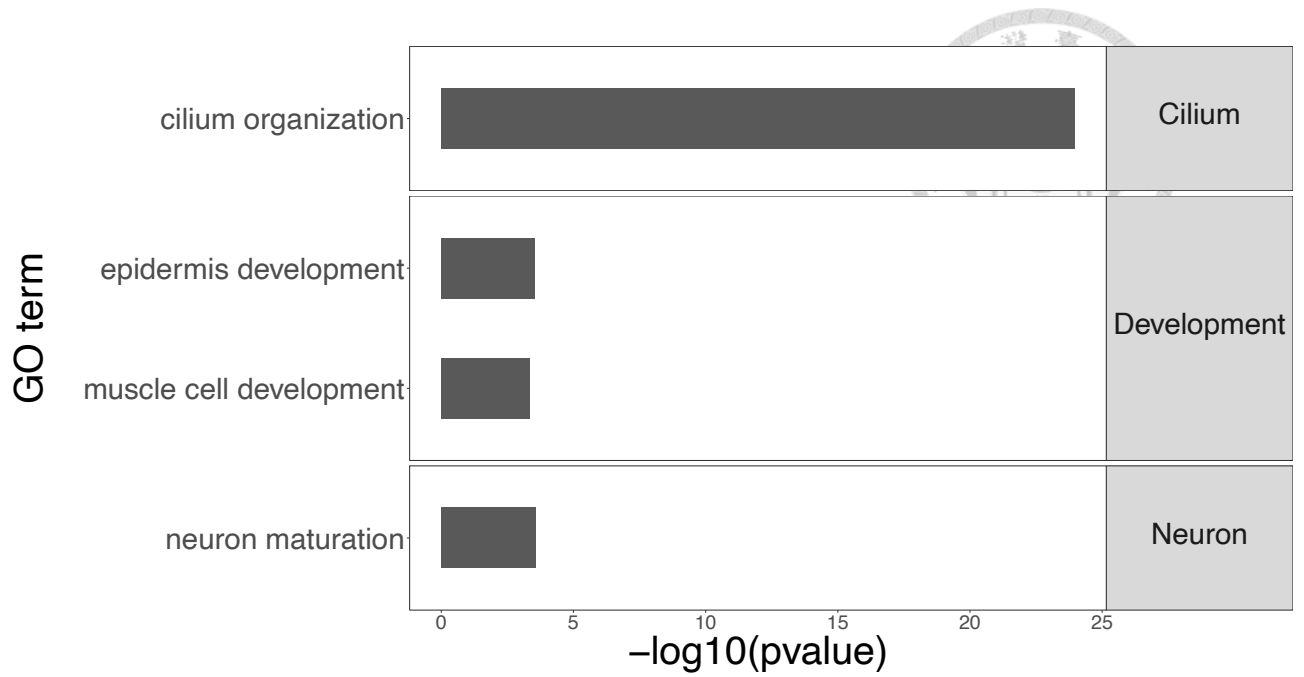


Figure 18. Selected GO terms in biological process related to germ layer development in down-regulated DEGs.

X-axis shows the $-\log_{10} p$ -values for the corresponding GO terms, Y-axis shows the name of the GO terms. Tags on the right represent key words used to selected the terms.

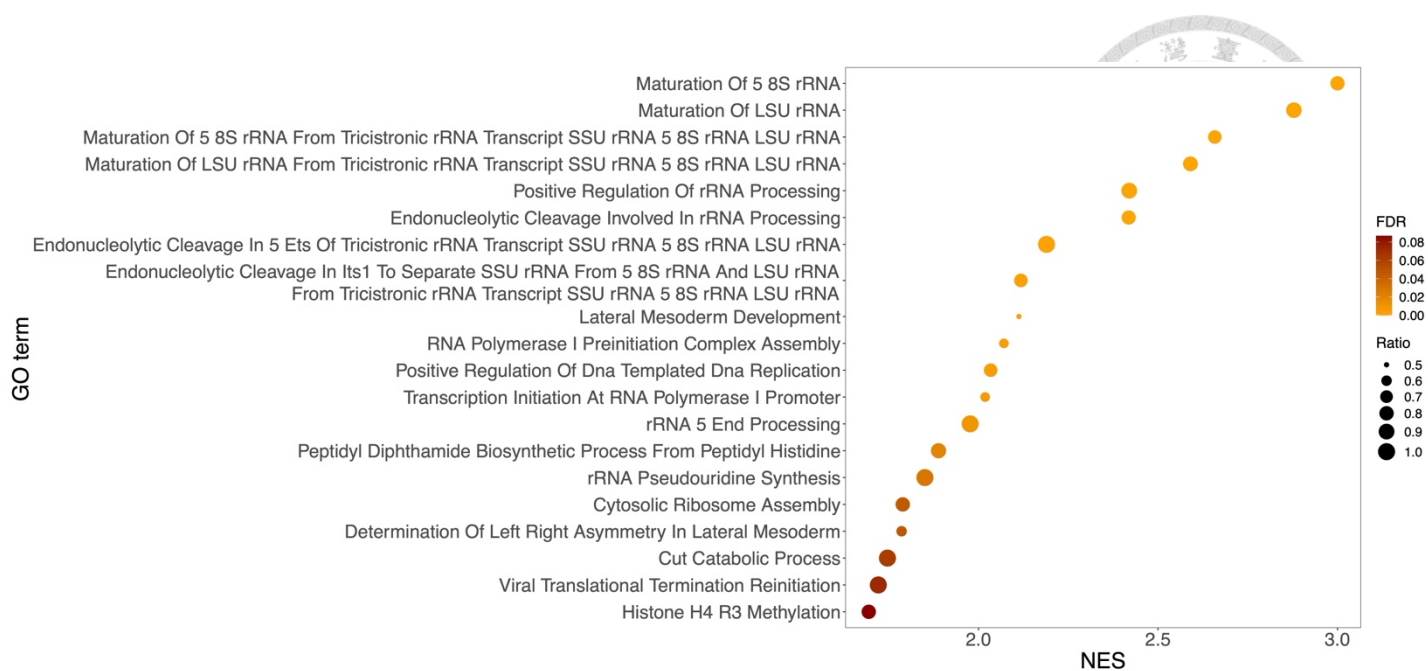


Figure 19. Top 20 GO terms in biological process in up-regulated gene sets by normalized enrichment score (NES).

X-axis represents the NES; Y-axis represents GO term. The dot color corresponds to false discovery rate for the respective GO terms. Size of dots indicate the ratio of genes enriched in the pathway to the gene set

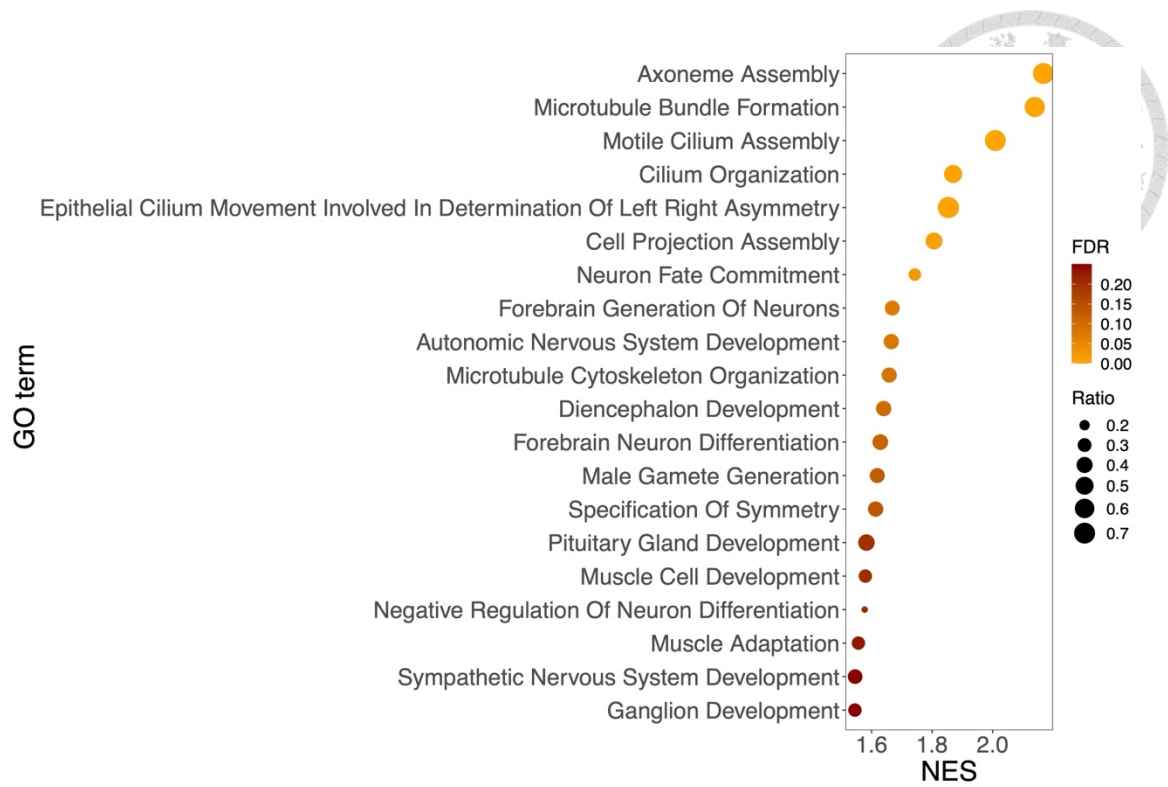


Figure 20. Top 20 GO terms in biological process enriched in down-regulated gene sets by normalized enrichment score (NES).

X-axis represents the NES; Y-axis represents GO term. The dot color indicates false discovery rate for the corresponding GO terms. Size of dots indicate the ratio of genes enriched in the pathway compared to the gene set

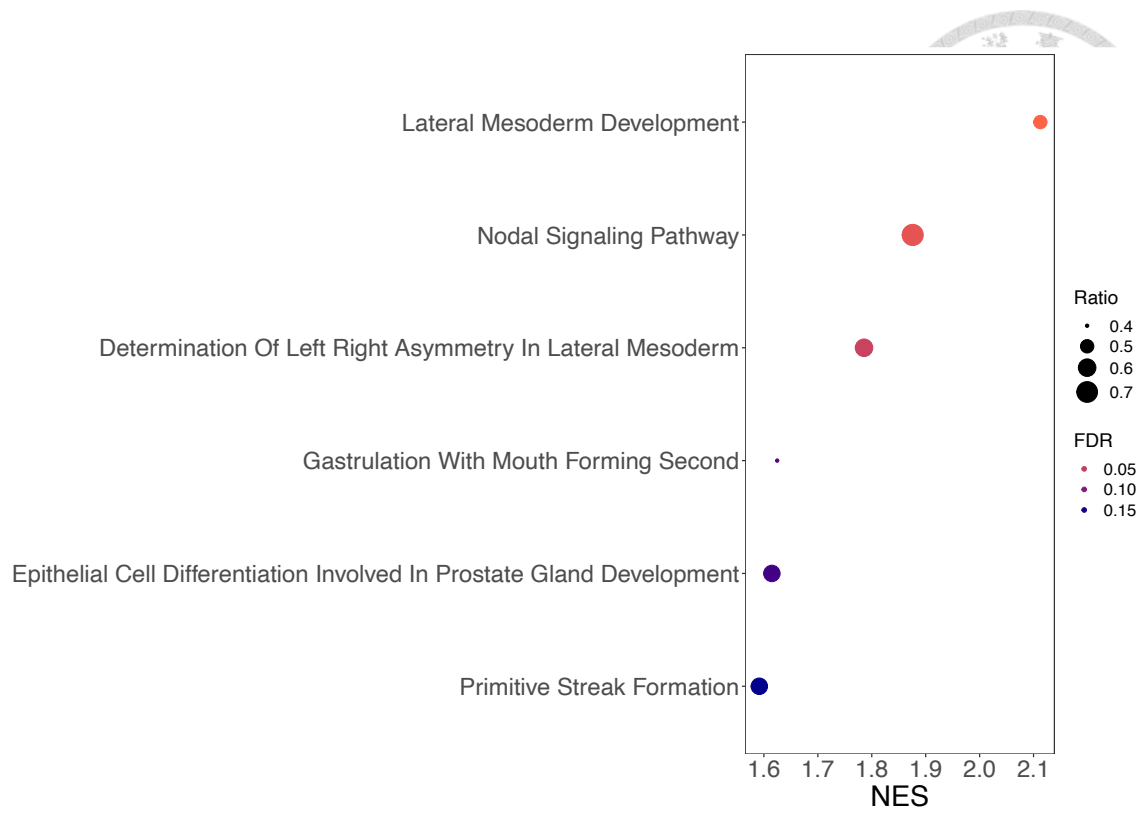


Figure 21. GO terms related to germ layer development in biological process in up-regulated genes by normalized enrichment score (NES).

X-axis represents the NES; Y-axis represents GO term. The dot color indicates false discovery rate for the corresponding GO terms. Size of dots indicate the ratio of genes enriched in the pathway compared to the gene set. Tags on the right represent key words used to select the terms.

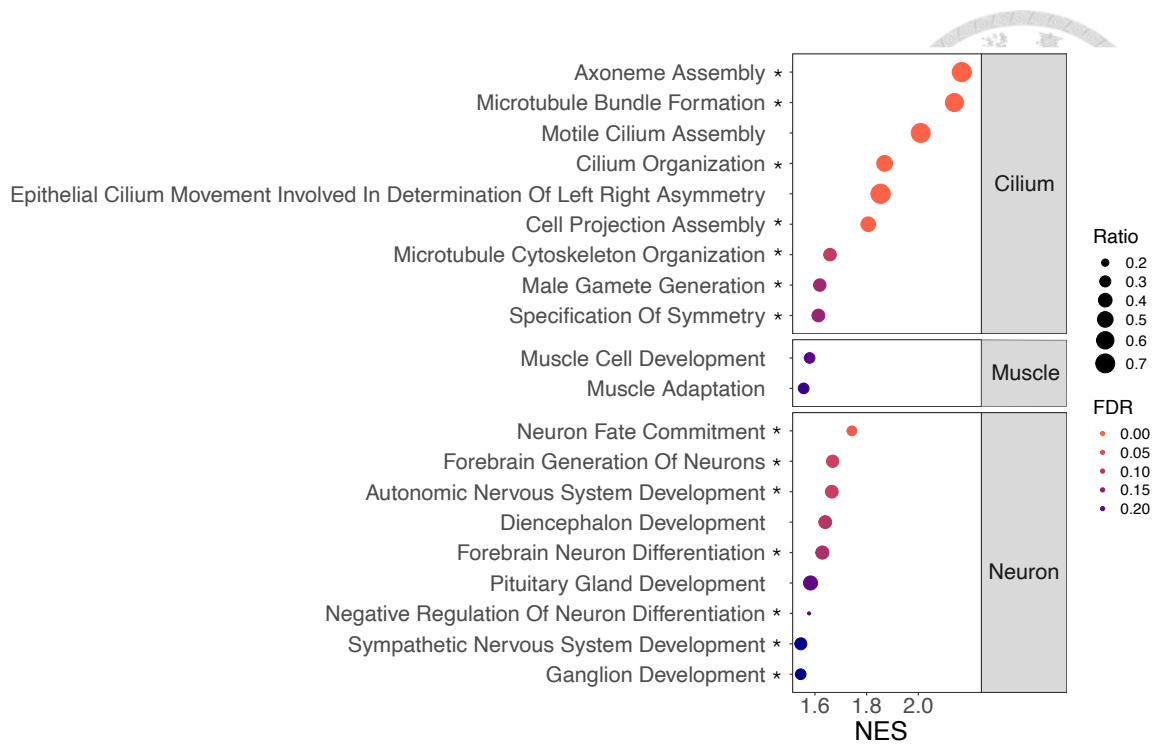


Figure 22. GO terms related to germ layer development in biological process in down-regulated gene sets by normalized enrichment score (NES).

X-axis represents the NES; Y-axis represents GO term. The dot color indicates false discovery rate (FDR) for the corresponding GO terms. Size of dots indicate the ratio of genes enriched in the pathway compared to the gene set. Cilium related terms involving *FoxJ1* and neuron related terms involving *Ash* were marked with star sign at the end of the term.

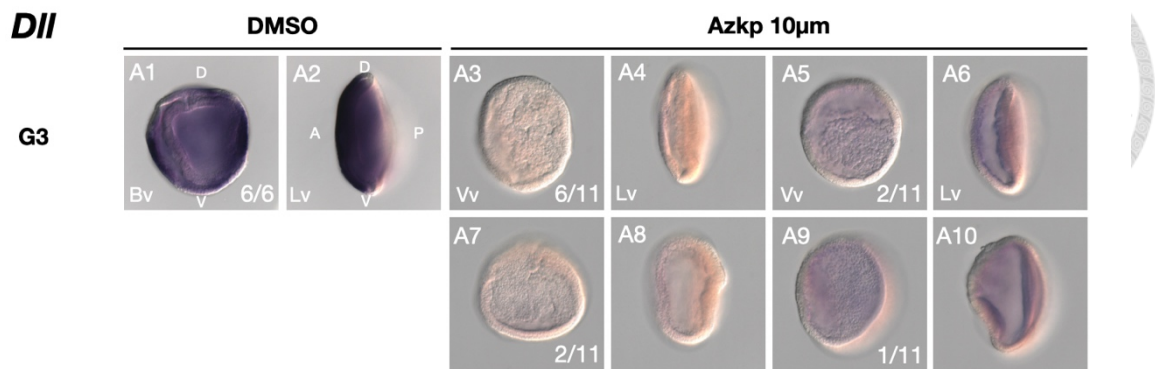


Figure 23. *Dll* expression at G3 stage in DMSO and Azkp treated embryos.

Whether embryos went through gastrulation did not influence the gene expression. In embryos treated with Azkp, two distinct phenotypes were observed: the upper two embryos successfully underwent gastrulation, while the lower two failed to do so. Phenotypic variation did not appear to have an impact on gene expression. The purple sites on the embryos indicate the presence of gene expression, while the transparent areas represent the absence of gene expression. The numbers on the bottom right corner of each embryos represent the counts of embryos exhibiting each respective phenotype. D: dorsal, V: ventral, A: anterior, P: posterior, Bv: blastopore view, Lv: lateral view, Vv: vegetal view.

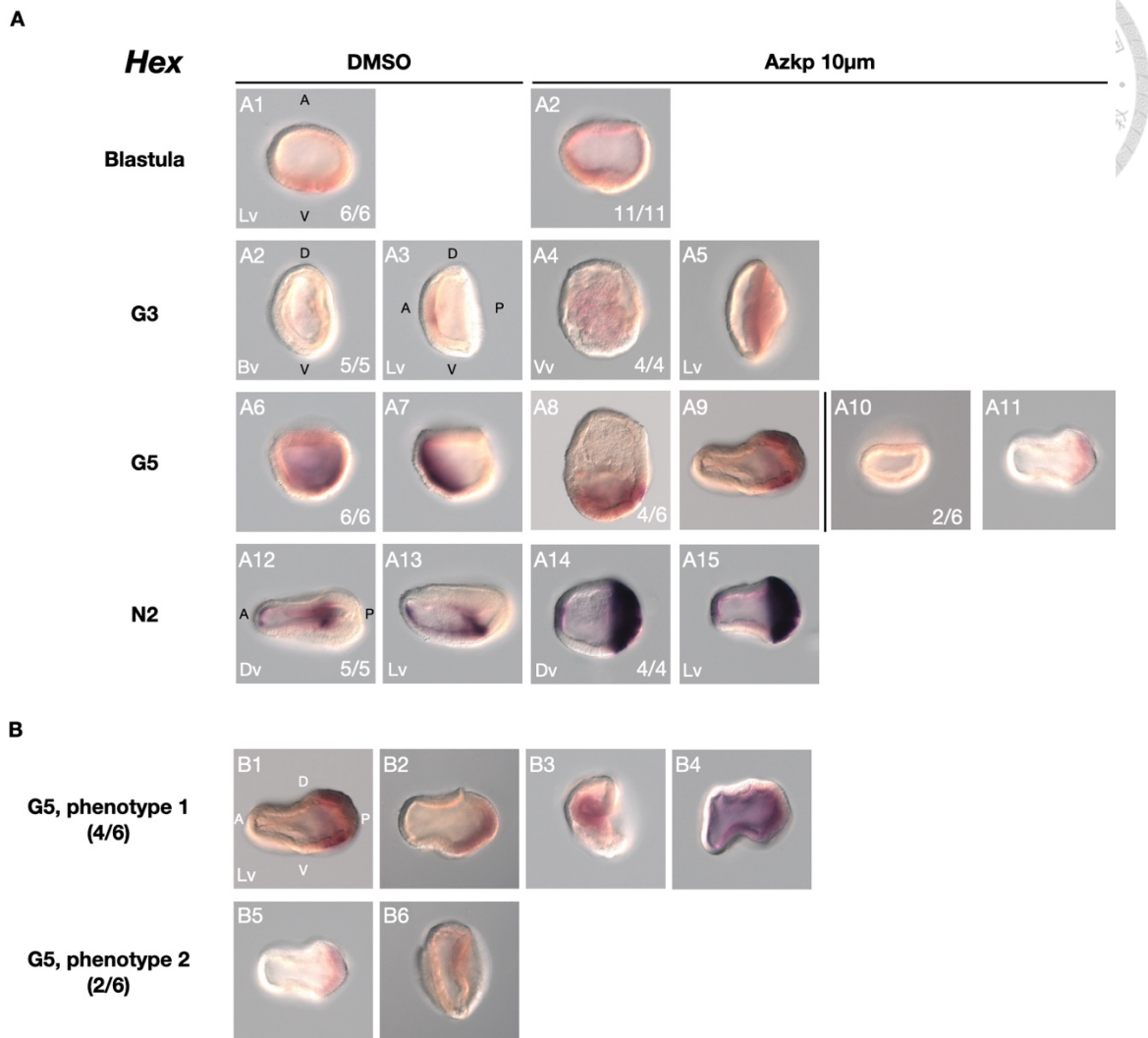
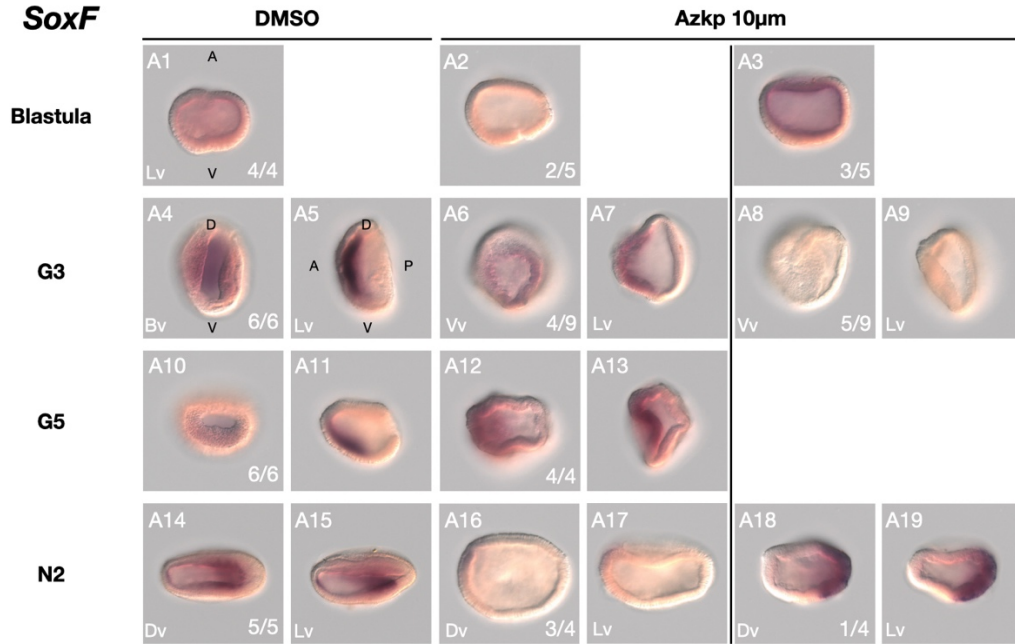


Figure 24. *Hex* expression at the blastula, G3, G5 and N2 stages in DMSO and Azkp-treated embryos.

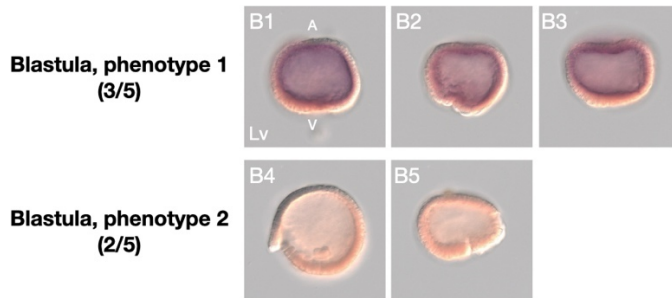
(A) *Hex* expression at blastula, G3, G5 and N2 stage in DMSO and Azkp-treated embryos. (B) *Hex* expression of all Azkp-treated embryos at G5 stage. The Azkp-treated embryos received continuous treatment from the one-cell stage. The purple sites on the embryos indicate the presence of gene expression, while the transparent areas represent the absence of gene expression. The developmental stages are on the left side of each row, and the treatments are on the top. In Azkp-treated embryos, different phenotypes are displayed when present. The numbers in the bottom right corner of each embryo indicate the count of embryos exhibiting each respective phenotype. In blastula stage, A: animal, V: vegetal. In G3, G5 and N2 stage, D: dorsal, V: ventral, A: anterior, P: posterior, Bv: blastopore view, Lv: lateral view, Vv: vegetal view.

A

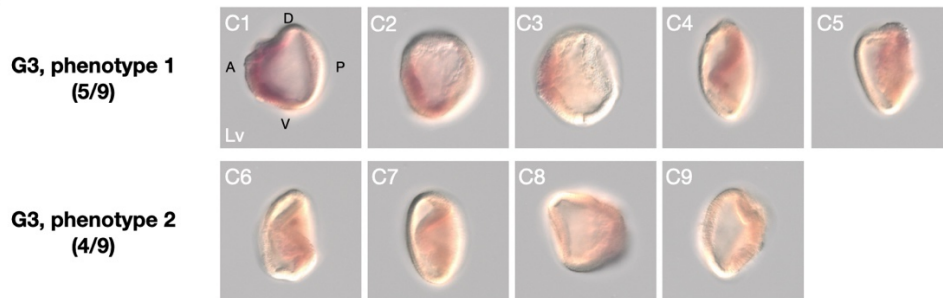
SoxF



B



C



D

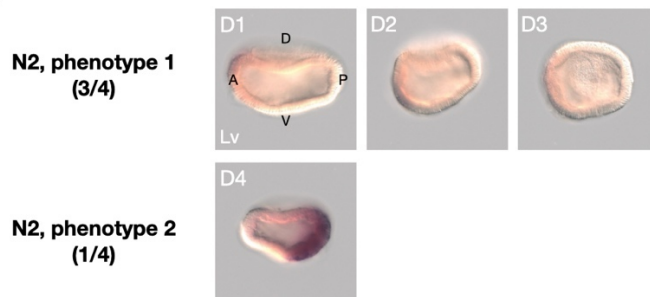


Figure 25. *SoxF* expression at the blastula, G3, G5 and N2 stage in DMSO and Azkp-treated embryos.

(A) *SoxF* expression at blastula, G3, G5 and N2 stage in DMSO and Azkp-treated embryos. (B) *SoxF* expression of all Azkp-treated embryos at blastula, (C) G3, and (D) N2 stage. The Azkp-treated embryos received continuous treatment from the one-cell stage. The purple sites on the embryos indicate the presence of gene expression, while the transparent areas represent the absence of gene expression. The developmental stages are on the left side of each row, and the treatments are on the top. In Azkp-treated embryos, different phenotypes are displayed when present. The numbers in the bottom right corner of each embryo indicate the count of embryos exhibiting each respective phenotype. In blastula stage, A: animal, V: vegetal. In G3, G5 and N2 stage, D: dorsal, V: ventral, A: anterior, P: posterior, Bv: blastopore view, Lv: lateral view, Vv: vegetal view.

Hey1

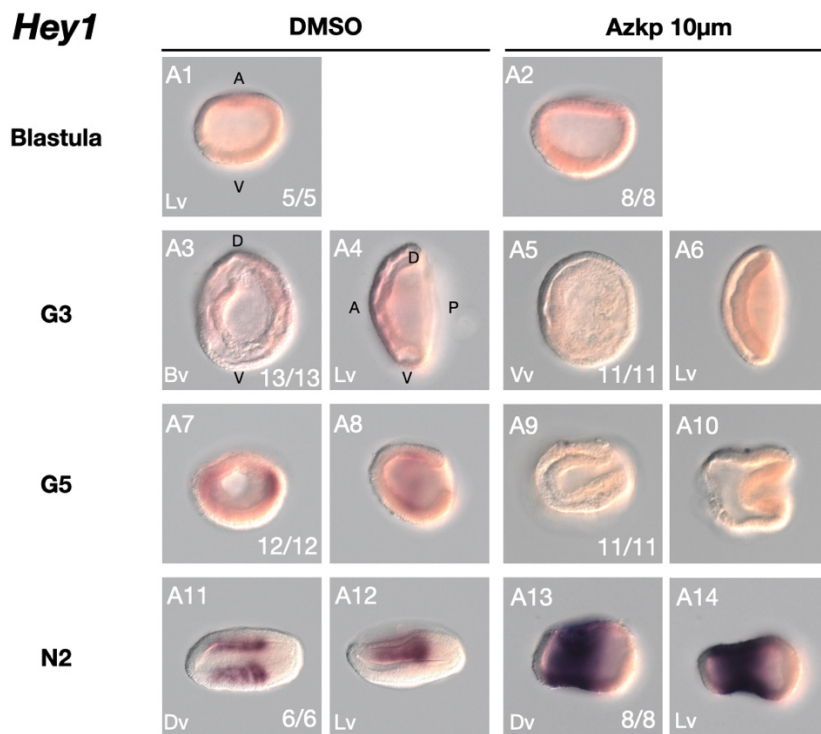


Figure 26. *Hey1* expression at the blastula, G3, G5 and N2 stage in DMSO and Azkp-treated embryos.

The Azkp-treated embryos received continuous treatment from the one-cell stage. The purple sites on the embryos indicate the presence of gene expression, while the transparent areas represent the absence of gene expression. The developmental stages are on the left side of each row, and the treatments are on the top. In Azkp-treated embryos, different phenotypes are displayed when present. The numbers in the bottom right corner of each embryo indicate the count of embryos exhibiting each respective phenotype. In blastula stage, A: animal, V: vegetal. In G3, G5 and N2 stage, D: dorsal, V: ventral, A: anterior, P: posterior, Bv: blastopore view, Lv: lateral view, Vv: vegetal view.

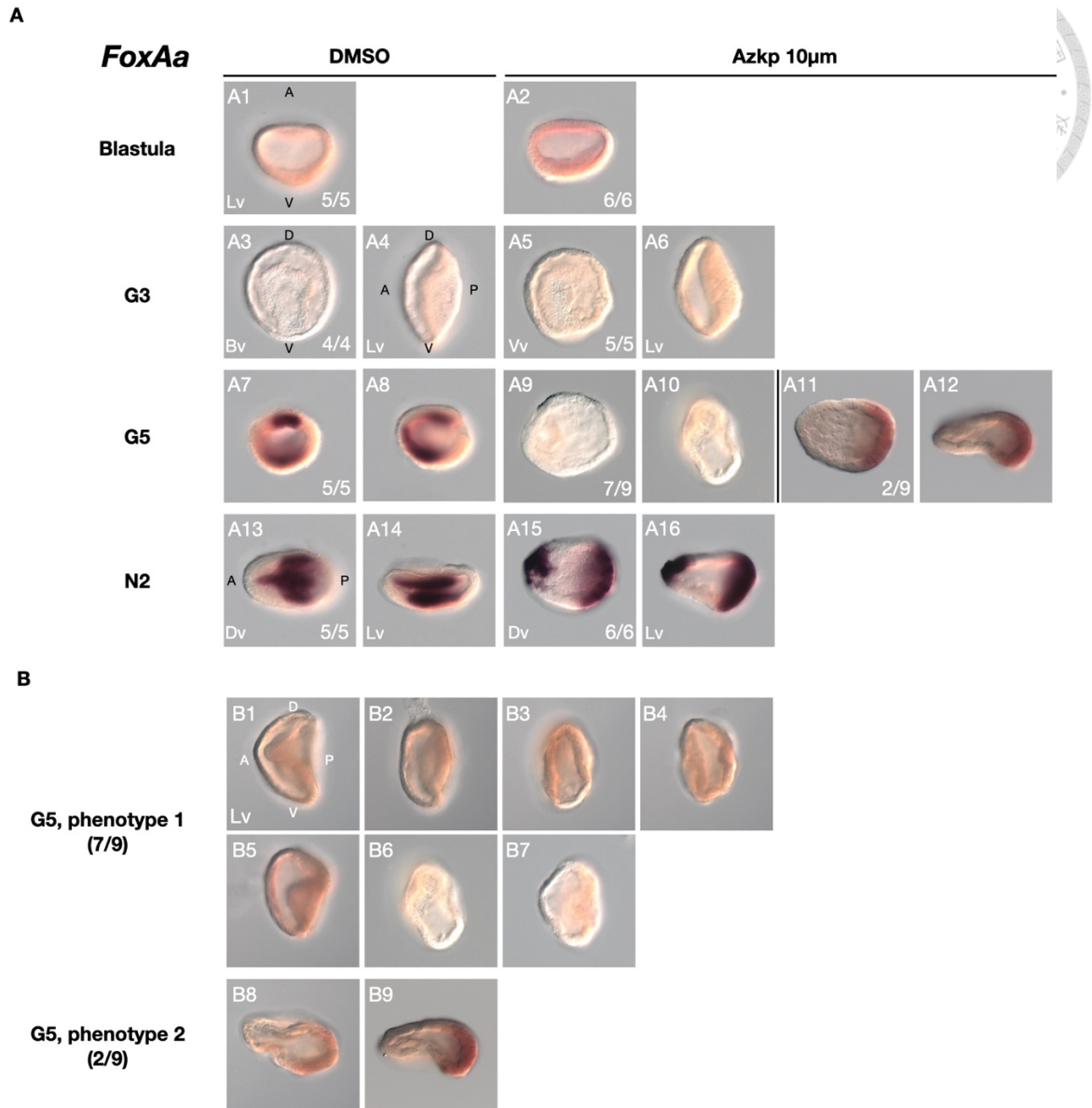
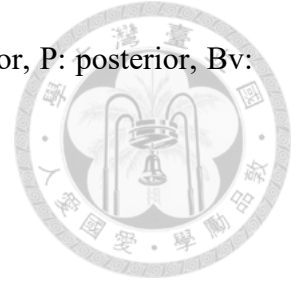


Figure 27. *FoxAa* expression at the blastula, G3, G5 and N2 stage in DMSO and Azkp-treated embryos.

(A) *SoxF* expression at blastula, G3, G5 and N2 stage in DMSO and Azkp-treated embryos. (B) *SoxF* expression of all Azkp-treated embryos at G5 stage. The Azkp-treated embryos received continuous treatment from the one-cell stage. The purple sites on the embryos indicate the presence of gene expression, while the transparent areas represent the absence of gene expression. The developmental stages are on the left side of each row, and the treatments are on the top. In Azkp-treated embryos, different phenotypes are displayed when present. The numbers in the bottom right corner of each embryo indicate the count of embryos exhibiting each respective phenotype. In blastula stage, A: animal,

V: vegetal. In G3, G5 and N2 stage, D: dorsal, V: ventral, A: anterior, P: posterior, Bv: blastopore view, Lv: lateral view, Vv: vegetal view.



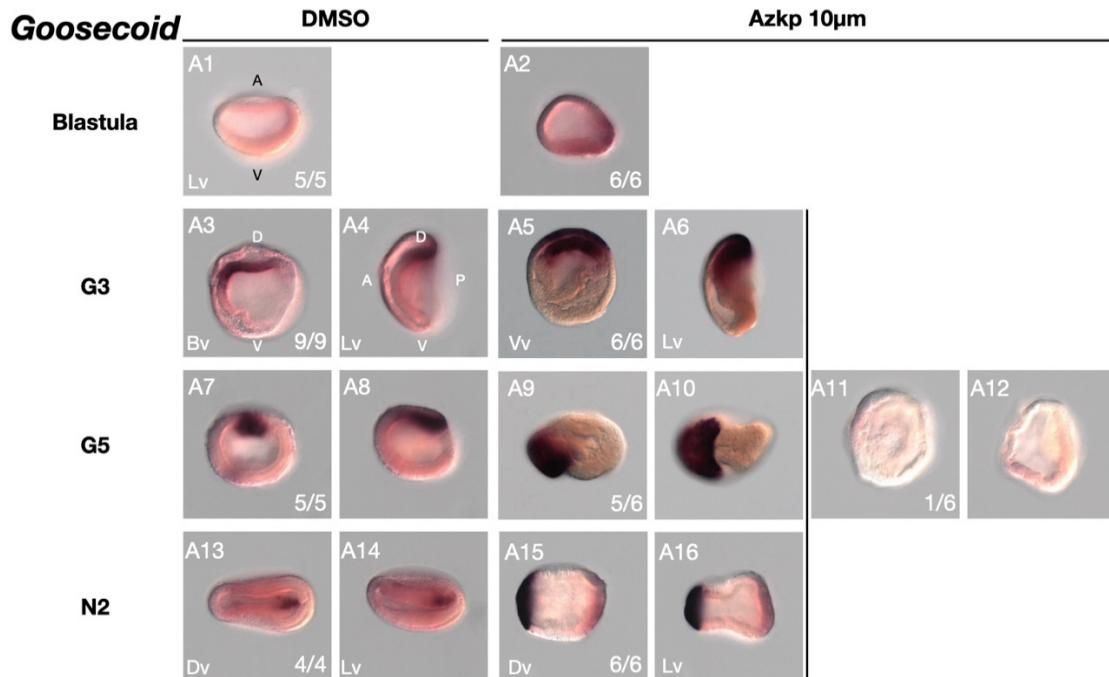


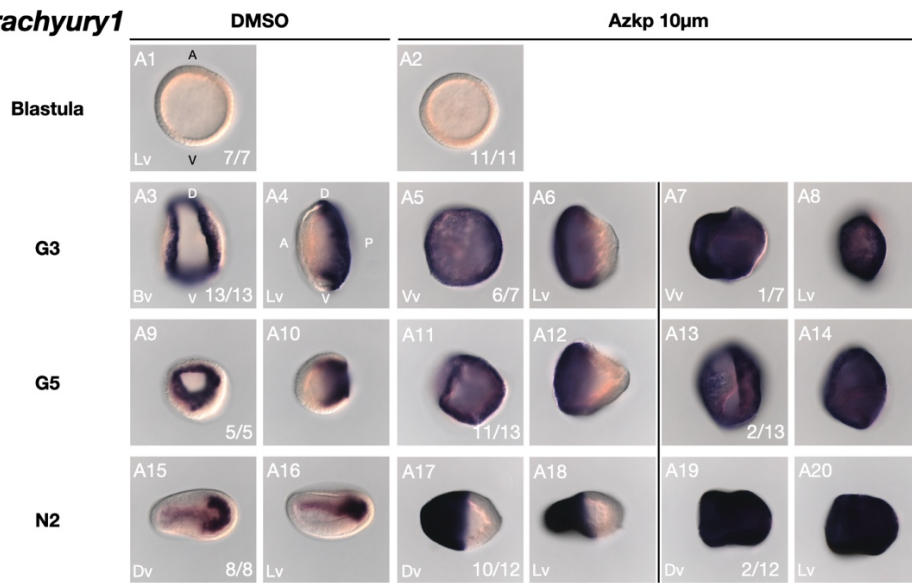
Figure 28. *Goosecoid* expression at the blastula, G3, G5 and N2 stage in DMSO and Azkp-treated embryos.

The Azkp-treated embryos received continuous treatment from the one-cell stage. The purple sites on the embryos indicate the presence of gene expression, while the transparent areas represent the absence of gene expression. The developmental stages are on the left side of each row, and the treatments are on the top. In Azkp-treated embryos, different phenotypes are displayed when present. The numbers in the bottom right corner of each embryo indicate the count of embryos exhibiting each respective phenotype. In blastula stage, A: animal, V: vegetal. In G3, G5 and N2 stage, D: dorsal, V: ventral, A: anterior, P: posterior, Bv: blastopore view, Lv: lateral view, Vv: vegetal view.

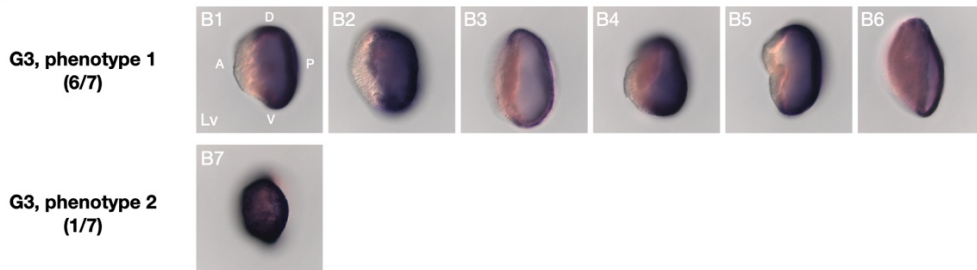


A

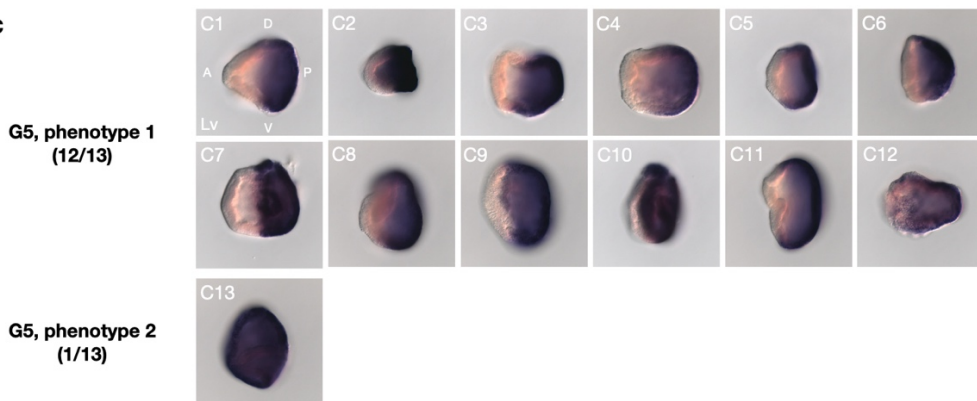
Brachyury1



B



C



D

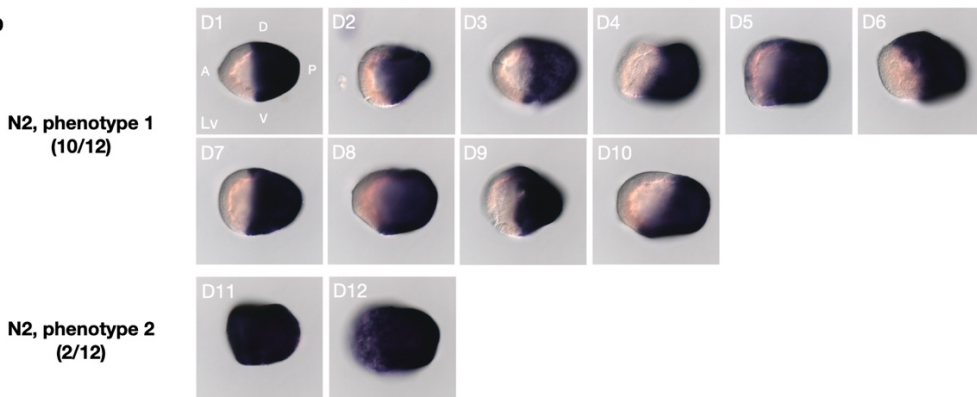


Figure 29. *Brachyury1* expression at the blastula, G3, G5 and N2 stage in DMSO and Azkp-treated embryos.

(A) *SoxF* expression at blastula, G3, G5 and N2 stage in DMSO and Azkp-treated embryos. (B) *SoxF* expression of all Azkp-treated embryos at G3, (C) G5, and (D) N2 stage. The Azkp-treated embryos received continuous treatment from the one-cell stage. The purple sites on the embryos indicate the presence of gene expression, while the transparent areas represent the absence of gene expression. The developmental stages are on the left side of each row, and the treatments are on the top. In Azkp-treated embryos, different phenotypes are displayed when present. The numbers in the bottom right corner of each embryo indicate the count of embryos exhibiting each respective phenotype. In blastula stage, A: animal, V: vegetal. In G3, G5 and N2 stage, D: dorsal, V: ventral, A: anterior, P: posterior, Bv: blastopore view, Lv: lateral view, Vv: vegetal view.

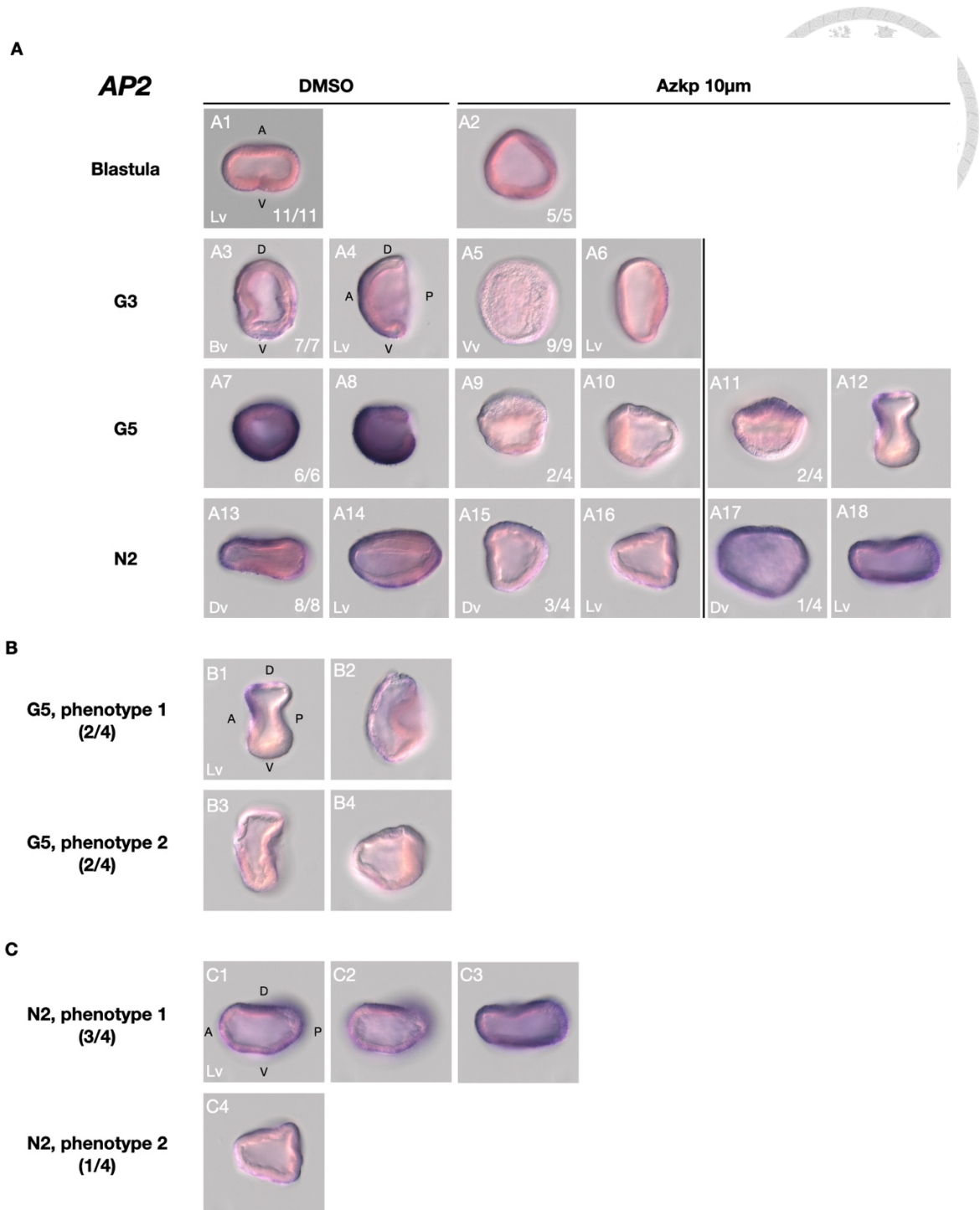
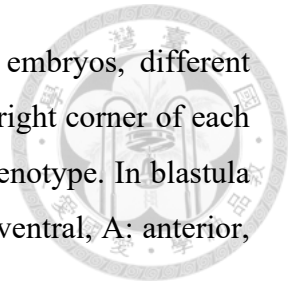


Figure 30. AP2 expression at the blastula, G3, G5 and N2 stage in DMSO and Azkp-treated embryos.

(A) *SoxF* expression at blastula, G3, G5 and N2 stage in DMSO and Azkp-treated embryos. (B) *SoxF* expression of all Azkp-treated embryos at G5 and (C) N2 stage. The Azkp-treated embryos received continuous treatment from the one-cell stage. The purple sites on the embryos indicate the presence of gene expression, while the transparent areas represent the absence of gene expression. The developmental stages are on the left side

of each row, and the treatments are on the top. In Azkp-treated embryos, different phenotypes are displayed when present. The numbers in the bottom right corner of each embryo indicate the count of embryos exhibiting each respective phenotype. In blastula stage, A: animal, V: vegetal. In G3, G5 and N2 stage, D: dorsal, V: ventral, A: anterior, P: posterior, Bv: blastopore view, Lv: lateral view, Vv: vegetal view.



FoxJ1

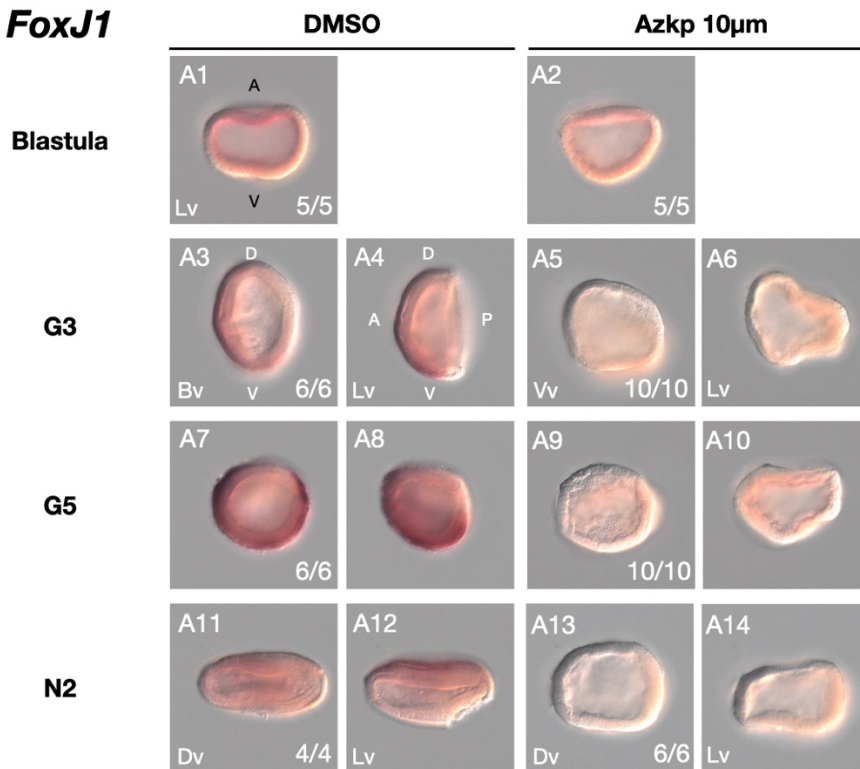
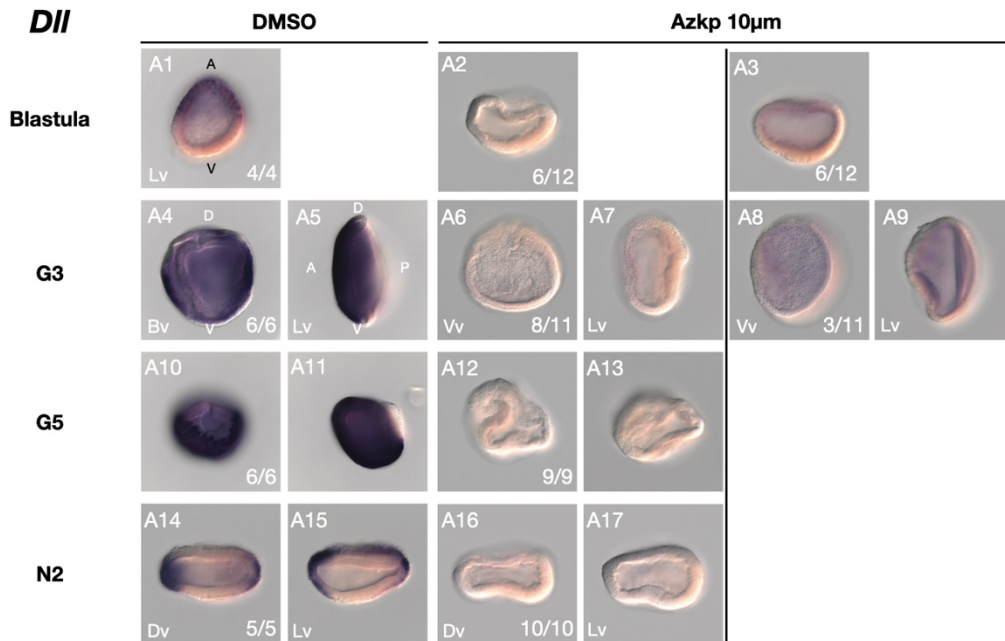


Figure 31. *FoxJ1* expression at the blastula, G3, G5 and N2 stage in DMSO and Azkp-treated embryos.

The Azkp-treated embryos received continuous treatment from the one-cell stage. The purple sites on the embryos indicate the presence of gene expression, while the transparent areas represent the absence of gene expression. The developmental stages are on the left side of each row, and the treatments are on the top. In Azkp-treated embryos, different phenotypes are displayed when present. The numbers in the bottom right corner of each embryo indicate the count of embryos exhibiting each respective phenotype. In blastula stage, A: animal, V: vegetal. In G3, G5 and N2 stage, D: dorsal, V: ventral, A: anterior, P: posterior, Bv: blastopore view, Lv: lateral view, Vv: vegetal view.

A



B

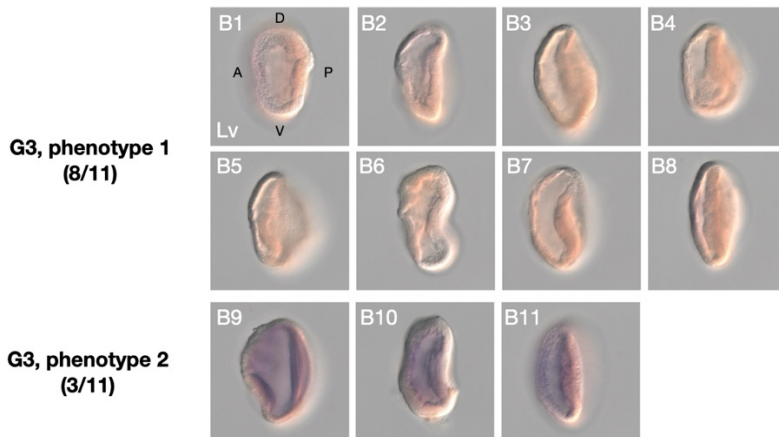
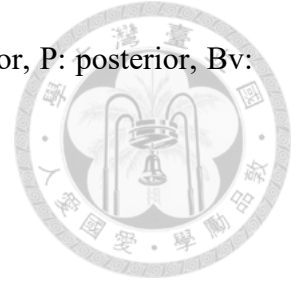


Figure 32. *Dll* expression at the blastula, G3, G5 and N2 stage in DMSO and Azkp-treated embryos.

(A) *SoxF* expression at blastula, G3, G5 and N2 stage in DMSO and Azkp-treated embryos. (B) *SoxF* expression of all Azkp-treated embryos at G3 stage. The Azkp-treated embryos received continuous treatment from the one-cell stage. The purple sites on the embryos indicate the presence of gene expression, while the transparent areas represent the absence of gene expression. The developmental stages are on the left side of each row, and the treatments are on the top. In Azkp-treated embryos, different phenotypes are displayed when present. The numbers in the bottom right corner of each embryo indicate the count of embryos exhibiting each respective phenotype. In blastula stage, A: animal,

V: vegetal. In G3, G5 and N2 stage, D: dorsal, V: ventral, A: anterior, P: posterior, Bv: blastopore view, Lv: lateral view, Vv: vegetal view.



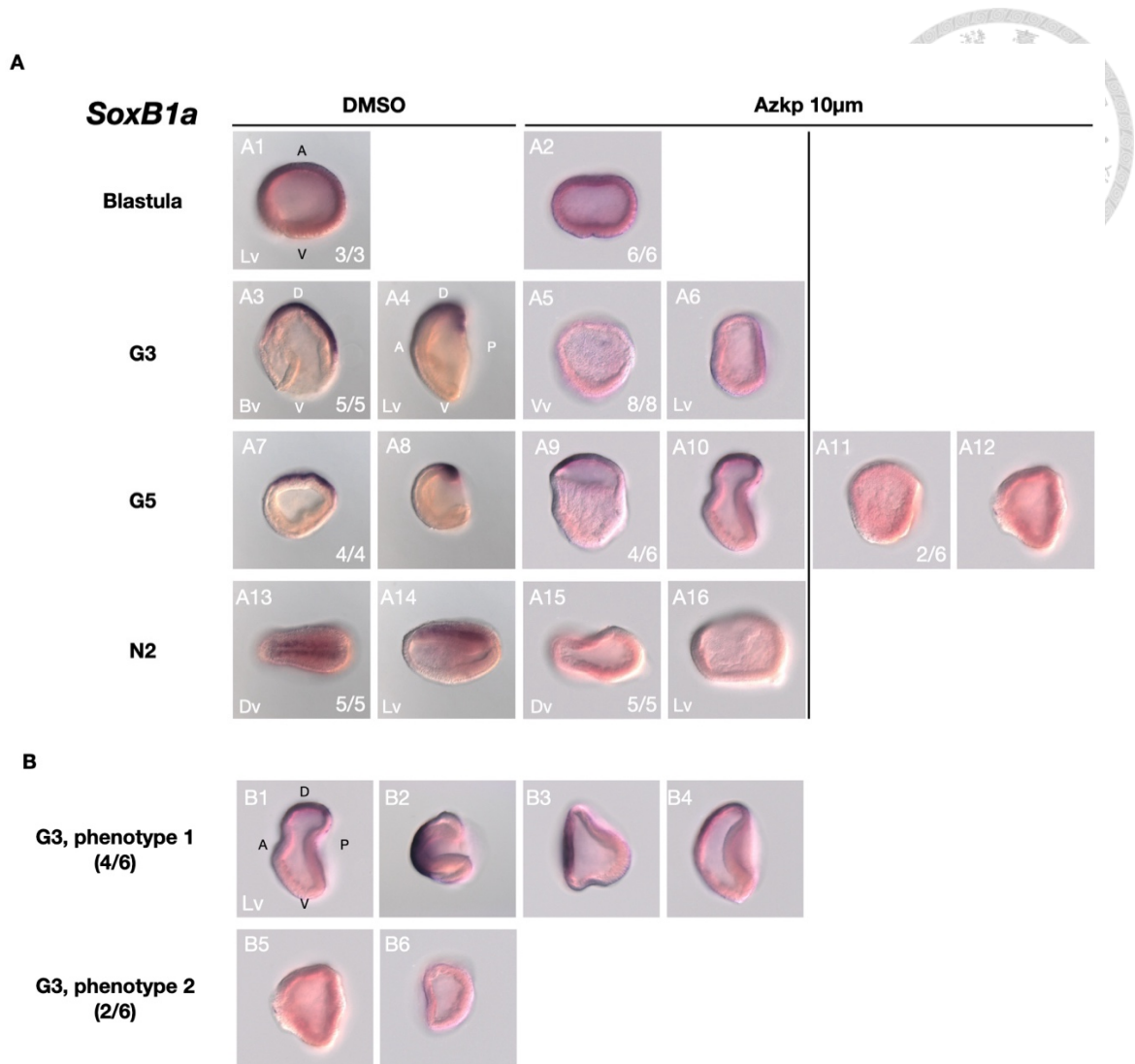


Figure 33. *SoxB1a* expression at the blastula, G3, G5 and N2 stage in DMSO and Azkp-treated embryos.

(A) *SoxF* expression at blastula, G3, G5 and N2 stage in DMSO and Azkp-treated embryos. (B) *SoxF* expression of all Azkp-treated embryos at G3 stage. The Azkp-treated embryos received continuous treatment from the one-cell stage. The purple sites on the embryos indicate the presence of gene expression, while the transparent areas represent the absence of gene expression. The developmental stages are on the left side of each row, and the treatments are on the top. In Azkp-treated embryos, different phenotypes are displayed when present. The numbers in the bottom right corner of each embryo indicate the count of embryos exhibiting each respective phenotype. In blastula stage, A: animal, V: vegetal. In G3, G5 and N2 stage, D: dorsal, V: ventral, A: anterior, P: posterior, Bv: blastopore view, Lv: lateral view, Vv: vegetal view.

Neurogenin

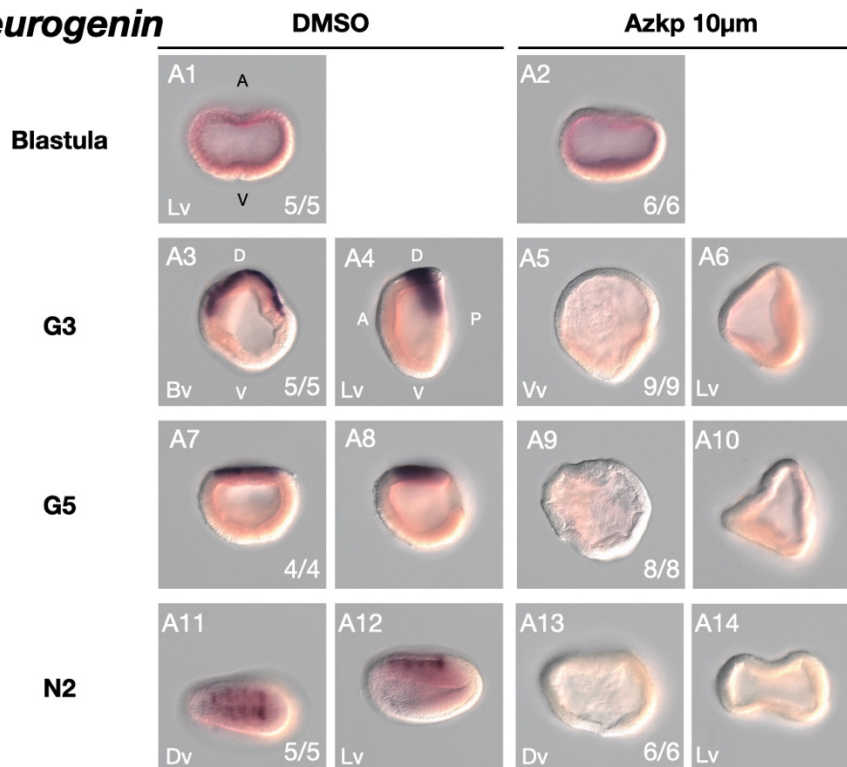


Figure 34. Neurogenin expression at the blastula, G3, G5 and N2 stage in DMSO and Azkp-treated embryos.

The Azkp-treated embryos received continuous treatment from the one-cell stage. The purple sites on the embryos indicate the presence of gene expression, while the transparent areas represent the absence of gene expression. The developmental stages are on the left side of each row, and the treatments are on the top. In Azkp-treated embryos, different phenotypes are displayed when present. The numbers in the bottom right corner of each embryo indicate the count of embryos exhibiting each respective phenotype. In blastula stage, A: animal, V: vegetal. In G3, G5 and N2 stage, D: dorsal, V: ventral, A: anterior, P: posterior, Bv: blastopore view, Lv: lateral view, Vv: vegetal view.

Tables



Table 1. Number of terms found in annotation result using different database as reference.

Database	“gastrula”	“mesoderm”	“endoderm”	“cilia”	“development”
nr metazoan	165	197	89	317	3870
5 species (nr)	343	407	277	578	7702
5 species (Swiss-Prot)	8	36	22	135	782

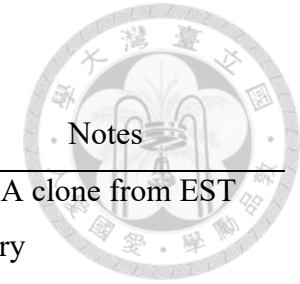


Table 2. Published genes in *Branchiostoma sp.*

Gene name	Gene accession	Protein ID	References	Notes
<i>Admp</i>	bfne048m24	XP_035670031.1	(Kozmikova et al., 2013)	cDNA clone from EST library
<i>Ahr</i>	KC305629.1	AGX25234.1	(Li et al., 2014)	
<i>Alx</i>	JF460798.1	JF460798.1	(McGonnell et al., 2011)	
<i>AP2</i>	XM_035808123.1	XP_035664016.1	(Meulemans & Bronner-Fraser, 2002)	
<i>APC</i>	XM_002596503.1	XP_002596549.1	(Wang et al., 2016)	
<i>Arnt</i>	KC305625.1	AGX25230.1	(Li et al., 2014)	
<i>Ash</i>	JF779676.1	AEH76906.1	(Lu et al., 2012)	achaete-scute homolog
<i>Axin</i>	MF479271.1	KAI8506568.1	(Onai, 2019)	<i>Branchiostoma belcheri</i>
<i>bHLHPAS-orphan</i>	KC305626.1	AGX25231.1	(Li et al., 2014)	
<i>Bmal</i>	KC305628.1	AGX25233.1	(Li et al., 2014)	
<i>BMP2/4</i>	AF068750.1	AAC97488.1	(Panopoulou et al., 1998)	
<i>BMP5/8</i>	BW827668.1	XP_035660238.1	(Yu et al., 2007)	
<i>Brachyury1</i>	X91903.1	CAA62999.1	(P. W. Holland et al., 1995)	
<i>Brachyury2</i>	EU685284.1	ACE79709.1	(Dailey et al., 2017)	<i>Branchiostoma belcheri</i>
<i>Brn1/2/4</i>	AY078995.1	AAL85498.1	(Candiani et al., 2002)	
<i>CAI</i>	D87406.1	BAA13350.1	(Kusakabe et al., 1999)	cytoplasmic actin




<i>Cerberus</i>	EU670254.1	ACF94996.1	(Li et al., 2017)	
<i>Chordin</i>	DQ644539.1	ABG66525.1	(Yu et al., 2007)	
<i>Ckl α</i>	XM_002588552.1	XP_002588598.1	(Wang et al., 2016)	
<i>Ckl δ</i>	XM_002599236.1	XP_002599282.1	(Wang et al., 2016)	
<i>Clock</i>	KC305627.1	AGX25232.1	(Li et al., 2014)	
<i>Coe</i>	AJ580840.1	CAE45569.1	(Mazet et al., 2004)	
<i>ColA</i>	AB612876.1	BAJ76654.1	(Daniel Meulemans & Marianne Bronner-Fraser, 2007)	<i>Branchiostoma belcheri</i>
<i>Dachshund</i>	AF541879.1	AAQ11368.1	(Candiani et al., 2003)	
<i>Delta</i>	HM359124.1	ADU32849.1	(Candiani et al., 2003)	<i>Branchiostoma belcheri</i>
<i>Dkk1</i>	DQ644491.2	ABG34307.1	(Zhang & Mao, 2010)	
<i>Dkk3</i>	JN019787.1	AEG80153.1	(Onai et al., 2012)	
<i>Dll</i>	U47058.1	AAB36860.1	(Holland et al., 1996)	
<i>DRAL</i>	AF071773.1	AAC69756.1	(Holland et al., 1996)	
<i>Dsh</i>	MF479273.1	AXY98025.1	(Onai, 2019)	
<i>Elav</i>	KY569299.1	ASW25830.1	(Sato et al., 2001)	<i>Branchiostoma belcheri</i>
<i>EmxA</i>	AF261146.1	AAF76327.1	(Williams & Holland, 2000)	
<i>EmxB</i>	AY040834.1	AAK93792.1	(Minguillón et al., 2002)	
<i>En</i>	U82487.2	AAB40144.1	(Holland et al., 1997)	
<i>Ets1/2</i>	AB219528.1	BAE46385.1	(Holland et al., 1997)	<i>Branchiostoma belcheri</i>

<i>EvxA</i>	AF374191.1	AAK58953.1	(Ferrier et al., 2001)
<i>EvxB</i>	AF374192.1	AAK58954.1	(Ferrier et al., 2001)
<i>Eya</i>	EF195740.1	AWV91590.1	(Kozmik et al., 2007)
<i>FGF1/2</i>	EU606032.1	ACF17006.1	(Bertrand et al., 2011)
<i>FGF8/17/18</i>	EU606035.1	ACF17009.1	(Bertrand et al., 2011)
<i>FGF9/16/20</i>	EU606036.1	ACF17010.1	(Bertrand et al., 2011)
<i>FGFA</i>	EU606033.1	ACF17007.1	(Bertrand et al., 2011)
<i>FGFB</i>	EU606034.1	ACF17008.1	(Bertrand et al., 2011)
<i>FGFC</i>	EU606038.1	ACF17012.1	(Bertrand et al., 2011)
<i>FGFD</i>	HM854710.1	ADU32860.1	(Bertrand et al., 2011)
<i>FGFE</i>	EU606037.1	ACF17011.1	(Bertrand et al., 2011)
<i>FoxAa</i>	X96519.1	CAA65368.1	(Shimeld, 1997)
<i>FoxAb</i>	EU581687.1	ACE79149.1	(Yu et al., 2008)
<i>FoxB</i>	EU581688.1	ACE79150.1	(Yu et al., 2008)
<i>FoxC</i>	EU581692.1	ACE79154.1	(Yu et al., 2008)
<i>FoxD</i>	AF512537.2	AAN03853.1	(Yu et al., 2002b)
<i>FoxEa</i>	EU581693.1	ACE79155.1	(Yu et al., 2008)
<i>FoxEb-Ei</i>	EU581694.1	ACE79156.1	(Yu et al., 2008)
<i>FoxF</i>	EU581676.1	ACE79138.1	(Yu et al., 2008)
<i>FoxG</i>	AF067203.1	AAC18392.1	(Toresson et al., 1998)



Branchiostoma belcheri
Branchiostoma belcheri
Branchiostoma belcheri
Branchiostoma belcheri
Branchiostoma belcheri
Branchiostoma belcheri
Branchiostoma belcheri
Branchiostoma belcheri
Branchiostoma belcheri

<i>FoxH</i>	EU581679.1	ACE79141.1	(Yu et al., 2008)
<i>FoxI</i>	XM_035818314.1	XP_035674207.1	
<i>FoxJ1</i>	EU581680.1	ACE79142.1	(Yu et al., 2008)
<i>FoxK</i>	EU581684.1	ACE79146.1	(Yu et al., 2008)
<i>FoxM</i>	EU581686.1	ACE79148.1	(Yu et al., 2008)
<i>FoxN1/4a</i>	EU581677.1	ACE79139.1	(Yu et al., 2008)
<i>FoxN1/4b</i>	EU581675.1	ACE79137.1	(Yu et al., 2008)
<i>FoxN2/3</i>	EU581678.1	ACE79140.1	(Yu et al., 2008)
<i>FoxO</i>	EU581697.1	ACE79159.1	(Yu et al., 2008)
<i>FoxP</i>	XM_035822257.1	XP_035678150.1	
<i>FoxQ1</i>	EU581681.1	ACE79143.1	(Yu et al., 2008)
<i>FoxQ2a</i>	EU581683.1	ACE79145.1	(Yu et al., 2008)
<i>FoxQ2c</i>	EU581685.1	ACE79147.1	(Yu et al., 2008)
<i>Fringe</i>	AJ566297.1	CAD97418.1	(Mazet & Shimeld, 2003)
<i>Fz1/2/7</i>	KC690271.1	AHB53231.1	(Li et al., 2014)
<i>Fz4</i>	KC690272.1	AHB53232.1	(Li et al., 2014)



No publication, blasted
to *FOXII* of Human and
Bos taurus

No publication,
bidirectional blasted to
Human *FOXP*

Branchiostoma belcheri
Branchiostoma belcheri

<i>Fz5/8</i>	KC690273.1	AHB53233.1	(Li et al., 2014)
<i>Fz9/10</i>	KC690274.1	AHB53234.1	(Li et al., 2014)
<i>GATA1/2/3</i>	FJ615537.1	ACR66214.1	(Zhang & Mao, 2009)
<i>GATA4/5/6</i>	JQ942474.1	AFJ79491.1	
<i>Goosecoid</i>	AF281674.1	AAF97935.1	(Neidert et al., 2000)
<i>Gremlin</i>	JX945168.1	AGS15318.1	(Le Petillon et al., 2013)
<i>Gro</i>	XM_002587088.1	XP_002587134.1	(Putnam et al., 2008)
<i>GSK3 β</i>	MF479270.1	AXY98022.1	(Onai, 2019)
<i>hairyA</i>	AY349467.1	AAQ93667.1	(Minguillón et al., 2003)
<i>hairyB</i>	AY349468.1	AAQ93668.1	(Minguillón et al., 2003)
<i>hairyC</i>	AY349469.1	AAQ93669.1	(Minguillón et al., 2003)
<i>hairyD</i>	AY349470.1	AAQ93670.1	(Minguillón et al., 2003)
<i>hairyE</i>	AY349471.1	AAQ93671.1	(Minguillón et al., 2003)
<i>hairyF</i>	AY349472.1	AAQ93672.1	(Minguillón et al., 2003)
<i>hairyG</i>	AY349473.1	AAQ93673.1	(Minguillón et al., 2003)
<i>hairyH</i>	AY349474.1	AAQ93674.1	(Minguillón et al., 2003)
<i>Hand</i>	HQ605708.1	AEL13770.1	(Onimaru et al., 2011)
<i>Hex</i>	EU296398.1	ABZ90156.1	(Onai et al., 2009)
<i>Hey1</i>	MF287249.1	AWV91612.1	(Beaster-Jones et al., 2008)
<i>Hif α</i>	KC305633.1	AGX25238.1	(Li et al., 2014)

Branchiostoma belcheri

Branchiostoma belcheri

Branchiostoma belcheri

Branchiostoma belcheri



<i>Hox1</i>	AB028206.2	BAA78620.2	(Wada et al., 1999)
<i>Hox2</i>	AB028207.1	BAA78621.1	(Wada et al., 1999)
<i>Hox3</i>	X68045.1	CAA48180.1	(Holland et al., 1992)
<i>Hox4</i>	AB028208.1	BAA78622.1	(Wada et al., 1999)
<i>Hox5</i>	Z35145.1	CAA84517.1	(Garcia-Fernández & Holland, 1994)
<i>Hox6</i>	Z35146.1	CAA84518.1	(Garcia-Fernández & Holland, 1994)
<i>Hox7</i>	Z35147.1	CAA84519.1	(Garcia-Fernández & Holland, 1994)
<i>Hox8</i>	Z35148.1	CAA84520.1	(Garcia-Fernández & Holland, 1994)
<i>Hox9</i>	JX508618.1	AFV93984.1	(Pascual-Anaya et al., 2012)
<i>Hox10</i>	Z35150.1	CAA84522.1	(Garcia-Fernández & Holland, 1994)
<i>Hox11</i>	AH009596.2	AAF81909.1	(Pascual-Anaya et al., 2012)
<i>Hox12</i>	AH009594.2	AAF81903.1	(Pascual-Anaya et al., 2012)
<i>Hox13</i>	AF276815.1	AAF81904.1	(Pascual-Anaya et al., 2012)
<i>Hox14</i>	AH009595.2	AAF81905.1	(Pascual-Anaya et al., 2012)
<i>Ifl1</i>	BN001292.1	CAU95878.1	(John et al., 2009)
<i>Ifl2</i>	BN001281.1	CAU95867.1	(John et al., 2009)
<i>IrxA</i>	EU754744.1	ACF10235.1	(Irimia et al., 2008)
<i>IrxB</i>	EU754747.1	ACF10238.1	(Irimia et al., 2008)
<i>IrxC</i>	EU754749.1	ACF10240.1	(Irimia et al., 2008)
<i>Islet</i>	AF226616.1	AAF34717.1	(Jackman et al., 2000)



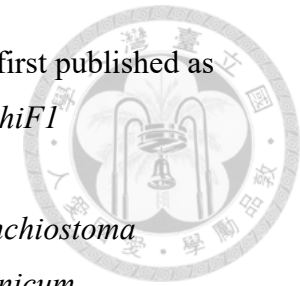
<i>Keratin1</i>	AF108192.1	AAD23384.1	(Luke & Holland, 1999)
<i>Klf1/2/4</i>	KT354037.1	AMQ13227.1	(Dailey et al., 2017)
<i>Lefty</i>	LC127056.1	BAV53928.1	(Li et al., 2017)
<i>Lrp5/6</i>	XM_002597561.1	XP_002597607.1	(Wang et al., 2016)
<i>mActin</i>	D87407.1	BAA13351.1	(Fagotti et al., 1998)
<i>MESP</i>	DQ395132.1	ABD57444.1	(Beaster-Jones et al., 2008)
<i>MRF1</i>	AY154744.2	AAN87801.2	(Schubert et al., 2003)
<i>MRF2</i>	AY154745.1	AAN87802.1	(Schubert et al., 2003)
<i>NBL1</i>	JX945167.1	AGS15317.1	(Le Petillon et al., 2013)
<i>Ncoa</i>	KC305624.1	AGX25229.1	(Li et al., 2014)
<i>Netrin</i>	AJ252166.1	CAB72422.1	(Shimeld, 2000)
<i>Neurogenin</i>	AF271788.1	AAF81766.1	(Holland et al., 2000)
<i>Nk2-5</i>	AF482469.1	AAM90855.1	(Holland et al., 2003)
<i>Nk2-1</i>	AF077840.1	AAC35350.1	(Venkatesh et al., 1999)
<i>Nk2-2</i>	AF032999.1	AAD01958.1	(Holland et al., 1998)
<i>Nodal</i>	AY083838.1	AAL99367.1	(Yu et al., 2002a)
<i>Noggin</i>	DQ644540.1	ABG66526.1	(Yong et al., 2021)
<i>Notch</i>	Y12539.2	CAC19873.1	(Yong et al., 2021)

K1, first published as
AmphiF1

Branchiostoma
japonicum

Branchiostoma belcheri

Amphink2-tin





<i>Npas1/3</i>	KC305632.1	AGX25237.1	(Li et al., 2014)	
<i>Npas4</i>	KC305630.1	AGX25235.1	(Li et al., 2014)	
<i>OligA</i>	MT166306.1	QRG28803.1	(Beaster-Jones et al., 2008)	
<i>Otx</i>	AF043740.1	AAC00193.1	(Williams & Holland, 1998)	
<i>Pax1/9</i>	U20167.1	AAA81364.1	(N. D. Holland et al., 1995)	
<i>Pax2/5/8</i>	AF053763.1	AAC12734.1	(Kozmik et al., 1999)	
<i>Pax3/7a</i>	MF979123.1	AXK16180.1	(Barton-Owen et al., 2018)	
<i>Pax3/7b</i>	MF979124.1	AXK16181.1	(Barton-Owen et al., 2018)	
<i>Pax6</i>	AJ223444.1	CAA11368.1	(Glardon et al., 1998)	
<i>Pitx</i>	AJ438768.1	CAD27489.1	(Xing et al., 2021)	
<i>POUIF1</i>	EF210455.1	ABP01321.1	(Candiani et al., 2008)	
<i>POU-IV</i>	DQ314242.1	ABC42926.1	(Candiani et al., 2006)	
<i>Runt</i>	AY146617.1	AAN08567.1	(Stricker et al., 2003)	
<i>Runx</i>	AB612879.1	BAJ76657.1	(Daniel Meulemans & Marianne Bronner-Fraser, 2007)	<i>Branchiostoma belcheri</i>
<i>Scl</i>	MW650860.1	USH99549.1	(Pascual-Anaya et al., 2013)	
<i>Sim</i>	KC305631.1	AGX25236.1	(Li et al., 2014)	
<i>Six1/2</i>	EF195742.1	AWV91584.1	(Kozmik et al., 2007)	<i>Branchiostoma belcheri</i>
<i>Six3/6</i>	EF195743.1	BAV53949.1	(Kozmik et al., 2007)	<i>Branchiostoma belcheri</i>
<i>Six4/5</i>	EF195741.1	AWV91598.1	(Kozmik et al., 2007)	<i>Branchiostoma belcheri</i>

<i>Smad1/5/8</i>	EF544709.1	ABQ23403.1	(Yu et al., 2011)
<i>Smad4</i>	HQ588925.1	AEU03847.1	(Yu et al., 2011)
<i>Snail</i>	AF081809.1	AAC35351.1	(Langeland et al., 1998)
<i>SoxB1a</i>	AF271787.1	AAF81765.1	(Holland et al., 2000)
<i>SoxB1b</i>	DQ644541.1	ABG66527.1	(D. Meulemans & M. Bronner-Fraser, 2007)
<i>SoxB2</i>	DQ644542.1	ABG66528.1	(D. Meulemans & M. Bronner-Fraser, 2007)
<i>SoxC</i>	FJ176301.1	ACI15223.1	(Lin et al., 2009)
<i>SoxD</i>	AB612878.1	BAJ76656.1	(Daniel Meulemans & Marianne Bronner-Fraser, 2007)
<i>SoxE</i>	AB612880.1	BAJ76658.1	(Daniel Meulemans & Marianne Bronner-Fraser, 2007)
<i>SoxF</i>	FE551779.1	XP_035667517.1	(Daniel Meulemans & Marianne Bronner-Fraser, 2007)
<i>SPARC</i>	MN400676.1	QJF54217.1	(Bertrand et al., 2013)
<i>Tbx1/10</i>	AF262562.2	AAG34887.2	(Ruvinsky et al., 2000)
<i>Tbx2/3</i>	AF262563.1	AAG34888.1	(Ruvinsky et al., 2000)
<i>Tbx4/5</i>	JQ942475.1	AFJ79492.1	(Minguillon et al., 2009)
<i>Tcf</i>	DQ148394.1	AAZ77711.1	(Lin et al., 2006)

Branchiostoma belcheri



Branchiostoma belcheri

Branchiostoma belcheri

Branchiostoma belcheri

Branchiostoma belcheri

Branchiostoma belcheri

<i>Tlx</i>	AJ551449.1	CAD83853.1	(Luke et al., 2003)
<i>Twist</i>	AF097914.1	AAD10038.1	(Yasui et al., 1998)
<i>Vent1</i>	AF303217.1	AAK58840.1	(Kozmik et al., 2001)
<i>Vent2</i>	AL671996.2	XP_035675293.1	(Kozmikova et al., 2011)
<i>Vgl</i>	EU670255.1	ACF94997.1	(Onai et al., 2010)
<i>Wnt1</i>	AF061974.1	AAC80432.1	(Schubert, Holland, Holland, et al., 2000)
<i>Wnt10</i>	AF361016.1	AAL37558.1	(Schubert et al., 2001)
<i>Wnt11</i>	AF187553.1	AAF80555.1	(Schubert, Holland, et al., 2000a)
<i>Wnt3</i>	AF361013.1	AAL37555.1	(Schubert et al., 2001)
<i>Wnt4</i>	AF061973.1	AAC80431.1	(Schubert, Holland, et al., 2000b)
<i>Wnt5</i>	AF361014.1	AAL37556.1	(Schubert et al., 2001)
<i>Wnt6</i>	AF361015.1	AAL37557.1	(Schubert et al., 2001)
<i>Wnt7b</i>	AF061975.1	AAC80433.1	(Schubert, Holland, et al., 2000b)
<i>Wnt8</i>	AF190470.1	AAF80559.1	(Schubert, Holland, Panopoulou, et al., 2000)
<i>Zic</i>	AJ252245.1	CAB96573.1	(Gostling & Shimeld, 2003)
β -catenin	DQ013259.1	AAAY34439.1	(Holland et al., 2005)





Table 3. RNA sequence counts in each analysis step.

Paired-end reads were mapped using STAR, which treats each paired-end read as a single entity. The percentage of reads at each step was calculated based on the number of reads remaining in the subsequent step.

	DMSO_1	DMSO_2	Azcp_2μ_1	Azcp_2μ_2	Azcp_10μ_1	Azcp_10μ_2
Sequencing reads	57866578	66211354	48265382	66864084	67730282	63735214
Trimmed reads passed fastp	28703198	32839086	23956595	33182812	33600082	31624929
Uniquely mapped by STAR	24061373 (83.83%)	27749817 (84.50%)	20780985 (86.74%)	27558590 (83.05%)	26510833 (78.90%)	27189636 (85.98%)
Assigned by featureCounts	20502559 (85.21%)	23615573 (85.10%)	17568680 (84.54%)	23415721 (84.97%)	22208034 (83.77%)	22756349 (83.69%)



Table 4. Down-regulated gene set in KEGG pathway by GSEA.

ES: enrichment score, NES: normalized enrichment score, FDR: false discovery rate.

Name	SIZE	ES	NES	FDR q-val
Arachidonic Acid Metabolism	18	0.7956533	1.7559038	0.03079086



Table 5. Up-regulated gene set in KEGG pathway by GSEA.

ES: enrichment score, NES: normalized enrichment score, FDR: false discovery rate.

Name	SIZE	ES	NES	FDR q-val
Spliceosome	96	0.641731	3.1959474	0
Ribosome	68	0.5968831	2.892845	0
RNA Degradation	45	0.6322586	2.5628371	0
RNA Polymerase	20	0.7086968	2.3434508	6.35E-04
Proteasome	31	0.53541905	2.147198	0.001692017
Aminoacyl TRNA Biosynthesis	32	0.5082564	1.9015156	0.015861835
Notch Signaling Pathway	20	0.5326073	1.7132096	0.058033954



Table 6. Gene set members involved in Notch signaling pathway in GSEA analysis.

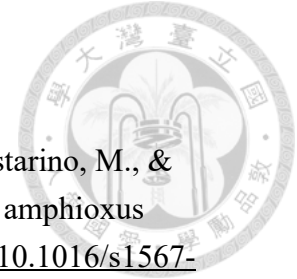
Genes with a “Yes” value in the column contributes to the enrichment result.

Gene symbol	Gene name	Core enrichment
Dll	delta like canonical Notch ligand	Yes
MFNG	MFNG O-fucosylpeptide 3-beta-N-acetylglucosaminyltransferase	Yes
HDAC2	histone deacetylase 2	Yes
KAT2B	lysine acetyltransferase 2B	Yes
SNW1	SNW domain containing 1	Yes
JAG1	jagged canonical Notch ligand 1	Yes
Notch	notch receptor	Yes
Dvl	dishevelled segment polarity protein	Yes
RBPJ	recombination signal binding protein for immunoglobulin kappa J region	Yes
MAML3	mastermind like transcriptional coactivator 3	Yes
NCSTN	nicastrin	Yes
NUMB	NUMB endocytic adaptor protein	Yes
CREBBP	CREB binding protein	Yes
DTX4	deltex E3 ubiquitin ligase 4	Yes
PSEN1	presenilin 1	Yes
PSENEN	presenilin enhancer, gamma-secretase subunit	No
APH1A	aph-1 homolog A, gamma-secretase subunit	No
CIR1	corepressor interacting with RBPJ, CIR1	No
ADAM17	ADAM metallopeptidase domain 17	No
HES1	Hes family bHLH transcription factor 1	No


References

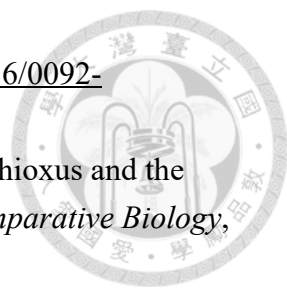


- Aldea, D., Leon, A., Bertrand, S., & Escriva, H. (2015). Expression of Fox genes in the cephalochordate *Branchiostoma lanceolatum*. *Front. Ecol. Evol.*, 3. <https://doi.org/10.3389/fevo.2015.00080>
- Ayers, T. N., Nicotra, M. L., & Lee, M. T. (2023). Parallels and contrasts between the cnidarian and bilaterian maternal-to-zygotic transition are revealed in *Hydractinia* embryos. *PLoS Genet*, 19(7), e1010845. <https://doi.org/10.1371/journal.pgen.1010845>
- Bairoch, A., & Apweiler, R. (1996). The SWISS-PROT protein sequence data bank and its new supplement TREMBL. *Nucleic Acids Res*, 24(1), 21-25. <https://doi.org/10.1093/nar/24.1.21>
- Barton-Owen, T. B., Ferrier, D. E. K., & Somorjai, I. M. L. (2018). Pax3/7 duplicated and diverged independently in amphioxus, the basal chordate lineage. *Sci Rep*, 8(1), 9414. <https://doi.org/10.1038/s41598-018-27700-x>
- Beaster-Jones, L., Kaltenbach, S. L., Koop, D., Yuan, S., Chastain, R., & Holland, L. Z. (2008). Expression of somite segmentation genes in amphioxus: a clock without a wavefront? *Dev Genes Evol*, 218(11), 599-611. <https://doi.org/10.1007/s00427-008-0257-5>
- Bertrand, S., Camasses, A., Somorjai, I., Belgacem, M. R., Chabrol, O., Escande, M. L., Pontarotti, P., & Escriva, H. (2011). Amphioxus FGF signaling predicts the acquisition of vertebrate morphological traits. *Proc Natl Acad Sci U S A*, 108(22), 9160-9165. <https://doi.org/10.1073/pnas.1014235108>
- Bertrand, S., Fuentealba, J., Aze, A., Hudson, C., Yasuo, H., Torrejon, M., Escriva, H., & Marcellini, S. (2013). A dynamic history of gene duplications and losses characterizes the evolution of the SPARC family in eumetazoans. *Proc Biol Sci*, 280(1757), 20122963. <https://doi.org/10.1098/rspb.2012.2963>
- Bolger, A. M., Lohse, M., & Usadel, B. (2014). Trimmomatic: a flexible trimmer for Illumina sequence data. *Bioinformatics*, 30(15), 2114-2120. <https://doi.org/10.1093/bioinformatics/btu170>
- Candiani, S., Castagnola, P., Oliveri, D., & Pestarino, M. (2002). Cloning and developmental expression of *AmphiBrn1/2/4*, a POU III gene in amphioxus. *Mech Dev*, 116(1-2), 231-234. [https://doi.org/10.1016/s0925-4773\(02\)00146-6](https://doi.org/10.1016/s0925-4773(02)00146-6)
- Candiani, S., Holland, N. D., Oliveri, D., Parodi, M., & Pestarino, M. (2008). Expression of the amphioxus Pit-1 gene (*AmphiPOU1F1/Pit-1*) exclusively in the developing preoral organ, a putative homolog of the vertebrate adenohypophysis.

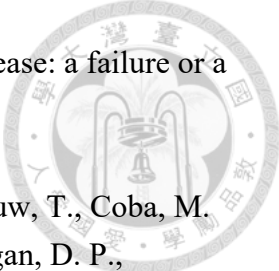


- Brain Res Bull*, 75(2-4), 324-330.
<https://doi.org/10.1016/j.brainresbull.2007.10.023>
- Candiani, S., Kreslova, J., Benes, V., Oliveri, D., Castagnola, P., Pestarino, M., & Kozmik, Z. (2003). Cloning and developmental expression of amphioxus Dachschild. *Gene Exp. Patterns*, 3(1), 65-69. [https://doi.org/10.1016/s1567-133x\(02\)00070-4](https://doi.org/10.1016/s1567-133x(02)00070-4)
- Candiani, S., Oliveri, D., Parodi, M., Bertini, E., & Pestarino, M. (2006). Expression of AmphipOU-IV in the developing neural tube and epidermal sensory neural precursors in amphioxus supports a conserved role of class IV POU genes in the sensory cells development. *Dev Genes Evol*, 216(10), 623-633.
<https://doi.org/10.1007/s00427-006-0083-6>
- Carnac, G., Kodjabachian, L., Gurdon, J. B., & Lemaire, P. (1996). The homeobox gene Siamois is a target of the Wnt dorsalisation pathway and triggers organiser activity in the absence of mesoderm. *Development*, 122(10), 3055-3065.
<https://doi.org/10.1242/dev.122.10.3055>
- Carvalho, J. E., Lahaye, F., Yong, L. W., Croce, J. C., Escrivá, H., Yu, J.-K., & Schubert, M. (2021). An Updated Staging System for Cephalochordate Development: One Table Suits Them All. *Front Cell Dev Biol*, 9.
<https://doi.org/10.3389/fcell.2021.668006>
- Cattell, M. V., Garnett, A. T., Klymkowsky, M. W., & Medeiros, D. M. (2012). A maternally established SoxB1/SoxF axis is a conserved feature of chordate germ layer patterning. *Evol Dev*, 14(1), 104-115. <https://doi.org/10.1111/j.1525-142X.2011.00525.x>
- Chang, C., Holtzman, D. A., Chau, S., Chickering, T., Woolf, E. A., Holmgren, L. M., Bodorova, J., Gearing, D. P., Holmes, W. E., & Brivanlou, A. H. (2001). Twisted gastrulation can function as a BMP antagonist. *Nature*, 410(6827), 483-487.
<https://doi.org/10.1038/35068583>
- Chen, S., Zhou, Y., Chen, Y., & Gu, J. (2018). fastp: an ultra-fast all-in-one FASTQ preprocessor. *Bioinformatics*, 34(17), i884-i890.
<https://doi.org/10.1093/bioinformatics/bty560>
- Dailey, S. C., Kozmikova, I., & Somorjai, I. M. L. (2017). Amphioxus Sp5 is a member of a conserved Specificity Protein complement and is modulated by Wnt/ β -catenin signalling. *Int J Dev Biol*, 61(10-11-12), 723-732.
<https://doi.org/10.1387/ijdb.170205is>
- Darras, S., Gerhart, J., Terasaki, M., Kirschner, M., & Lowe, C. J. (2011). β -catenin specifies the endomesoderm and defines the posterior organizer of the hemichordate *Saccoglossus kowalevskii*. *Development*, 138(5), 959-970.
<https://doi.org/10.1242/dev.059493>

- 
- Dobin, A., & Gingeras, T. R. (2015). Mapping RNA-seq Reads with STAR. *Curr Protoc Bioinformatics*, 51, 11.14.11-11.14.19. <https://doi.org/10.1002/0471250953.bi1114s51>
- Erter, C. E., Wilm, T. P., Basler, N., Wright, C. V. E., & Solnica-Krezel, L. (2001). Wnt8 is required in lateral mesendodermal precursors for neural posteriorization in vivo. *Development*, 128(18), 3571-3583. <https://doi.org/10.1242/dev.128.18.3571>
- Fagotti, A., Di Rosa, I., Simoncelli, F., Chaponnier, C., Gabbiani, G., & Pascolini, R. (1998). Actin isoforms in amphioxus *Branchiostoma lanceolatum*. *Cell Tissue Res*, 292(1), 173-176. <https://doi.org/10.1007/s004410051047>
- Ferrier, D. E., Minguillón, C., Cebrián, C., & Garcia-Fernández, J. (2001). Amphioxus *Evx* genes: implications for the evolution of the Midbrain-Hindbrain Boundary and the chordate tailbud. *Dev Biol*, 237(2), 270-281. <https://doi.org/10.1006/dbio.2001.0375>
- Garcia-Fernández, J., & Holland, P. W. (1994). Archetypal organization of the amphioxus Hox gene cluster. *Nature*, 370(6490), 563-566. <https://doi.org/10.1038/370563a0>
- Glardon, S., Holland, L. Z., Gehring, W. J., & Holland, N. D. (1998). Isolation and developmental expression of the amphioxus Pax-6 gene (AmphiPax-6): insights into eye and photoreceptor evolution. *Development*, 125(14), 2701-2710. <https://doi.org/d>
- Gostling, N. J., & Shimeld, S. M. (2003). Protochordate *Zic* genes define primitive somite compartments and highlight molecular changes underlying neural crest evolution. *Evol Dev*, 5(2), 136-144. <https://doi.org/10.1046/j.1525-142x.2003.03020.x>
- Götz, S., García-Gómez, J. M., Terol, J., Williams, T. D., Nagaraj, S. H., Nueda, M. J., Robles, M., Talón, M., Dopazo, J., & Conesa, A. (2008). High-throughput functional annotation and data mining with the Blast2GO suite. *Nucleic Acids Research*, 36(10), 3420-3435. <https://doi.org/10.1093/nar/gkn176>
- Haegel, H., Larue, L., Ohsugi, M., Fedorov, L., Herrenknecht, K., & Kemler, R. (1995). Lack of β -catenin affects mouse development at gastrulation. *Development*, 121(11), 3529-3537. <https://doi.org/10.1242/dev.121.11.3529>
- Hall, B. K. (1998). Evolutionary Developmental Biology. In (2nd ed., pp. 78-84, 129-138, 155-160). Springer Netherlands.
- Heasman, J., Crawford, A., Goldstone, K., Garner-Hamrick, P., Gumbiner, B., McCrea, P., Kintner, C., Noro, C. Y., & Wylie, C. (1994). Overexpression of cadherins and underexpression of beta-catenin inhibit dorsal mesoderm induction in early

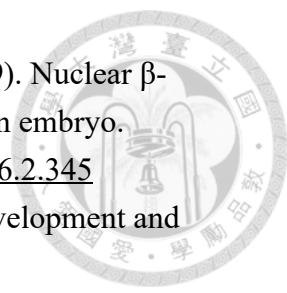
- 
- Xenopus embryos. *Cell*, 79(5), 791-803. [https://doi.org/10.1016/0092-8674\(94\)90069-8](https://doi.org/10.1016/0092-8674(94)90069-8)
- Holland, L. Z., & Holland, N. D. (2007). A revised fate map for amphioxus and the evolution of axial patterning in chordates. *Integrative and Comparative Biology*, 47(3), 360-372. <https://doi.org/10.1093/icb/icm064>
- Holland, L. Z., Kene, M., Williams, N. A., & Holland, N. D. (1997). Sequence and embryonic expression of the amphioxus engrailed gene (AmphiEn): the metameric pattern of transcription resembles that of its segment-polarity homolog in Drosophila. *Development*, 124(9), 1723-1732. <https://doi.org/10.1242/dev.124.9.1723>
- Holland, L. Z., & Onai, T. (2012). Early development of cephalochordates (amphioxus). *Wiley Interdiscip Rev Dev Biol*, 1(2), 167-183. <https://doi.org/10.1002/wdev.11>
- Holland, L. Z., Panfilio, K. A., Chastain, R., Schubert, M., & Holland, N. D. (2005). Nuclear β -catenin promotes non-neural ectoderm and posterior cell fates in amphioxus embryos. *Dev Dyn*, 233(4), 1430-1443. <https://doi.org/10.1002/dvdy.20473>
- Holland, L. Z., Schubert, M., Holland, N. D., & Neuman, T. (2000). Evolutionary Conservation of the Presumptive Neural Plate Markers AmphiSox1/2/3 and AmphiNeurogenin in the Invertebrate Chordate Amphioxus. *Dev. Biol.*, 226(1), 18-33. <https://doi.org/10.1006/dbio.2000.9810>
- Holland, L. Z., Venkatesh, T. V., Gorlin, A., Bodmer, R., & Holland, N. D. (1998). Characterization and developmental expression of AmphiNk2-2, an NK2 class homeobox gene from Amphioxus. (Phylum Chordata; Subphylum Cephalochordata). *Dev Genes Evol*, 208(2), 100-105. <https://doi.org/10.1007/s004270050159>
- Holland, N. D., Holland, L. Z., & Kozmik, Z. (1995). An amphioxus Pax gene, AmphiPax-1, expressed in embryonic endoderm, but not in mesoderm: implications for the evolution of class I paired box genes. *Mol Mar Biol Biotechnol*, 4(3), 206-214.
- Holland, N. D., Panganiban, G., Henyey, E. L., & Holland, L. Z. (1996). Sequence and developmental expression of AmphiDll, an amphioxus Distal-less gene transcribed in the ectoderm, epidermis and nervous system: insights into evolution of craniate forebrain and neural crest. *Development*, 122(9), 2911-2920. <https://doi.org/10.1242/dev.122.9.2911>
- Holland, N. D., Venkatesh, T. V., Holland, L. Z., Jacobs, D. K., & Bodmer, R. (2003). AmphiNk2-tin, an amphioxus homeobox gene expressed in myocardial progenitors: insights into evolution of the vertebrate heart. *Dev Biol*, 255(1), 128-137. [https://doi.org/10.1016/s0012-1606\(02\)00050-7](https://doi.org/10.1016/s0012-1606(02)00050-7)

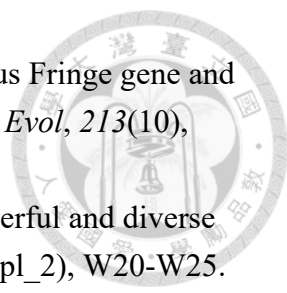
- 
- Holland, P. W., Garcia-Fernández, J., Williams, N. A., & Sidow, A. (1994). Gene duplications and the origins of vertebrate development. *Dev Suppl*, 125-133.
- Holland, P. W., Holland, L. Z., Williams, N. A., & Holland, N. D. (1992). An amphioxus homeobox gene: sequence conservation, spatial expression during development and insights into vertebrate evolution. *Development*, 116(3), 653-661. <https://doi.org/10.1242/dev.116.3.653>
- Holland, P. W., Koschorz, B., Holland, L. Z., & Herrmann, B. G. (1995). Conservation of Brachyury (T) genes in amphioxus and vertebrates: developmental and evolutionary implications. *Development*, 121(12), 4283-4291. <https://doi.org/10.1242/dev.121.12.4283>
- Hudson, C., Kawai, N., Negishi, T., & Yasuo, H. (2013). β -Catenin-driven binary fate specification segregates germ layers in ascidian embryos. *Curr Biol*, 23(6), 491-495. <https://doi.org/10.1016/j.cub.2013.02.005>
- Huelsken, J., Vogel, R., Brinkmann, V., Erdmann, B., Birchmeier, C., & Birchmeier, W. (2000). Requirement for β -catenin in anterior-posterior axis formation in mice. *J Cell Biol*, 148(3), 567-578. <https://doi.org/10.1083/jcb.148.3.567>
- Irimia, M., Maeso, I., & Garcia-Fernández, J. (2008). Convergent evolution of clustering of Iroquois homeobox genes across metazoans. *Mol Biol Evol*, 25(8), 1521-1525. <https://doi.org/10.1093/molbev/msn109>
- Jackman, W. R., Langeland, J. A., & Kimmel, C. B. (2000). islet reveals segmentation in the Amphioxus hindbrain homolog. *Dev Biol*, 220(1), 16-26. <https://doi.org/10.1006/dbio.2000.9630>
- John, L. B., Yoong, S., & Ward, A. C. (2009). Evolution of the Ikaros gene family: implications for the origins of adaptive immunity. *J Immunol*, 182(8), 4792-4799. <https://doi.org/10.4049/jimmunol.0802372>
- Kemler, R., Hierholzer, A., Kanzler, B., Kuppig, S., Hansen, K., Taketo, M. M., de Vries, W. N., Knowles, B. B., & Solter, D. (2004). Stabilization of β -catenin in the mouse zygote leads to premature epithelial-mesenchymal transition in the epiblast. *Development*, 131(23), 5817-5824. <https://doi.org/10.1242/dev.01458>
- Kiecker, C., & Niehrs, C. (2001). A morphogen gradient of Wnt/ β -catenin signalling regulates anteroposterior neural patterning in *Xenopus*. *Development*, 128(21), 4189-4201. <https://doi.org/10.1242/dev.128.21.4189>
- Kim, C. H., Oda, T., Itoh, M., Jiang, D., Artinger, K. B., Chandrasekharappa, S. C., Driever, W., & Chitnis, A. B. (2000). Repressor activity of headless/Tcf3 is essential for vertebrate head formation. *Nature*, 407(6806), 913-916. <https://doi.org/10.1038/35038097>

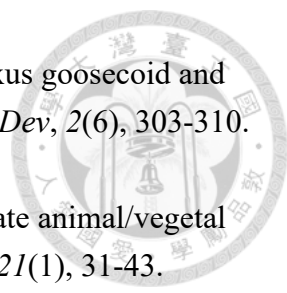
- 
- Königshoff, M., & Eickelberg, O. (2010). WNT signaling in lung disease: a failure or a regeneration signal? *Am J Respir Cell Mol Biol*, 42(1), 21-31.
<https://doi.org/10.1165/rcmb.2008-0485TR>
- Koopmans, F., van Nierop, P., Andres-Alonso, M., Byrnes, A., Cijssouw, T., Coba, M. P., Cornelisse, L. N., Farrell, R. J., Goldschmidt, H. L., Howrigan, D. P., Hussain, N. K., Imig, C., de Jong, A. P. H., Jung, H., Kohansalnodehi, M., Kramarz, B., Lipstein, N., Lovering, R. C., MacGillavry, H., . . . Verhage, M. (2019). SynGO: An Evidence-Based, Expert-Curated Knowledge Base for the Synapse. *Neuron*, 103(2), 217-234.e214.
<https://doi.org/10.1016/j.neuron.2019.05.002>
- Kozmik, Z., Holland, L. Z., Schubert, M., Lacalli, T. C., Kreslova, J., Vlcek, C., & Holland, N. D. (2001). Characterization of Amphioxus *AmphiVent*, an evolutionarily conserved marker for chordate ventral mesoderm. *Genesis*, 29(4), 172-179. <https://doi.org/10.1002/gene.1021>
- Kozmik, Z., Holland, N. D., Kalousova, A., Paces, J., Schubert, M., & Holland, L. Z. (1999). Characterization of an amphioxus paired box gene, *AmphiPax2/5/8*: developmental expression patterns in optic support cells, nephridium, thyroid-like structures and pharyngeal gill slits, but not in the midbrain-hindbrain boundary region. *Development*, 126(6), 1295-1304. <https://doi.org/10.1242/dev.126.6.1295>
- Kozmik, Z., Holland, N. D., Kreslova, J., Oliveri, D., Schubert, M., Jonasova, K., Holland, L. Z., Pestarino, M., Benes, V., & Candiani, S. (2007). Pax-Six-Eya-Dach network during amphioxus development: conservation in vitro but context specificity in vivo. *Dev Biol*, 306(1), 143-159.
<https://doi.org/10.1016/j.ydbio.2007.03.009>
- Kozmikova, I., Candiani, S., Fabian, P., Gurska, D., & Kozmik, Z. (2013). Essential role of Bmp signaling and its positive feedback loop in the early cell fate evolution of chordates. *Dev Biol*, 382(2), 538-554.
<https://doi.org/10.1016/j.ydbio.2013.07.021>
- Kozmikova, I., & Kozmik, Z. (2020). Wnt/ β -catenin signaling is an evolutionarily conserved determinant of chordate dorsal organizer. *Elife*, 9.
<https://doi.org/10.7554/eLife.56817>
- Kozmikova, I., Smolikova, J., Vlcek, C., & Kozmik, Z. (2011). Conservation and Diversification of an Ancestral Chordate Gene Regulatory Network for Dorsoventral Patterning. *PLoS One*, 6(2), e14650.
<https://doi.org/10.1371/journal.pone.0014650>
- Kunick, C., Lauenroth, K., Leost, M., Meijer, L., & Lemcke, T. (2004). 1-Azakenpaullone is a selective inhibitor of glycogen synthase kinase-3 beta.

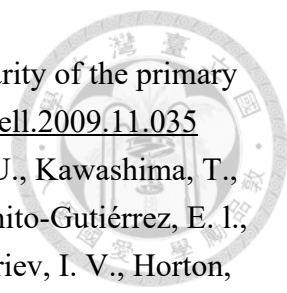


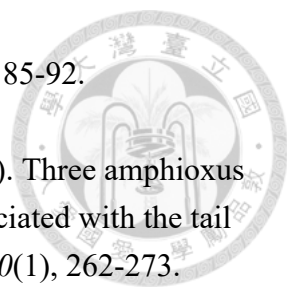
- Bioorg Med Chem Lett*, 14(2), 413-416.
<https://doi.org/10.1016/j.bmcl.2003.10.062>
- Kusakabe, R., Satoh, N., Holland, L. Z., & Kusakabe, T. (1999). Genomic organization and evolution of actin genes in the amphioxus *Branchiostoma belcheri* and *Branchiostoma floridae*. *Gene*, 227(1), 1-10. [https://doi.org/10.1016/S0378-1119\(98\)00608-8](https://doi.org/10.1016/S0378-1119(98)00608-8)
- Langeland, J. A., Tomsa, J. M., Jackman, W. R., Jr., & Kimmel, C. B. (1998). An amphioxus snail gene: expression in paraxial mesoderm and neural plate suggests a conserved role in patterning the chordate embryo. *Dev Genes Evol*, 208(10), 569-577. <https://doi.org/10.1007/s004270050216>
- Le Petillon, Y., Oulion, S., Escande, M. L., Escriva, H., & Bertrand, S. (2013). Identification and expression analysis of BMP signaling inhibitors genes of the DAN family in amphioxus. *Gene Exp. Patterns*, 13(8), 377-383. <https://doi.org/10.1016/j.gep.2013.07.005>
- Li, G., Liu, X., Xing, C., Zhang, H., Shimeld, S. M., & Wang, Y. (2017). Cerberus-Nodal-Lefty-Pitx signaling cascade controls left-right asymmetry in amphioxus. *Proc Natl Acad Sci U S A*, 114(14), 3684-3689. <https://doi.org/10.1073/pnas.1620519114>
- Li, K. L., Lu, T. M., & Yu, J. K. (2014). Genome-wide survey and expression analysis of the bHLH-PAS genes in the amphioxus *Branchiostoma floridae* reveal both conserved and diverged expression patterns between cephalochordates and vertebrates. *Evodevo*, 5, 20. <https://doi.org/10.1186/2041-9139-5-20>
- Liao, Y., Smyth, G. K., & Shi, W. (2014). featureCounts: an efficient general purpose program for assigning sequence reads to genomic features. *Bioinformatics*, 30(7), 923-930. <https://doi.org/10.1093/bioinformatics/btt656>
- Lin, H. C., Holland, L. Z., & Holland, N. D. (2006). Expression of the *AmphiTcf* gene in amphioxus: insights into the evolution of the TCF/LEF gene family during vertebrate evolution. *Dev Dyn*, 235(12), 3396-3403. <https://doi.org/10.1002/dvdy.20971>
- Lin, Y., Chen, D., Fan, Q., & Zhang, H. (2009). Characterization of *SoxB2* and *SoxC* genes in amphioxus (*Branchiostoma belcheri*): implications for their evolutionary conservation. *Sci China C Life Sci*, 52(9), 813-822. <https://doi.org/10.1007/s11427-009-0111-7>
- Liu, P., Wakamiya, M., Shea, M. J., Albrecht, U., Behringer, R. R., & Bradley, A. (1999). Requirement for *Wnt3* in vertebrate axis formation. *Nat Genet*, 22(4), 361-365. <https://doi.org/10.1038/11932>

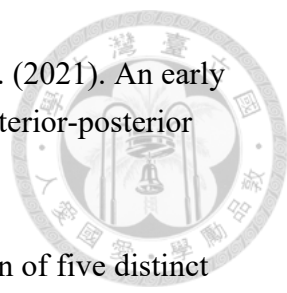
- 
- Logan, C. Y., Miller, J. R., Ferkowicz, M. J., & McClay, D. R. (1999). Nuclear β -catenin is required to specify vegetal cell fates in the sea urchin embryo. *Development*, *126*(2), 345-357. <https://doi.org/10.1242/dev.126.2.345>
- Logan, C. Y., & Nusse, R. (2004). The Wnt signaling pathway in development and disease. *Annu Rev Cell Dev Biol*, *20*, 781-810. <https://doi.org/10.1146/annurev.cellbio.20.010403.113126>
- Love, M. I., Huber, W., & Anders, S. (2014). Moderated estimation of fold change and dispersion for RNA-seq data with DESeq2. *Genome Biol*, *15*(12), 550. <https://doi.org/10.1186/s13059-014-0550-8>
- Lu, T. M., Luo, Y. J., & Yu, J. K. (2012). BMP and Delta/Notch signaling control the development of amphioxus epidermal sensory neurons: insights into the evolution of the peripheral sensory system. *Development*, *139*(11), 2020-2030. <https://doi.org/10.1242/dev.073833>
- Luke, G. N., Castro, L. F., McLay, K., Bird, C., Coulson, A., & Holland, P. W. (2003). Dispersal of NK homeobox gene clusters in amphioxus and humans. *Proc Natl Acad Sci U S A*, *100*(9), 5292-5295. <https://doi.org/10.1073/pnas.0836141100>
- Luke, G. N., & Holland, P. W. (1999). Amphioxus type I keratin cDNA and the evolution of intermediate filament genes. *J Exp Zool*, *285*(1), 50-56. [https://doi.org/http://doi.org/10.1002/\(sici\)1097-010x\(19990415\)285:1<50::aid-jez6>3.0.co;2-c](https://doi.org/http://doi.org/10.1002/(sici)1097-010x(19990415)285:1<50::aid-jez6>3.0.co;2-c)
- Marikawa, Y. (2006). Wnt/ β -catenin signaling and body plan formation in mouse embryos. *Semin. Cell Dev. Biol.*, *17*(2), 175-184. <https://doi.org/10.1016/j.semcdb.2006.04.003>
- Marlétaz, F., Firbas, P. N., Maeso, I., Tena, J. J., Bogdanovic, O., Perry, M., Wyatt, C. D. R., de la Calle-Mustienes, E., Bertrand, S., Burguera, D., Acemel, R. D., van Heeringen, S. J., Naranjo, S., Herrera-Ubeda, C., Skvortsova, K., Jimenez-Gancedo, S., Aldea, D., Marquez, Y., Buono, L., . . . Irimia, M. (2018). Amphioxus functional genomics and the origins of vertebrate gene regulation. *Nature*, *564*(7734), 64-70. <https://doi.org/10.1038/s41586-018-0734-6>
- Martin, B. L., & Kimelman, D. (2012). Canonical Wnt signaling dynamically controls multiple stem cell fate decisions during vertebrate body formation. *Dev Cell*, *22*(1), 223-232. <https://doi.org/10.1016/j.devcel.2011.11.001>
- Martindale, M. Q. (2005). The evolution of metazoan axial properties. *Nat Rev Genet*, *6*(12), 917-927. <https://doi.org/10.1038/nrg1725>
- Mazet, F., Masood, S., Luke, G. N., Holland, N. D., & Shimeld, S. M. (2004). Expression of AmphiCoe, an amphioxus COE/EBF gene, in the developing central nervous system and epidermal sensory neurons. *Genesis*, *38*(2), 58-65. <https://doi.org/10.1002/gene.20006>

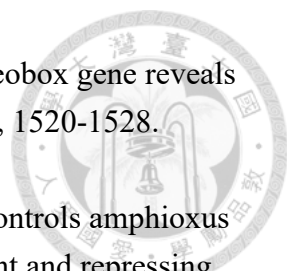
- 
- Mazet, F., & Shimeld, S. M. (2003). Characterisation of an amphioxus Fringe gene and the evolution of the vertebrate segmentation clock. *Dev Genes Evol*, 213(10), 505-509. <https://doi.org/10.1007/s00427-003-0351-7>
- McGinnis, S., & Madden, T. L. (2004). BLAST: at the core of a powerful and diverse set of sequence analysis tools. *Nucleic Acids Research*, 32(suppl_2), W20-W25. <https://doi.org/10.1093/nar/gkh435>
- McGonnell, I. M., Graham, A., Richardson, J., Fish, J. L., Depew, M. J., Dee, C. T., Holland, P. W., & Takahashi, T. (2011). Evolution of the Alx homeobox gene family: parallel retention and independent loss of the vertebrate Alx3 gene. *Evol Dev*, 13(4), 343-351. <https://doi.org/10.1111/j.1525-142X.2011.00489.x>
- Meulemans, D., & Bronner-Fraser, M. (2002). Amphioxus and lamprey AP-2 genes: implications for neural crest evolution and migration patterns. *Development*, 129(21), 4953-4962. <https://doi.org/10.1242/dev.129.21.4953>
- Meulemans, D., & Bronner-Fraser, M. (2007). The amphioxus SoxB family: implications for the evolution of vertebrate placodes. *Int J Biol Sci*, 3(6), 356-364. <https://doi.org/10.7150/ijbs.3.356>
- Meulemans, D., & Bronner-Fraser, M. (2007). Insights from Amphioxus into the Evolution of Vertebrate Cartilage. *PLoS One*, 2(8), e787. <https://doi.org/10.1371/journal.pone.0000787>
- Minguillón, C., Ferrier, D. E., Cebrián, C., & Garcia-Fernández, J. (2002). Gene duplications in the prototypical cephalochordate amphioxus. *Gene*, 287(1-2), 121-128. [https://doi.org/10.1016/s0378-1119\(01\)00828-9](https://doi.org/10.1016/s0378-1119(01)00828-9)
- Minguillón, C., Gibson-Brown, J. J., & Logan, M. P. (2009). Tbx4/5 gene duplication and the origin of vertebrate paired appendages. *Proc Natl Acad Sci U S A*, 106(51), 21726-21730. <https://doi.org/10.1073/pnas.0910153106>
- Minguillón, C., Jiménez-Delgado, S., Panopoulou, G., & Garcia-Fernández, J. (2003). The amphioxus Hairy family: differential fate after duplication. *Development*, 130(24), 5903-5914. <https://doi.org/10.1242/dev.00811>
- Moon, R. T., Kohn, A. D., Ferrari, G. V. D., & Kaykas, A. (2004). WNT and β -catenin signalling: diseases and therapies. *Nature Reviews Genetics*, 5(9), 691-701. <https://doi.org/10.1038/nrg1427>
- Mukhopadhyay, M., Shtrom, S., Rodriguez-Esteban, C., Chen, L., Tsukui, T., Gomer, L., Dorward, D. W., Glinka, A., Grinberg, A., Huang, S. P., Niehrs, C., Belmonte, J. C. I., & Westphal, H. (2001). Dickkopf1 Is Required for Embryonic Head Induction and Limb Morphogenesis in the Mouse. *Dev. Cell*, 1(3), 423-434. [https://doi.org/10.1016/S1534-5807\(01\)00041-7](https://doi.org/10.1016/S1534-5807(01)00041-7)

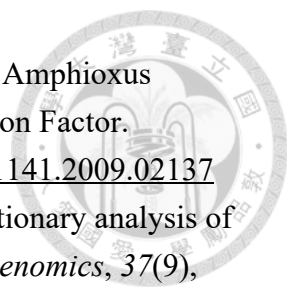
- 
- Neidert, A. H., Panopoulou, G., & Langeland, J. A. (2000). Amphioxus goosecoid and the evolution of the head organizer and prechordal plate. *Evol Dev*, 2(6), 303-310. <https://doi.org/10.1046/j.1525-142x.2000.00073.x>
- Onai, T. (2019). Canonical Wnt/ β -catenin and Notch signaling regulate animal/vegetal axial patterning in the cephalochordate amphioxus. *Evol Dev*, 21(1), 31-43. <https://doi.org/10.1111/ede.12273>
- Onai, T., Lin, H.-C., Schubert, M., Koop, D., Osborne, P. W., Alvarez, S., Alvarez, R., Holland, N. D., & Holland, L. Z. (2009). Retinoic acid and Wnt/ β -catenin have complementary roles in anterior/posterior patterning embryos of the basal chordate amphioxus. *Dev. Biol.*, 332(2), 223-233. <https://doi.org/10.1016/j.ydbio.2009.05.571>
- Onai, T., Takai, A., Setiamarga, D. H., & Holland, L. Z. (2012). Essential role of Dkk3 for head formation by inhibiting Wnt/ β -catenin and Nodal/Vg1 signaling pathways in the basal chordate amphioxus. *Evol Dev*, 14(4), 338-350. <https://doi.org/10.1111/j.1525-142X.2012.00552.x>
- Onai, T., Yu, J.-K., Blitz, I. L., Cho, K. W. Y., & Holland, L. Z. (2010). Opposing Nodal/Vg1 and BMP signals mediate axial patterning in embryos of the basal chordate amphioxus. *Dev. Biol.*, 344(1), 377-389. <https://doi.org/10.1016/j.ydbio.2010.05.016>
- Onimaru, K., Shoguchi, E., Kuratani, S., & Tanaka, M. (2011). Development and evolution of the lateral plate mesoderm: comparative analysis of amphioxus and lamprey with implications for the acquisition of paired fins. *Dev Biol*, 359(1), 124-136. <https://doi.org/10.1016/j.ydbio.2011.08.003>
- Ota, C., Baarsma, H. A., Wagner, D. E., Hilgendorff, A., & Konigshoff, M. (2016). Linking bronchopulmonary dysplasia to adult chronic lung diseases: role of WNT signaling. *Mol Cell Pediatr*, 3(1), 34. <https://doi.org/10.1186/s40348-016-0062-6>
- Panopoulou, G. D., Clark, M. D., Holland, L. Z., Lehrach, H., & Holland, N. D. (1998). AmphiBMP2/4, an amphioxus bone morphogenetic protein closely related to *Drosophila* decapentaplegic and vertebrate BMP2 and BMP4: insights into evolution of dorsoventral axis specification. *Dev Dyn*, 213(1), 130-139. [https://doi.org/10.1002/\(sici\)1097-0177\(199809\)213:1](https://doi.org/10.1002/(sici)1097-0177(199809)213:1)
- Pascual-Anaya, J., Adachi, N., Alvarez, S., Kuratani, S., D'Aniello, S., & Garcia-Fernández, J. (2012). Broken colinearity of the amphioxus Hox cluster. *Evodevo*, 3(1), 28. <https://doi.org/10.1186/2041-9139-3-28>
- Pascual-Anaya, J., Albuixech-Crespo, B., Somorjai, I. M., Carmona, R., Oisi, Y., Alvarez, S., Kuratani, S., Muñoz-Chápuli, R., & Garcia-Fernández, J. (2013). The evolutionary origins of chordate hematopoiesis and vertebrate endothelia. *Dev Biol*, 375(2), 182-192. <https://doi.org/10.1016/j.ydbio.2012.11.015>

- 
- Petersen, C. P., & Reddien, P. W. (2009). Wnt signaling and the polarity of the primary body axis. *Cell*, *139*(6), 1056-1068. <https://doi.org/10.1016/j.cell.2009.11.035>
- Putnam, N. H., Butts, T., Ferrier, D. E. K., Furlong, R. F., Hellsten, U., Kawashima, T., Robinson-Rechavi, M., Shoguchi, E., Terry, A., Yu, J.-K., Benito-Gutiérrez, E. I., Dubchak, I., Garcia-Fernández, J., Gibson-Brown, J. J., Grigoriev, I. V., Horton, A. C., de Jong, P. J., Jurka, J., Kapitonov, V. V., . . . Rokhsar, D. S. (2008). The amphioxus genome and the evolution of the chordate karyotype. *Nature*, *453*(7198), 1064-1071. <https://doi.org/10.1038/nature06967>
- Range, R. (2014). Specification and positioning of the anterior neuroectoderm in deuterostome embryos. *Genesis*, *52*(3), 222-234. <https://doi.org/10.1002/dvg.22759>
- Rhinn, M., Lun, K., Luz, M., Werner, M., & Brand, M. (2005). Positioning of the midbrain-hindbrain boundary organizer through global posteriorization of the neuroectoderm mediated by Wnt8 signaling. *Development*, *132*(6), 1261-1272. <https://doi.org/10.1242/dev.01685>
- Ruvinsky, I., Silver, L. M., & Gibson-Brown, J. J. (2000). Phylogenetic analysis of T-Box genes demonstrates the importance of amphioxus for understanding evolution of the vertebrate genome. *Genetics*, *156*(3), 1249-1257. <https://doi.org/10.1093/genetics/156.3.1249>
- Satoh, G., Wang, Y., Zhang, P., & Satoh, N. (2001). Early development of amphioxus nervous system with special reference to segmental cell organization and putative sensory cell precursors: a study based on the expression of pan-neuronal marker gene *Hu/elav*. *J Exp Zool*, *291*(4), 354-364. <https://doi.org/10.1002/jez.1134>
- Schubert, M., Holland, L. Z., & Holland, N. D. (2000a). Characterization of an amphioxus wnt gene, *AmphiWnt11*, with possible roles in myogenesis and tail outgrowth. *Genesis*, *27*(1), 1-5. [https://doi.org/10.1002/1526-968X\(200005\)27:1<1::AID-GENE10>3.0.CO;2-3](https://doi.org/10.1002/1526-968X(200005)27:1<1::AID-GENE10>3.0.CO;2-3)
- Schubert, M., Holland, L. Z., & Holland, N. D. (2000b). Characterization of two amphioxus Wnt genes (*AmphiWnt4* and *AmphiWnt7b*) with early expression in the developing central nervous system. *Dev Dyn*, *217*(2), 205-215. [https://doi.org/10.1002/\(sici\)1097-0177\(200002\)217:2<205::Aid-dvdy7>3.0.Co;2-f](https://doi.org/10.1002/(sici)1097-0177(200002)217:2<205::Aid-dvdy7>3.0.Co;2-f)
- Schubert, M., Holland, L. Z., Holland, N. D., & Jacobs, D. K. (2000). A phylogenetic tree of the Wnt genes based on all available full-length sequences, including five from the cephalochordate amphioxus. *Mol Biol Evol*, *17*(12), 1896-1903. <https://doi.org/10.1093/oxfordjournals.molbev.a026291>
- Schubert, M., Holland, L. Z., Panopoulou, G. D., Lehrach, H., & Holland, N. D. (2000). Characterization of amphioxus *AmphiWnt8*: insights into the evolution of

- 
- patterning of the embryonic dorsoventral axis. *Evol Dev*, 2(2), 85-92.
<https://doi.org/10.1046/j.1525-142x.2000.00047.x>
- Schubert, M., Holland, L. Z., Stokes, M. D., & Holland, N. D. (2001). Three amphioxus Wnt genes (AmphiWnt3, AmphiWnt5, and AmphiWnt6) associated with the tail bud: the evolution of somitogenesis in chordates. *Dev Biol*, 240(1), 262-273.
<https://doi.org/10.1006/dbio.2001.0460>
- Schubert, M., Meulemans, D., Bronner-Fraser, M., Holland, L. Z., & Holland, N. D. (2003). Differential mesodermal expression of two amphioxus MyoD family members (AmphiMRF1 and AmphiMRF2). *Gene Exp. Patterns*, 3(2), 199-202.
[https://doi.org/10.1016/s1567-133x\(02\)00099-6](https://doi.org/10.1016/s1567-133x(02)00099-6)
- Seal, R. L., Braschi, B., Gray, K., Jones, T. E. M., Tweedie, S., Haim-Vilmovsky, L., & Bruford, E. A. (2023). Genenames.org: the HGNC resources in 2023. *Nucleic Acids Res*, 51(D1), D1003-d1009. <https://doi.org/10.1093/nar/gkac888>
- Shimeld, S. (2000). An amphioxus netrin gene is expressed in midline structures during embryonic and larval development. *Dev Genes Evol*, 210(7), 337-344.
<https://doi.org/10.1007/s004270000073>
- Shimeld, S. M. (1997). Characterisation of amphioxus HNF-3 genes: conserved expression in the notochord and floor plate. *Dev Biol*, 183(1), 74-85.
<https://doi.org/10.1006/dbio.1996.8481>
- Shimizu, T., Bae, Y.-K., Muraoka, O., & Hibi, M. (2005). Interaction of Wnt and caudal-related genes in zebrafish posterior body formation. *Dev. Biol.*, 279(1), 125-141. <https://doi.org/10.1016/j.ydbio.2004.12.007>
- Sokol, S. Y. (1993). Mesoderm formation in *Xenopus* ectodermal explants overexpressing Xwnt8: evidence for a cooperating signal reaching the animal pole by gastrulation. *Development*, 118(4), 1335-1342.
<https://doi.org/10.1242/dev.118.4.1335>
- Stricker, S., Poustka, A. J., Wiecha, U., Stiege, A., Hecht, J., Panopoulou, G., Vilcinskis, A., Mundlos, S., & Seitz, V. (2003). A single amphioxus and sea urchin runt-gene suggests that runt-gene duplications occurred in early chordate evolution. *Dev Comp Immunol*, 27(8), 673-684. [https://doi.org/10.1016/s0145-305x\(03\)00037-5](https://doi.org/10.1016/s0145-305x(03)00037-5)
- Strutt, D. (2003). Frizzled signalling and cell polarisation in *Drosophila* and vertebrates. *Development*, 130(19), 4501-4513. <https://doi.org/10.1242/dev.00695>
- Subramanian, A., Tamayo, P., Mootha, V. K., Mukherjee, S., Ebert, B. L., Gillette, M. A., Paulovich, A., Pomeroy, S. L., Golub, T. R., Lander, E. S., & Mesirov, J. P. (2005). Gene set enrichment analysis: a knowledge-based approach for interpreting genome-wide expression profiles. *PNAS*, 102(43), 15545-15550.
<https://doi.org/10.1073/pnas.0506580102>

- 
- Sun, H., Peng, C.-f. J., Wang, L., Feng, H., & Wikramanayake, A. H. (2021). An early global role for Axin is required for correct patterning of the anterior-posterior axis in the sea urchin embryo. *Development*, 148(7).
<https://doi.org/10.1242/dev.191197>
- Tendeng, C., & Houart, C. (2006). Cloning and embryonic expression of five distinct sfrp genes in the zebrafish *Danio rerio*. *Gene Exp. Patterns*, 6(8), 761-771.
<https://doi.org/10.1016/j.modgep.2006.01.006>
- Toresson, H., Martinez-Barbera, J. P., Bardsley, A., Caubit, X., & Krauss, S. (1998). Conservation of BF-1 expression in amphioxus and zebrafish suggests evolutionary ancestry of anterior cell types that contribute to the vertebrate telencephalon. *Dev Genes Evol*, 208(8), 431-439.
<https://doi.org/10.1007/s004270050200>
- Veeman, M. T., Axelrod, J. D., & Moon, R. T. (2003). A Second Canon: Functions and Mechanisms of β -Catenin-Independent Wnt Signaling. *Dev. Cell*, 5(3), 367-377.
[https://doi.org/10.1016/S1534-5807\(03\)00266-1](https://doi.org/10.1016/S1534-5807(03)00266-1)
- Venkatesh, T. V., Holland, N. D., Holland, L. Z., Su, M. T., & Bodmer, R. (1999). Sequence and developmental expression of amphioxus *AmphiNk2-1*: insights into the evolutionary origin of the vertebrate thyroid gland and forebrain. *Dev Genes Evol*, 209(4), 254-259. <https://doi.org/10.1007/s004270050250>
- Wada, H., Garcia-Fernández, J., & Holland, P. W. (1999). Colinear and segmental expression of amphioxus Hox genes. *Dev Biol*, 213(1), 131-141.
<https://doi.org/10.1006/dbio.1999.9369>
- Wang, J., Li, G., Qian, G. H., Hua, J. H., & Wang, Y. Q. (2016). Expression analysis of eight amphioxus genes involved in the Wnt/ β -catenin signaling pathway. *Dongwuxue Yanjiu*, 37(3), 136-143. <https://doi.org/10.13918/j.issn.2095-8137.2016.3.136>
- Weitzel, H. E., Illies, M. R., Byrum, C. A., Xu, R., Wikramanayake, A. H., & Etensohn, C. A. (2004). Differential stability of β -catenin along the animal-vegetal axis of the sea urchin embryo mediated by dishevelled. *Development*, 131(12), 2947-2956. <https://doi.org/10.1242/dev.01152>
- Wikramanayake, A. H., Huang, L., & Klein, W. H. (1998). β -catenin is essential for patterning the maternally specified animal-vegetal axis in the sea urchin embryo. *PNAS*, 95(16), 9343-9348. <https://doi.org/doi:10.1073/pnas.95.16.9343>
- Williams, N. A., & Holland, P. W. (1998). Gene and domain duplication in the chordate *Otx* gene family: insights from amphioxus *Otx*. *Mol Biol Evol*, 15(5), 600-607.
<https://doi.org/10.1093/oxfordjournals.molbev.a025961>

- 
- Williams, N. A., & Holland, P. W. (2000). An amphioxus Emx homeobox gene reveals duplication during vertebrate evolution. *Mol Biol Evol*, *17*(10), 1520-1528. <https://doi.org/10.1093/oxfordjournals.molbev.a026251>
- Xing, C., Pan, R., Hu, G., Liu, X., Wang, Y., & Li, G. (2021). Pitx controls amphioxus asymmetric morphogenesis by promoting left-side development and repressing right-side formation. *BMC Biology*, *19*(1), 166. <https://doi.org/10.1186/s12915-021-01095-0>
- Yasui, K., Zhang, S. C., Uemura, M., Aizawa, S., & Ueki, T. (1998). Expression of a twist-related gene, Bbtwist, during the development of a lancelet species and its relation to cephalochordate anterior structures. *Dev Biol*, *195*(1), 49-59. <https://doi.org/10.1006/dbio.1997.8834>
- Yong, L. W., Lu, T. M., Tung, C. H., Chiou, R. J., Li, K. L., & Yu, J. K. (2021). Somite Compartments in Amphioxus and Its Implications on the Evolution of the Vertebrate Skeletal Tissues. *Front Cell Dev Biol*, *9*, 607057. <https://doi.org/10.3389/fcell.2021.607057>
- Yu, J. K., & Holland, L. Z. (2009). Cephalochordates (amphioxus or lancelets): a model for understanding the evolution of chordate characters. *Cold Spring Harb Protoc*, *2009*(9), pdb.emo130. <https://doi.org/10.1101/pdb.emo130>
- Yu, J. K., Holland, L. Z., & Holland, N. D. (2002a). An amphioxus nodal gene (AmphiNodal) with early symmetrical expression in the organizer and mesoderm and later asymmetrical expression associated with left-right axis formation. *Evol Dev*, *4*(6), 418-425. <https://doi.org/10.1046/j.1525-142x.2002.02030.x>
- Yu, J. K., Holland, N. D., & Holland, L. Z. (2002b). An amphioxus winged helix/forkhead gene, AmphiFoxD: insights into vertebrate neural crest evolution. *Dev Dyn*, *225*(3), 289-297. <https://doi.org/10.1002/dvdy.10173>
- Yu, J. K., Mazet, F., Chen, Y. T., Huang, S. W., Jung, K. C., & Shimeld, S. M. (2008). The Fox genes of *Branchiostoma floridae*. *Dev Genes Evol*, *218*(11-12), 629-638. <https://doi.org/10.1007/s00427-008-0229-9>
- Yu, J. K., Satou, Y., Holland, N. D., Shin, I. T., Kohara, Y., Satoh, N., Bronner-Fraser, M., & Holland, L. Z. (2007). Axial patterning in cephalochordates and the evolution of the organizer. *Nature*, *445*(7128), 613-617. <https://doi.org/10.1038/nature05472>
- Yu, X., Li, J., Liu, H., Li, X., Chen, S., Zhang, H., & Xu, A. (2011). Identification and expression of amphioxus AmphiSmad1/5/8 and AmphiSmad4. *Sci. China Life Sci.*, *54*(3), 220-226. <https://doi.org/10.1007/s11427-011-4136-3>
- Yuan, L., Wang, Y., & Li, G. (2020). Differential expression pattern of two Brachyury genes in amphioxus embryos. *Gene Exp. Patterns*, *38*, 119152. <https://doi.org/10.1016/j.gep.2020.119152>

- 
- Zhang, Y. J., & Mao, B. Y. (2009). Developmental Expression of an Amphioxus (*Branchiostoma belcheri*) Gene Encoding a GATA Transcription Factor. *Zoological Research*, 30(2), 137. <https://doi.org/10.3724/sp.J.1141.2009.02137>
- Zhang, Y. J., & Mao, B. Y. (2010). Embryonic expression and evolutionary analysis of the amphioxus Dickkopf and Kremen family genes. *J Genet Genomics*, 37(9), 637-645. [https://doi.org/10.1016/S1673-8527\(09\)60082-5](https://doi.org/10.1016/S1673-8527(09)60082-5)
- Zhou, M., Yan, J., Ma, Z., Zhou, Y., Abbood, N. N., Liu, J., Su, L., Jia, H., & Guo, A. Y. (2012). Comparative and evolutionary analysis of the HES/HEY gene family reveal exon/intron loss and teleost specific duplication events. *PLoS One*, 7(7), e40649. <https://doi.org/10.1371/journal.pone.0040649>
- Zinski, J., Tajer, B., & Mullins, M. C. (2018). TGF- β Family Signaling in Early Vertebrate Development. *Cold Spring Harb Perspect Biol*, 10(6). <https://doi.org/10.1101/cshperspect.a033274>